International University of Africa

Deanship of Graduate Studies

Modification of Natural Clays and Their Applications in the Remediation of Selected Contaminants from Aqueous Media

A Thesis Submitted in Fulfillment of the Requirements for the Degree of Doctor of Philosophy in Chemistry

by

Omer Sakin Omer

M.Sc. (Chemistry), University of Khartoum
B.(Sc. and Edu.) Honors 1st Class, (Chemistry), University of Khartoum

Supervisor

Prof. Mohammed Ali Hussein

ربيع الثاني 1440هـ

December 2018

استهلال

قَالَ تَعَالَىٰ:

﴿ فَمَن زُحۡزِحَ عَنِ ٱلنَّارِ وَأُدۡخِلَ ٱلۡجَنَّةَ فَقَدۡ فَازَۗ وَمَا ٱلۡحَيَوٰةُ ٱلدُّنۡيَآ إِلَّا مَتَٰعُ ٱلۡغُرُورِ ١٨٥ ﴾

سورة آل عمران

Dedication

To: the soul of my father,
my mother, bothers, sisters, wife and daughter.

Acknowledgements

I would like to thank Allah, Almighty, for the giving me the strength to complete this work.

I would like to express my sincere gratitude to my supervisor Prof. Mohammed Ali Hussein for the unceasing support during my study, for his patience and vast knowledge that he shared during this period. I am also thankful to him for going through my work, commenting and assisting me to apprehend and develop my ideas.

I also take this opportunity to express a deep sense of gratitude to Prof. Arabi Mgaidi and Dr. Belal M. Hussein for the motivation, invaluable guidance and cordial support that helped me in completing this task, through various stages.

I owe my heartiest gratitude to Prof. Omer Hago, Dr. Sufyan Abdulgader, Dr. Khadija Emran, Dr. Omer Adam and Mr. Omer Aljaldy, for providing moral support and technical assistance during my work.

Finally, I would like to express my deepest gratitude to my family members and dear friends for their supports, encouragement and well wishes.

Abstract

Purification and modification of clays may be a useful approach to produce an effective and low-cost adsorbent to control water pollution. In this work, Sudanese and Morocco natural clay samples were purified, modified and characterized then their adsorption capacity for removing As(III), methylene blue, crystal violet, Congo red, phenol and nitrate were studied. Brunauer-Emmett-Teller (BET) analysis and transmission electron microscope images showed that these materials were mesoporous, non-rigid aggregates of plate-like particles. X-ray diffraction showed that Sudanese clay sample mainly contains smectite and illite, whereas Morocco sample contains illite and kaolinite. Fourier transform infrared, FTIR, analysis and scanning electron microscope images confirmed the success of the modification process. Purified Morocco clay, Na-MO, proved to be an effective adsorbent for the remediation of As(III), methylene blue and crystal violet. The adsorption of As(III) was found to be controlled by the intraparticle diffusion model. In addition, the adsorption of methylene blue was found to be endothermic while that of crystal violet was found to be exothermic. Both prepared organoclay adsorbents showed higher adsorption capacities than Na-MO sample for Congo red removal. i.e., 91.7, 83.3 and 5.8 $mg.g^{-1}$ for Surf-NI, Surf-MO and Na-MO samples, respectively. The modification of clay with a cationic surfactant can produce a highly effective and efficient low-cost adsorbent for the removal of anionic dyes from contaminated water. Both organoclays adsorbents showed relatively similar adsorption capacities for phenol removal under same conditions. The results of this study proved that natural clays with simple modification process have high possibility to be used as an effective and low-cost adsorbent for chemical pollutants control. Further studies emphasized on using column approach are suggested to assess the adsorption capacities of the modified natural clay towards the studied and other contaminants.

مستخلص البحث

تنقية وتطوير الطين الطبيعي قد تكون من المداخل المهمة للحصول على مواد مُمتزَّة منخفضة التكلفة وفعالة للسيطرة على تلوث المياه. في هذه الدراسة تمت تنقية عينات من الطين الطبيعي، من المغرب ومن السودان، عن طريق التبادل الأيوني مع محلول كلوريد الصوديوم. ثم تطويرها بإدخال (intercalation) بروميد ثنائي ديسيل ثنائي مثيل الأمونيوم بين طبقات الطين، ثم تشخيصها بالطرق المختلفة، ثم دراسة فعاليتها كمواد مُمتزَّة منخفضة التكلفة لإزالة الزرنيخ الثلاثي، وصبغة الميثايلن الأزرق، وصبغة الكريستال البنفسجي، وصبغة الكونغو الحمراء، والفينول، والنترات. أوضحت نتائج طريقة بروناور–إيميت–تيلر وصور المجهر الإلكتروني النافذ أن عينات الطين عبارة عن مواد مسامية، مكونة من تجمعات مرنة لها شكل الألواح، وتصل مساحة سطحها إلى (23 و 128) م^2/غم، للعينة النيلية والعينة المغربية على التوالي. بينما أظهرت نتائج تحليل العينات بجهاز حيود الأشعة السينية أن عينة الطين السوداني تتكون من معادن السميستايت (smectite) والإليت (illite)، بينما تتكون عينة الطين المغربي من معادن الإليت والكاولينيت (kaolinite). تم التأكد من نجاح عملية التطوير بمقارنة نتائج تحليل عينات الطين قبل وبعد التطوير، باستعمال جهاز الأشعة تحت الحمراء. أظهرت عينة الطين المغربي المُنقاة Na–MO كفاءة عالية في إزالة: الزرنيخ الثلاثي وصبغتي الميثايلن الأزرق والكريستال البنفسجي، من المحاليل المائية في مدى الأس الهيدروجيني 10.8–9، حيث وصلت قيمة امتزاز الزرنيخ الثلاثي القصوى إلى 233.1 ملغم/غرام. من جهة أخرى فقد وُجد أن عملية إمتزاز الميثايلن الأزرق عملية طاردة للحرارة بينما عملية إمتزاز الكريستال البنفسجي مصحوبة بامتصاص للحرارة. أبدت العينتان (Surf–NI) و (Surf–MO) قدرة عالية على إزالة صبغة الكونغو الحمراء من المحاليل المائية مقارنة مع العينة (Na–MO)، حيث كانت قيم الإمتزاز القصوى 91.7 و 83.3 و 5.8 ملغم/غم لكل من (Surf–NI) و (Surf–MO) و (Na–MO)، على التوالي. هذه النتائج تبين بوضوح أن تنقية وتطوير الطين الطبيعي يمكن أن تساهم في إنتاج ممتزات عالية الكفاءة ومنخفضة التكلفة تصلُح لإزالة الأصباغ من المياه الملوثة. من جهة أخرة فقد أظهرت العينتان (Surf–NI) و (Surf–MO) كفاءة إمتزاز متماثلة عند استعمالهما لإزالة الفينول من المياه وذلك عند نفس الظروف التجريبية. وقد أوضحت الدراسات الحرارية أن عملية إمتزاز الفينول عملية تلقائية ماصة للحرارة، مصحوبة بزيادة في الأنتروبيا، مما يعكس قدرة كلتا المادتين على إزالة الفينول. النتائج الإجمالية لهذه الدراسة أوضحت أن تنقية وتطوير الطين الطبيعي تسهم بشكل كبير في زيادة كفاءته الامتزازية بالتالي يمكن استعماله كمادة مُمتزَّة قليلة التكلفة للسيطرة على تلوث المياه. إجراء دراسات إضافية باستعمال نمط العمود (column mode) لتقييم كفاءة الطين الطبيعي المطور على إزالة الملوثات المذكورة أو غيرها من الملوثات الكيميائية الأخرى من أهم توصيات هذه الدراسة.

Table of Contents

List of Tables

Title **page**

List of Figures

Title **page**

List of Abbreviations

As(III)	arsenite
BET	Brunauer, Emmett, and Teller
CEC	cation exchange capacity
CR	Congo red
CV	crystal violet
DSC	Deferential scanning calorimetry
DTGS	deuterated triglycine sulfate
EDS	Energy dispersive x-ray spectroscopy
FTIR	Fourier-transform infrared spectroscopy
IC	Ion chromatography
ICP-MS	inductively coupled plasma mass spectroscopy
LOI	loss on ignition
MB	Methylene blue
MSE	The mean square error
Na-MO	Sodium-exchanged Morocco clay sample
Na-NI	Sodium-exchanged Nile clay sample
PFO	Pseudo-first order
pH_{pzc}	pH point of zero charge
PSO	Pseudo-second order
q_e	Adsorption capacity ($mg.g^{-1}$)
RMSE	The root mean square error
SEM	Scanning electron microscopy
Surf-MO	surfactant-exchanged Morocco clay sample
Surf-NI	surfactant-exchanged Nile clay sample
TEM	Transmission electron microscopy
TGA	Thermogravimetric analysis
US-EPA	Environmental protection agency
UV-Vis	Ultraviolet visible spectroscopy
WHO	World Health Organization
XRD	X-ray diffraction
ΔG^0	Free energy
ΔH^0	Enthalpy
ΔS^0	Entropy changes

Publications

1) Sakin Omer, O., Hussein, B. H. M., Hussein, M. A. & Mgaidi, A. Mixture of illite-kaolinite for efficient water purification: Removal of As(III) from aqueous solutions. *Desalin. Water Treat.* 79, 273–281 (2017).

2) Sakin Omer, O., Hussein, M. A., Hussein, B. H. M. & Mgaidi, A. Adsorption thermodynamics of cationic dyes (methylene blue and crystal violet) to a natural clay mineral from aqueous solution between 293.15 and 323.15 K. *Arab. J. Chem.* 11, 615–623 (2018).

3) Sakin Omer, O., Hussein, B. H. M., Ouf, A. M., Hussein, M. A. & Mgaidi, A. An organified mixture of illite-kaolinite for the removal of Congo red from wastewater. *J. Taibah Univ. Sci.* 12, 858–866 (2018).

CHAPTER ONE

1. INTRODUCTION

1.1. Water Scarcity

Globally, water scarcity has been concerned as an immense threat to individuals, living organisms and environment (Dell, Cristina and Odorico, 2018). By 2050, world population is estimated to reach 9.6 billion (The United Nations World Water Development Report 2017)**,** hence, people living in urban areas are expected to grow rapidly, especially in developing countries.

The increased growth in population and urbanization in addition to the impacts of droughts related to the climate change, have enormous effects on the quality and quantity of water supplies. Moreover, water demand is predicted to increase drastically, mainly in the agriculture, municipal, industry, and energy invention sectors (Wang *et al.*, 2016). These sectors yield huge quantity of wastewater, therefore considered among the major sources of water pollution.

The recent industrial revolution added massive chemical wastes such as, heavy metals, organics, dyes and others, to water bodies. The developing countries are suffering more from dumping such wastes into the water bodies, because ecological policies are not defined nor implemented, and water treatment facilities are limited (Distefano and Kelly, 2017). The situation is expected to become worse because the economy of many developing countries depends on the most water polluting industrial sectors that release huge wastewater load without prior treatment (Mondal *et al.*, 2016).

The Sudan, a third world country, is a typical example, where there is a notable growth in such polluting industries like; (i) the dye and textile industry which generates wastewater containing reactive and nonreactive dyes and many organic pollutants, (ii) the iron and steel industry which generates wastewater containing many pollutants such as: phenols, acids and salts; and (iii) the mining industry that produces high volumes of wastewater containing fine particulates, metals, ...

The adverse public health risks and environmental bad effects of wastewater, in addition to the water scarcity and the growing demand for alternatives sources of water; have stimulated efforts intended to control and manage wastewater effectively. For example developed countries treat about 70% of their wastewater while the ratio drops to only 8% in developing countries (Development, 2017). However, the prospect of using treated water is varied notably, depending upon the degree of treatment and more significantly on community acceptance. Hence, few countries use treated water for drinking purposes, while several countries use it for irrigation purposes.

To push the growing demand for water, World Health Organization, (WHO), describes guidance for a suitable management system for production of potable water from municipal wastewater (WHO 2017). Settlement of this strategy put extra pressure on researchers, chemists and water treatment specialists to solve problems associated to water contaminants, and to reduce pollutants to the allowed level.

Although there is a wide range of methods available for that purpose, adsorption process gained growing concern as a purification method because of its high efficiency and relatively low cost compared to the other available technologies. Moreover, several low-cost adsorbents have been investigated to achieve a high-quality treated water.

1.2. Impacts of Water Pollution

Water pollution is caused due to anthropogenic activities that release many contaminants into waterways and sources, then reduce its usefulness to humans and other organisms in the environment. Agricultural, industrial and domestic activities produce several types of pollutants. The pollutants have adverse health effects, so they have been of growing concern worldwide.

Many severe risks due to point source and non-point source chemical pollution have been reported over the last decades, a part of such risky events includes: the first public health disaster that was caused by mercury toxicity in Minamata, Japan, where large amounts of methyl mercury discharged from a chemical factory to Minamata bay. Hence, various neurological damage, as well as irritability, insanity, and loss of sight were reported as the main toxicological effects of mercury in people who eat fish containing methyl mercury (Bernhoft, 2012).

Globally, the Sukinda valley in India is considered as one of the most polluted area, due to the mining processes for chromite ore deposits. The resultant Cr(VI) is a highly toxic element and has an adverse effects on lungs, liver, and kidneys (Pattnaik and Equeenuddin, 2016).

Besides, the two famous oil spills; Exxon Valdez in Alaska and the British Petroleum in the gulf of Mexico had caused major short-term and long-term troubles to ecological processes and threatened many populations of land, marine and coastal species (Perrons, 2013).

To control pollution and minimize its hazards, pollution prevention act of 1990, as testified by the United States Environmental Protection Agency, (US-EPA), strongly suggested the following rules; (i) reduce waste at the source by modifying production methods, (ii) promote usage of nontoxic or less toxic things, (iii) apply protection procedure, and (iv) recover materials in state of dumping them into wastewater.

1.3. Pollutants Sources and Health Risks

The sources of water pollutants are found where human activities continue to influence the environment, because these events are often accompanied with the discharge of chemical contaminants, among others. Industrial wastewater gets more concern since it produces the major types of pollutants.

1.3.1. Heavy Metals

Generally, heavy metals reach the environment from natural sources, industrial activities, mining activities, agrochemicals, wastewater treatment systems, etc. Some heavy metals; e.g. selenium and zinc, are essential to sustain the living species metabolism. Inversely, others are harmful as they tend to bioaccumulate; e.g. cadmium and lead. Bioaccumulation of heavy metals in living organisms and in the environment cause a wide spectrum of adverse effects, including ecological costs and human diseases.

From the viewpoint of the health impacts, each metal imparts diverse effects and symptoms. Thus, cadmium, chromium, lead, cobalt, arsenic, mercury, manganese, nickel, copper, and tin are considered of highest concern, so their acceptable levels have been proposed by local or international environmental authorities, such as WHO.

For example, cadmium is used in many industrial areas such as the pigments, coatings, and production of alkaline batteries. It has been recognized as very toxic to human beings since it acts synergistically with other elements such as copper and zinc, to increase toxicity. The toxicological properties of cadmium arise from its chemical similarity to zinc, an essential element for human and various living organisms (Antoine, Fung and Grant, 2017). In humans and animals, long-term exposure to cadmium is linked to renal disfunction, obstructive lung disease, and bone defects. The allowable limit of cadmium in drinking water recommended by WHO is 3 ppb (Sari and Tuzen, 2014).

1.3.2. Dyes

Thousands of types of dyes are commercially available and widely employed in the pharmaceutical, food, cosmetic, photographic, paper, plastics and textile industries. Wastewater effluents of these industries frequently contain high levels of dyes. A well-known example is the textile dyeing where 10-15% of the dyes used are washed out into the wastewater effluent (Abidi *et al.*, 2015).

Commonly, dyes are classified to three types, based on their particle charge upon dissolution in aqueous application: (i) cationic (all basic dyes), (ii) anionic (direct, acid, and reactive dyes), and (iii) non-ionic (dispersed dyes) (Yagub *et al.*, 2014).

Occurrence of dyes in water bodies reduces the penetration of sunlight to benthic organisms, decreases the dissolved oxygen quantity and damaging aerobic processes. Moreover, the release of dyes into water streams may result in the formation of toxic carcinogenic degradation products (Tireli *et al.*, 2014). Besides, dyes are highly persistent in natural environments because they are designed to be chemically and photolytically stable. Therefore, dyes present an eco-toxic hazard and introduce the potential danger of bio-accumulation that may finally affects human by transport through the food chains (Santos, Oliveira and Boaventura, 2016).

1.3.3. Phenols

Phenols are considered among the primary organic contaminants due to their hazardous effects on human health and the environment. Phenols are commonly found in wastewater of many industries, such as: leather, paper, disinfectants, paints, plastics, drugs, pesticides and wood preservatives (Nourmoradi *et al.*, 2016). Phenols were reported as known or suspected human carcinogens (Mubarik *et al.*, 2016). They have a strong and unpleasant odor and are extremely toxic to water flora and animals, the

presence of phenols in drinking water give unpleasant taste and odor, even at concentrations as low as 0.1 $mg.L^{-1}$ (Anirudhan and Ramachandran, 2014). Moreover, consuming phenolic-polluted waters can affect the central nervous system or results in liver, kidney and pancreas disorders in human (Anirudhan and Ramachandran, 2014).

1.3.4. Nitrate

Nitrate is a widespread contaminant as it is highly water soluble. It reaches the water systems from different activities such as agricultural and urban runoff, improper treatment of industrial wastes, and sewage effluents. Although it serves as an essential source of nitrogen for plants, but high level of nitrate in various water sources is hazardous. It is known to cause many health complications such as blue baby syndrome in infants, gastric cancer in adults, diabetes and formation of carcinogenic nitrosamine compounds (Bhatnagar and Sillanpää, 2011). Likewise, high levels of nitrate stimulate heavy algal growth and adversely affect cattle through nitrate poisoning. Due to the above health hazards associated with nitrate from contaminated water, US-EPA has set 10 $mg.g^{-1}$ for nitrate as the maximum contaminant level (Tyagi *et al.*, 2018).

Usually, wastewater may contain several types of contaminants, such as heavy metals, dyes, nitrate and phenols. Thus, wastewater must be treated before being discharged.

1.4. Methods of Water Treatment

Clean water is vital, and globally is considered as a human right. Since water pollution seriously affects water quality, it needs to be properly treated to mitigate the impacts of pollutants. Numerous treatment methods have been developed to remove chemical pollutants from water (Mu and Wang, 2016; Ezzatahmadi *et al.*, 2017; XU *et al.*, 2017).

Examples of the common methods in practice for the removal of chemical pollutants from water were summarized in **Table 1-1**, with some of their advantages and disadvantages.

Most of these methods are expensive, non-selective, useless at low pollutants concentrations, and cannot recover the contaminants. By contrast, contaminants removal by adsorption has been reported to have distinct advantages over other methods. Hence, the following section gives a brief account about adsorption.

Table 1-1: Pollutants removal methods with their advantages and disadvantages (Carolin *et al.*, 2017; Burakov *et al.*, 2018; Mohd *et al.*, 2018)

Methods	Advantages	disadvantages
Chemical treatment		
Oxidative process	Simplicity of application	(H_2O_2) agent needs to be activated by some means
H_2O_2+Fe(II) salts (Fenton's reagent)	Fenton's reagent is a suitable chemical means	Sludge generation
Ozonation	Applied in its gaseous state and does not increase the volume of wastewater and sludge	Short half-life, by-products formation
Photochemical	No sludge formation nor foul odors are produced	Formation of by-products
Sodium hypochlorite	Initiate and accelerates azo bond cleavage	Release of aromatic amines
Electrochemical destruction	No consumption of chemicals and no sludge	In high flow rates may decreases dye removal
Biological treatments		
Decolorization by white rot fungi	the fungi can degrade dyes using enzymes	Enzymes production has been shown to be unreliable
Other microbial cultures (mixed bacterial)	Decolorized in 24–30 h	Under aerobic conditions azo dyes are not readily metabolized
Adsorption by living/dead microbial biomass	Certain dyes have an affinity for binding with microbial species	Not effective for all dyes
Anaerobic textile – dye bioremediation system	Allows azo and other water-soluble dyes to be decolorized	Anaerobic breakdown yields methane and hydrogen sulfide
Physical treatments		
Adsorption by activated carbon	Good removal of wide variety of dyes	Very expensive
Membrane filtration	Removes all dye types	Concentrated sludge production
Ion exchange	Regeneration: no adsorbent loss	Not effective for all dyes
Irradiation	Effective oxidation at laboratory scale	Requires a lot of dissolved O_2
Electro-kinetic coagulation	Economically feasible	High sludge production

1.5. Problem statement

Pollution of water bodies with chemicals is a current problem worldwide because high levels of such contaminants pose threat to human life and the environment. Several treatment methods are available with diverse degree of success to minimize or remove contaminants. Many of these methods facing problems such as; high operational and maintenance costs, generation of toxic sludge, and complicated procedure are involved in the treatment.

Relatively, adsorption is considered a better choice for water treatment as a result of convenience, ease of operation and simplicity of design. Activated carbon is a famous adsorbent, that is frequently used for the removal of many contaminants from water, but its applications in wastewater treatment are limited due to its higher cost and the regeneration problems. Therefore, there is a growing need to find effective, low-cost and eco-friendly materials for the adsorption processes.

Clays and clay minerals have been selected as suitable materials for removal of water contaminants due to their brilliant properties; (i) clays have a high cation exchange capacity (CEC), (ii) large surface areas, which confer strong adsorption-absorption properties, (iii) clays are naturally abundant, moreover (iv) clay particles composed of edges and faces that can adsorb anions, cations, non-ionic and polar contaminants.

However, application of raw natural clay as adsorbent is restricted due to; high impurities, heterogeneous functional surfaces, breakable molecular structure. These drawbacks can be treated by adopting a modification method prior to application, such as: acid or base treatment, thermal activation, mechanical grinding, sodium chloride conditioning, surfactant intercalation, chemical grafting.

Variation of the clay structures based on their types and origins could result in different performances and behaviors toward the treatments. Therefore, it

is essential to gain in-depth information on the clay features and their adsorption properties toward a targeted pollutant. This leads to a requirement of the adsorption isotherms and kinetic studies, where the removal performance and mechanisms of the clays can be determined. Furthermore, the significant effects of important systematic parameters on the adsorption capacity such as solution pH, adsorbate initial concentration, adsorbents dosage, and temperature are also needed.

In this study, raw natural Sudanese clay and Morocco clay samples, which are considered relatively cheap materials, were purified and modified with simple routes, then used with the hope of achieving materials with enhanced adsorption properties for the removal selected contaminants from aqueous solution.

1.6. Aims of This Study

The aim of this project is to modify natural clay samples as low-cost adsorbents, and study their adsorption properties towards selected contaminants: The objectives of this study included the following:

(1) To separate a purer Na-clay from the natural clay samples from Sudan and Morocco through saturating these clays with NaCl solution.

(2) To prepare an organo-clay by treating each Na-clay with a surfactant didecyl dimethyl ammonium bromide

(3) To characterize these adsorbents with available techniques; XRD, BET, SEM-EDX, FTIR, DSC, and TGA.

(4) To investigate the adsorption performance and the mechanisms of removal of methylene blue, crystal violet, and As(III) using the Na-clays then fitting the experimental data to different isotherms and kinetics models.

(5) To investigate the adsorption performance and the mechanisms of removal of Congo red, nitrate and phenol using the organo-clay then fitting the experimental data to different isotherms and kinetics models.

(6) Compare the performance of all adsorbents for removal of the selected contaminants.

CHAPTER TOW

2. LITERATURE REVIEW

2.1. Adsorption Process

Adsorption process has become one of the preferred methods for water pollution treatment. It is well documented as an effective, efficient, simple and economic method. Moreover, adsorption process is applicable at moderate and low concentrations, suitable for using batch and continuous processes, capable for the remediation of both organic and inorganic pollutants, and the adsorbents can be regenerated and reused (Rosales *et al.*, 2017). Hence, the processes have got global importance for water treatments and become a significant addition to green chemistry events.

Adsorption is an equilibrium process. It involves a solid phase (adsorbent) and a gas or liquid phase containing a dissolved species to be adsorbed (adsorbate). Because of many physical or chemical attraction forces between adsorbate species and the chemical groups on the adsorbent surface, adsorbate species accumulate on the adsorbent till an equilibrium is reached (Yagub *et al.*, 2014; Tan and Hameed, 2017). The basic terms used in the adsorption process were shown in **Figure 2.1**.

Adsorption process system consist of three components; the adsorbent, the adsorbate, and the solution. Adsorption system is influenced by several factors such as: (i) the nature of the adsorbent, its physical and chemical nature and functional groups, (ii) the activation conditions of the raw solid material, (iii) the influence of process variable; concentration, time, dosage, stirring rate (iv) the chemistry of the pollutants; polarity, size and functional groups, and (v) the solution conditions; pH, ionic strength, and impurities

(Tran *et al.*, 2017). The relationship between the three components is shown schematically in **Figure 2-2** .Usually the affinity between the adsorbent and adsorbate is the main interaction force.

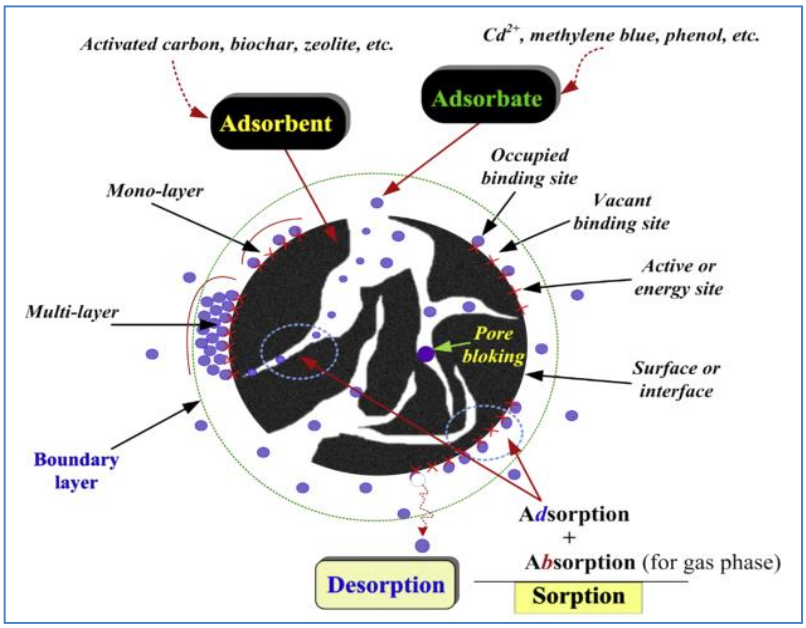

Figure 2-1: Some basic terms used in adsorption process (Tran *et al.*, 2017)

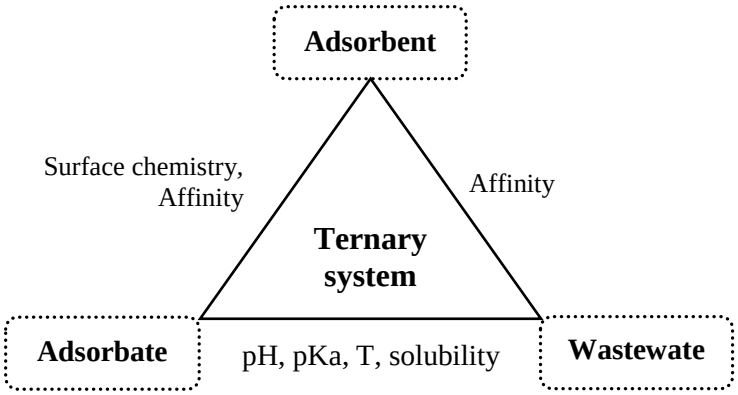

Figure 2-2: Relation between the three components of an adsorption system (Crini, Grégorio, Badot, 2010)

Interaction forces were grouped into two main types, (i) physical forces, (dipole moments, polarization forces, dispersive forces, or short range repulsive interactions), and (ii) chemical forces, (involving chemical reaction and the interactions that responsible for the formation of chemical compounds)(Yagub *et al.*, 2014; Ismadji, Soetaredjo and Ayucitra, 2015d).

Removal of the pollutants from water or wastewater during adsorption can be proceed through one or a combination of two or more of these forces.

However, the major obstruction to the application of the adsorption process by industry is the high cost of adsorbent materials currently available for commercial use, i.e. activated carbon. Therefore, there have been increased studies into the production and developing of low-cost adsorbents to replace the costly activated carbon.

The following part explains the use of low-cost materials as adsorbents for pollutants removal from aqueous solutions.

2.2. Low-Cost Adsorbents

Adsorption process based on binding capacities of various low-cost materials have alert attention to a variety of agricultural wastes, industrial by-products, clay, and other natural materials (De Gisi *et al.*, 2016).

The term Low-cost adsorbents commonly used to describe adsorbents that are abundant in nature, or are by-products or waste materials, from industry or agriculture, in addition they are requiring limited processing (Yagub *et al.*, 2014). **Figure 2-3** shows a broad classification of these materials.

The common features of a good low-cost adsorbent which determine its applications include: mechanical and chemical properties, abundance, handling, regeneration capability, and adsorption capacity, as summarized in **Figure 2-4**.

However, it is difficult that an adsorbent hold all of these features, thus accomplish many of these properties is crucial (Nguyen *et al.*, 2013; Rosales *et al.*, 2017; Tran *et al.*, 2017).

2.2.1. Agriculture Wastes

Extensive studies have been carried for the production of low-cost adsorbents from agricultural wastes and plant materials that otherwise

discarded usually after harvesting; i.e., leaves, seeds, parks, peels, husks, and fibers, amongst others (Gupta and Suhas, 2009; Omo-okoro, Daso and Okonkwo, 2017; Turk Sekulić *et al.*, 2018). These studies were documented and reviewed in several published works. Examples include: cotton and gingelly seed shell (Thinakaran *et al.*, 2008), lignocellulose from wood and tree leaves (Tran *et al.*, 2015), agricultural peels (Anastopoulos and Kyzas, 2014),

Figure 2-3: Common low-cost adsorbents for pollutants removal from water (Mu and Wang, 2016)

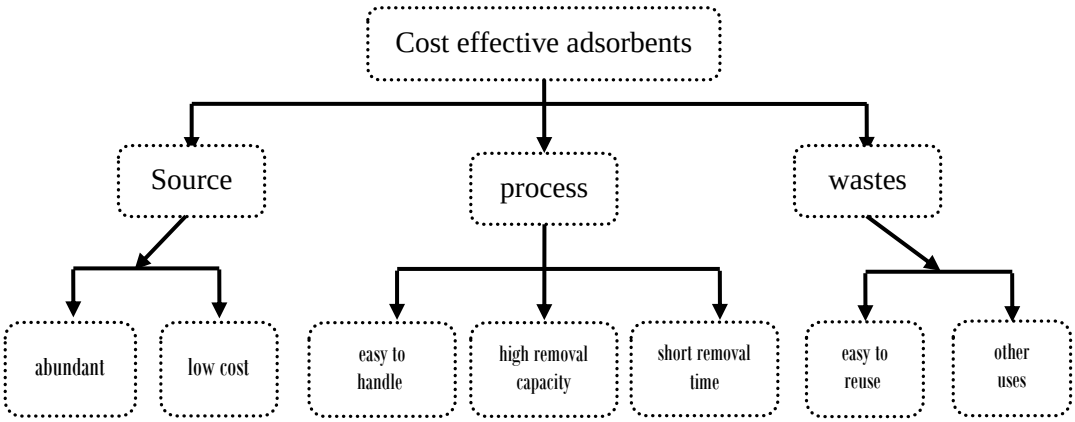

Figure 2-4: Basic features of a good low-cost adsorbent (Huang *et al.*, 2018).

agricultural peels (Anastopoulos and Kyzas, 2014), banana waste (Ahmad and Danish, 2018), oil palm (Montoya-Suarez *et al.*, 2016), neem park (Khattri and Singh, 2009), date palm (Ahmad *et al.*, 2012), rice husk (de Azevedo *et al.*, 2017), wheat bran (Adegoke and Bello, 2015), sugarcane bagasse (Yu *et al.*, 2017), carrot residues (Kyzas and Kostoglou, 2014), fruit juice residue (Yadav *et al.*, 2015), tea wastes (Yang *et al.*, 2016), Egyptian mandarin peel (Husein, 2013), garden grass (Hossain *et al.*, 2012), grapefruit peel (Zou, Zhao and Zhu, 2012), mango peel waste (Iqbal, Saeed and Kalim, 2009), groundnut shell (Malik, Ramteke and Wate, 2007) have been studied for the removal of many pollutants from water.

Adsorbents from agricultural wastes and plant materials normally rich with proteins, polysaccharides and lignin. These components provide a lot of surface functional groups responsible for adsorbate adsorbent interactions (Fosso-Kankeu and Mulaba-Bafubiandi, 2014). The main functional groups that play a significant role in determining the adsorption capacities of these adsorbents, include but not limited to: carboxyl, sulfaoxyl, hydroxyls, and amino groups (Adegoke and Bello, 2015).

Agricultural wastes are available, economic and eco-friendly. They are used either as treated or as untreated form, but the untreated materials need to be cleaned, ground to fine grains, sieved to the required size, and dried before adsorption studies (De Gisi *et al.*, 2016).

Applications of the untreated agricultural adsorbents can bring many troubles such as increasing chemical and biological oxygen demand and raising the total organic carbon due to the soluble organic components of the adsorbent, adversely causes a reduction of the dissolved oxygen content (Omo-okoro, Daso and Okonkwo, 2017). In the other hand, treatment of waste can be carried out with many common methods. The treatment of these adsorbents is significant to enhance adsorption capacities by increasing

number of active binding sites, improving ion-exchange properties and forming of new functional groups (Anjum, 2017). Adsorption capacities of agricultural adsorbents were listed in **Table 2-1.**

Table 2-1: Adsorption capacities of adsorbents from agricultural waste

Adsorbent	adsorbate	Capacity ($mg.g^{-1}$)	References
Rejected tea	MB	487.40	(M Azharul Islam *et al.*, 2015)
Tea waste	MB	402.25	(Borah, Goswami and Phukan, 2015)
Palm date seed	MB	612.1	(Md. Azharul Islam *et al.*, 2015)
Rice straw	MB	52.90	(Kim, Saif Ur Rehman and Han, 2014)
Banana peel	MB	385.12	(Liu *et al.*, 2014)
Papaya powder	CV	85.99	(Pavan *et al.*, 2014)
Wheat straw	CR	665.00	(Zhang *et al.*, 2014)
Sugarcane bagasse	CR	38.20	(Zhang *et al.*, 2011)
Peanut hull	Cu (II)	14	(Ali *et al.*, 2016)
Orange peel	Zn (II)	56	(Feng and Guo, 2012)

2.2.2. Industrial Byproducts

Industrial activities usually accompanied with the generation of several types of waste materials that are used rarely for any function, hence they are inexpensive and available in huge quantities. Following the impression of using waste to treat waste, numerous byproducts and industrial waste materials have been tested for their feasibility to remove contaminants from water and wastewater.

Examples of such materials include, but not limited to: fly ash, a waste material from combustion processes (Sun *et al.*, 2013), red mud, a waste material from aluminum industry (Sutar *et al.*, 2014), blast furnace slag, sludge and dust from the steel industry (De Gisi *et al.*, 2016), chlor-alkali waste (slurry) from the electrolysis of NaCl (Jayaraj *et al.*, 2012), lignin from black liquor waste of paper industry (Rao *et al.*, 2011), polystyrene plastic waste (Miandad *et al.*, 2018), the waste from the leather-processing industry (Xu and McKay, 2017), waste pomace of olive oil factory waste (Tripathi and Rawat Ranjan, 2015), battery industry wastes.

Active sites of concern in these materials include: amino and hydroxyl groups in chitin (Wan Ngah, Teong and Hanafiah, 2011), carboxylic acid and phenolic hydroxyl functional groups in low grade coal and SiO_2 and unburned carbon in fly ash. Adsorptive capacity of these wastes could be increased followed by slight processing. Adsorption capacities of adsorbents from industrial byproduct were listed in **Table 2-2.**

Table 2-2: Adsorption capacities of adsorbents from industrial waste

Adsorbent	adsorbate	Capacity ($mg.g^{-1}$)	References
Steel plant waste sludge	Zn(II)	7.26	(Mishra, Paul and Bandyopadhaya, 2013)
Palm oil mill sludge	MB	22.4	(Zaini *et al.*, 2013)
Metal hydroxide	CR	40	(Attallah, Ahmed and Hamed, 2013)
Print circuit board waste	As(III)	41.2	(Tu *et al.*, 2013)
Sewage sludge	chlorophenol	47.98	(Bousba and Meniai, 2013)
digested sludge	Cr(VI)	70.15	(Gorzin and Ghoreyshi, 2013)
Sewage sludge	Phenol	96.15	(Zou *et al.*, 2013)
Dried activated sludge	Cu(II)	149	(Zare *et al.*, 2015)
Concrete sludge	As(V)	175	(Sasaki *et al.*, 2014)

2.2.3. Bio-adsorbents

The term bio-adsorbents commonly used to describe any solid surface of a living or dead biomass that used in an adsorption process for removal of contaminants, but with different mechanisms (Fomina and Gadd, 2014).

In living biomass the process is called bioaccumulation, during which pollutants were removed via an active mechanism involving metabolic activities (Fosso-Kankeu and Mulaba-Bafubiandi, 2014), while dead cells adsorb contaminants through biosorption mentioned in adsorbents from agricultural wastes.

Several studies reported utilization of bacteria, fungi, algae, and yeasts as low cost adsorbents for water treatment (Toczyłowska-Mamińska, 2017). The biomass molecules involve many binding sites in both microbial cell walls and extracellular polymeric substances, the constituents of these

adsorbents are nucleic acid, carbohydrates, proteins, lipids, and phenolic compounds. The main functional groups of concern include: hydroxyl, amine, imidazole, phosphate, sulphate, and carboxyl (Li and Yu, 2014).

These adsorbents were found to be attractive and very promising referring to their high adsorption capacities, selective elimination of metals over a wide range of pH and temperature, and a negligible amount of chemical or biological sludge. However, bio adsorbents require special media and skilled workers for culturing these microbes that adds to the total cost of bio accumulation process (Fosso-Kankeu and Mulaba-Bafubiandi, 2014).

2.2.4. Natural Materials

Clays, zeolites and sediment are low-cost, abundant natural materials, and can be used as adsorbent or precursors. Of these, clay, clay minerals, and zeolites have gained special attentions due to their good adsorption capacities for removal of many pollutants from wastewater (Xu and McKay, 2017).

Zeolites are naturally occurring crystalline aluminosilicates with different cavity structures that involve a symmetrically ordered alumina and silica tetrahedral sheets linked with each other by shared oxygen atoms. Zeolites are highly hydrophilic materials because of their electrostatic charged framework, plenty of extra-framework cations, defect sites, surface nature, metal components in the framework, and the amount of coke deposits (Reeve and Fallow, 2018). Zeolites consist of more than 40 natural species, among which clinoptilolite is the most abundant and frequently studied one (Xu and McKay, 2017).

Clays and clay minerals are familiar and well known to human from the earliest days. Clays are considered as host materials for many pollutants therefore can be used as an alternative to activated carbon. **Table 2-3** shows the adsorption capacities of some natural materials that were used as adsorbents.

Table 2-3: Adsorption capacities of some natural adsorbents

Adsorbent	Adsorbate	Capacity $mg.g^{-1}$	References
Clinoptilolite zeolite	Cr(VI)	5.38	(Jorfi *et al.*, 2017)
Modified bentonite	CR	7.14	(Toor and Jin, 2012)
Acid Activated Kaolinite	CR	12.36	(Hai *et al.*, 2015)
Jordanian zeolite	Cd(II)	25.9	(Taamneh and Sharadqah, 2017)
Acid bentonite	CR	69.44	(Toor and Jin, 2012)
Montmorillonite	MB	74	(Hai *et al.*, 2015)
Zeolites from flay ash	Cd(II)	95.24	(Nicoleta Popa, 2015)
Modified clay beads	MB	101	(Auta and Hameed, 2013)
Palygorskite	MB	132.72	(Mu and Wang, 2016)
Safi raw clays	MG	156.43	(Elmoubarki *et al.*, 2015)
Acid modified clay	MB	223.19	(Auta and Hameed, 2012)

The previous survey indicates that numerous low-cost materials have been tried by number of researchers, and many of them have been sued the adsorbents to be most appropriate for pollutants removal from water or wastewater. However, many of the low cost materials face some problems, for example: the tendency of agricultural materials to burn off easily during thermal activation (Omo-okoro, Daso and Okonkwo, 2017), and some have low adsorption capacities, hence, an economical and effective treatment methods are required to improve the adsorption capacity while controlling the cost of the process at the same time.

This study will focus on simple treatments procedures of natural clay to prepare effective low-cost adsorbents for pollutants removal from aqueous media. Thus, the following parts will review the different types of clay minerals and their use as adsorbents in water treatment.

2.3. Clays and Clay Minerals

Clays and clay minerals are found at or near earth surface, they were recognized among the most important materials of the 21st century (Wang, Wang and Wang, 2013). Clays and clay minerals are abundant, low-cost and none polluting and can be used in pollution control (Vicente, Gil and

Bergaya, 2013). Clays have been identified, and used by, humans since antiquity. Currently clays are used widely in many ceramic products such as porcelain, bricks, tiles and sanitary ware as well as an important additive in plastics, paints, paper, rubber and cosmetics.

Although there is slightly different meanings across scientific disciplines, but the terms clays and clay minerals are commonly used interchangeably, "clay" is used by engineering geologists to describe geological materials less than 4μm in size, by soil scientists to denote the soil fraction containing particles less than 2 μm size, and colloidal scientists less than 1 μm (Zhou and Keeling, 2013). Clays may therefore be mixtures of fine-grained clay minerals and clay-sized crystals of other minerals such as quartz and metal oxides. In the other hand, the term clay minerals refers to phyllosilicate minerals and to minerals which impart plasticity to clay, and which harden upon drying or firing (Guggenheim and Martins, 1995; Moore, 1996; Ngulube *et al.*, 2017).

The properties of clays are origin-dependent because each clay may contain: (i) several clay minerals, (ii) non-clay minerals like quartz, calcite, (iii) organic matter in the form of discrete wood particles, leaves, etc., (iv) surface absorbed molecules, and (v) exchangeable ions that are entrapped in clays. Therefore, the physicochemical properties of clay are varied due to the differences in the components (Galán and Ferrell, 2013).

2.3.1. Structure of the Clay Minerals

Clays properties and their useful environmental and industrial applications are due to their mineralogy, structure, surface and crystal chemistry. Valuable work of several scientists such as; Ross, Hendricks, Hendricks and Fry, and Pauling, put the basis of the crystallinity in the structures of clay minerals (Uddin, 2017).

Many clay minerals are porous phyllosilicates or layered silicates. Their porosity is due to many cracks in the particle surfaces, staggered layer edges. Moreover, overlapping of layers, particles and aggregates resultant in forming interlayer, interparticle, and interaggregate pores (Bergaya and Lagaly, 2013). Clay are found as assembly of aggregates of particles, each particle is composed of a group of ordered layers as shown in **Figure 2-5**.

Each layer of clay minerals is built from one alumina octahedral sheet and one or two silica tetrahedral sheets that fit together to form a basic repeating unit of either 1:1 or 2:1 layers (Schoonheydt, 2014). The structure of a typical clay material is shown in **Figure 2-6**.

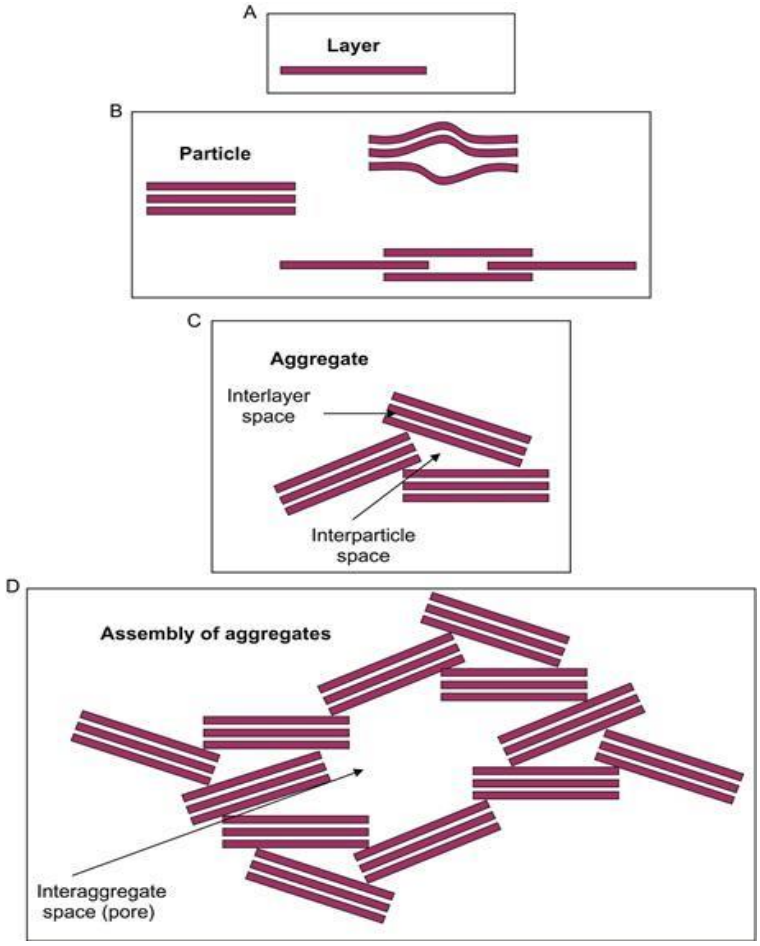

Figure 2-5: Diagram showing a clay mineral layer (A); a particle (B); an aggregate (C); and an assembly of aggregates (D) (Schoonheydt, 2014)

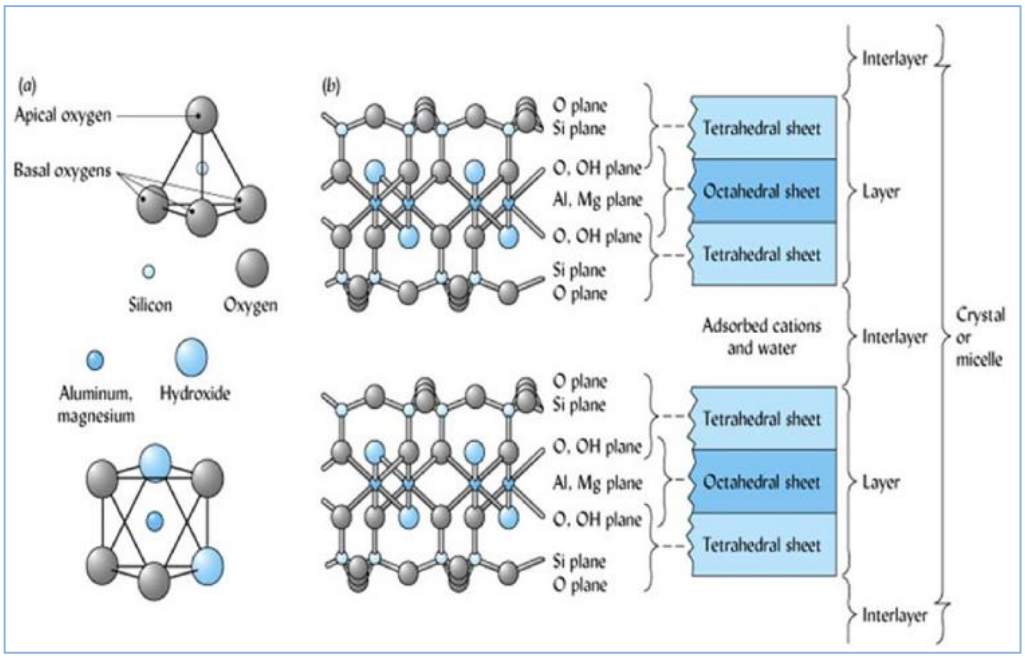

Figure 2-6: Structure of a typical clay material (Ngulube *et al.*, 2017).

2.3.2. The Active Sides in a Clay Mineral

Clay minerals normally have a complex surface chemistry due to the heterogeneity of the charged edges and faces of these layers. The basal faces carry a permanent pH-independent negative charge, while the edges hold a pH-dependent charge (Liu, Edraki and Berry, 2017).

In many clay minerals, the layers are found to have an excess negative charge, due to: (i) Substitution of Si^{4+} in tetrahedral position by trivalent (e.g., Al^{3+}) or bivalent (e.g. Mg^{2+}) cations, (ii) Substitution of Al^{3+} in octahedral positions by bivalent (e.g. Mg^{2+}) or monovalent (e.g. Li^{+}) cations, (iii) Vacancies in the octahedral positions, and (iv) as a result of dissociation of the hydrogen in various hydroxyl groups, including Si-OH and Al-OH groups, of which the dissociated propensity increases with an increase in pH. Thus, occurrence of cations in the interlayer space is essential to neutralize this negative charge. Moreover, hydration of these cations increase the interlayer distance, resultant in forming a swelling phenomenon of the clay (Brigatti, Galán and Theng, 2013; Schoonheydt, 2014; Komadel, 2016).

Schematic drawing of the active adsorbent's sites of 2:1 clay mineral is shown in **Figure 2-7**.

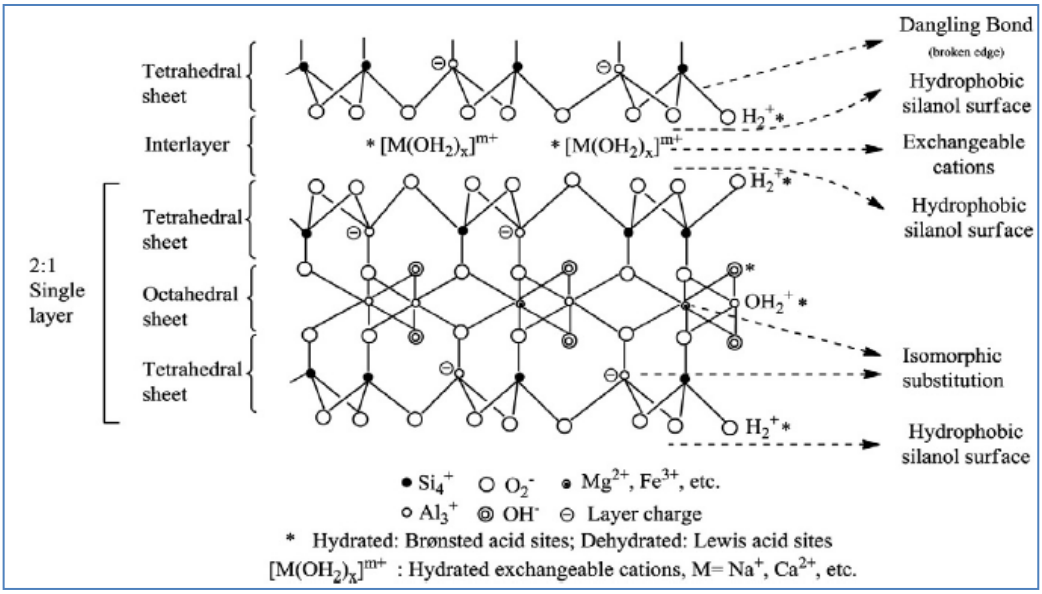

Figure 2-7: Schematic drawing of 2:1-type clay mineral showing active sites (Bergaya and Lagaly, 2013).

In the other hand, there are several types of active sites in clays such as (i) Brönsted acid or proton donor sites, created by interactions of adsorbed or interlayer water molecules; (ii) Lewis acid or electron acceptor sites occurring due to dehydroxilation; (iii) oxidizing sites, due to the presence of some cations (e.g. Fe^{3+}) in octahedral positions or due to adsorbed oxygen on surfaces; (iv) reducing sites produced due to the presence of some cations (e.g. Fe^{2+}); and (v) Surface hydroxyl groups, mostly found in the edges, bound to Si, Al or other octahedral cations (Vasconcelos *et al.*, 2013).

2.3.3. Clay Minerals Classification

The classification of clay minerals was firstly proposed by Grim (1962), and this classification becomes the basis for outlining the nomenclature and the differences between the various clay minerals (Ismadji, Soetaredjo and Ayucitra, 2015b). there are four main groups of clays: kaolinite, smectite-illite, sepiolite and chlorite. Kaolinite group includes the mineral kaolinite,

dickite, halloysite and nacrite. Smectite-illite group includes pyrophyllite, montmorillonite, talc, vermiculite, sauconite, saponite, and nontronite. The sepiolite and attapulgite group. Grimm's classification of clay minerals is shown in **Figure 2-8.**

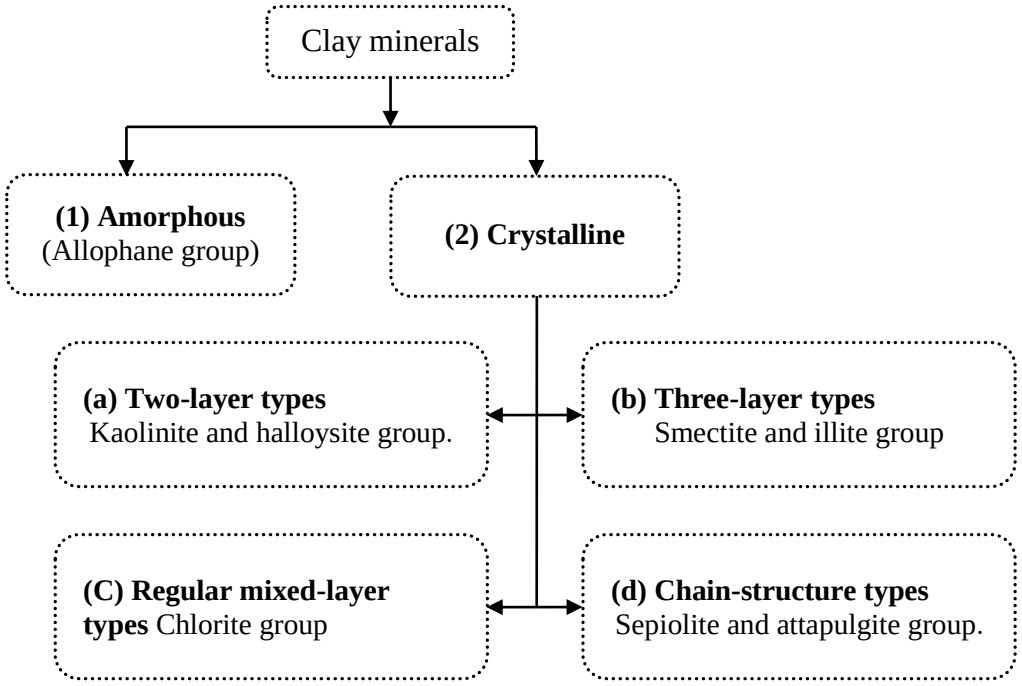

Figure 2-8: Classification of clay minerals according to Grim (Uddin, 2017).

Table 2-4: Properties of the kaolinite, illite and smectite clays (Kurniawan *et al.*, 2014)

Property	Kaolinite	Illite	Smectite
Structure type	1 : 1	2 : 1	2 : 1
Octahedral component	Dioctahedral	Mostly Dioctahedral	Di or tri-octahedral
Interlayer cation	None	K^+	Ca^{2+}, Na^+
Interlayer water	None (*except halloysite*)	None (*except hydromuscovite*)	Ca: 2 layers Na: 1 layer
Basal spacing	7.1°A	10°A	Variable; 15 °A
CEC meq/100g	3-15	10-40	70-120
Layer charge per unit cell	<0.001	1.4-2.0	0.05-1.2
Example	kaolinite	illite	Montmorillonite

Commonly, clay minerals are classified according to: (i) their magnitude of net layer charge, (ii) layer structure arrangement, and (iii) interlayer species

(Ismadji, Soetaredjo and Ayucitra, 2015e). Three types of clay minerals, kaolinite, illite and smectite, were applied widely in wastewater treatment. Summary of the properties of kaolinite, illite and smectite clay minerals is shown in **Table 2-4**.

2.3.4. Modification of Clay Minerals

Modification of clay and clay materials, chemically or physically, is essential to enhance their adsorption capacity and improve the mineralogy, adsorptive and electro kinetic properties so that they can be widely applicable.

Several modification methods have been applied such as impregnation with acids, bases or salts; pillaring with multivalent cations, organic treatment with surfactants, functionalization with grafting process (Auta and Hameed, 2012).

a) Thermal Activation Process

The general purposes of thermal activation are to remove any impurity, organic matter, and moisture attached to the clay particles. It is generally performed by heating the clay to elevated temperature, up to 1000 °C. The resulting material, called calcined or sintered clay, have a poorer amount of crystallinity, or amorphous with coarse-shaped pores, low dispersibility in aqueous solutions and generally lower sorption capacity in conjunction with a reduced specific surface area.

Thermal activation process is accompanied with two types of reactions, dehydration reaction that causes the release of hydrated and intercalated water moieties from the clay structure, and (ii) dehydroxylation reaction which require higher temperature (500 to 600 °C) to remove water from hydroxyls of clay frame. Increasing heat may cause phase transformation of the clay minerals into a meta-phase and further into a crystalline phase (Vasconcelos *et al.*, 2013).

b) Chemical Activation Process

The chemical activation process is achieved by soaking the clay or clay minerals in an acid solution, such as hydrochloric acid, sulfuric acid, nitric acid; or using salts solution such as potassium dihydrogen phosphate, potassium orthophosphate and sodium chloride, or using basic solutions such as sodium hydroxide, potassium hydroxide or calcium hydroxide.

The purpose of acid treatment is to enhance the adsorption capability of clay through the increasing of surface area, pore volume, and number of acid sites, since acid treatments influence the clay particles aggregation, remove impurities, and dissolution of the external layers.

Chemical conditioning process is a technique used to chemically altering the surface chemical nature of clays and clay minerals to expand their adsorption capacities. During this process, certain exchangeable cations in the clay layers are replaced with other cations from the solution. NaCl solution is frequently used in this process (Dammak *et al.*, 2013), to reduce the attractive interaction between the layers of the clay, permitting for better dispersion of solution into the clay layers. Thus, enhances the cation exchange ability of Na-Clay (Ismadji, Soetaredjo and Ayucitra, 2015a).

c) Pillaring Process

Pillaring process is used to expand the layer of clay minerals through three steps (i) polymerization of a multivalent cation such as iron (Tireli *et al.*, 2014), zirconium, manganese (Sari and Tuzen, 2014) (ii) intercalation of this polycation in the interlayer space of the clay, and (iii) calcination to change the polycations into stable oxide or hydroxide forms, since they retain the clay layered structure (Tireli *et al.*, 2014). Pillared clays are microporous or mesoporous with improved adsorption capacities (Ruiz-hitzky, Aranda and Belver, 2012).

d) Surfactant Modifications

Surfactant modification is a famous and preferential method to enhance clay adsorption capacity (de Paiva, Morales and Valenzuela Díaz, 2008), principally towards non-ionic organic pollutants (Ismadji, Soetaredjo and Ayucitra, 2015a), or anionic dyes. Surfactant modification is carried out by the intercalation of surfactant ions onto the clay or clay mineral structure, hence altering the hydrophilic clay or clay mineral particles into hydrophobic organo-clays and improving it is adsorption efficiency (Churchman *et al.*, 2006).

Surfactants are a large group of surface active compounds with a large number of applications such as wetting agents, emulsifying agents and detergents (Reeve and Fallow, 2018)**.** Surfactants are grouped according to their dissociation in water as: cationic, anionic, and non-ionic surfactants (Ismadji, Soetaredjo and Ayucitra, 2015a). Cationic surfactants have been widely used for clay modification, examples are listed in **Table 2-5**.

Table 2-5: Common cationic surfactants used for clay modification

Name	**Formula**
Hexadecyl trimethyl ammonium bromide	$CH_3(CH_2)_{15}N(Br)(CH_3)_3$
Octadecyl trimethyl ammonium bromide	$CH_3(CH_2)_{17}N(Br)\ (CH_3)_3$
Tetramethyl ammonium bromide	$(CH_3)_4N(Br)$
Myristyl trimethyl ammonium bromide	$CH_3(CH_2)_{13}N(Br)\ (CH_3)_3$
Dodecyl trimethyl ammonium bromide	$CH_3(CH_2)_{11}N(CH_3)_3Br$
Hexadecyl trimethyl ammonium chloride	$CH_3(CH_2)_{15}N(Cl)(CH_3)_3$
Dioctadecyl dimethyl ammonium bromide	$[CH_3(CH_2)_{17}]_2N(Br)\ (CH_3)_2$
Didodecyl dimethyl ammonium bromide	$[CH_3(CH_2)_{11}]_2N(CH_3)_2(Br)$

During the modification, the surfactant replaces the cations of clay interlayer and then bonding of its hydrophobic moiety in the clay layers. Moreover, the negative surface charge of Na-clay may be altered to positive charge. The resultant organo-clay properties such as: particle size, hydrophobicity, interlayer spacing, and thermal properties, are strongly affected with the

length of the alkyl chain and the concentration of the surfactant, and the type of the surfactant (Sun *et al.*, 2017).

e) Grafting Process

Chemical grafting of functional polymers can provide the ability to control and modify the properties of clay mineral surfaces. Grafting forms a stable chemical bond between the reactive silanol groups and silane-coupling agents which may be positioned at the loose edges of the clay mineral layers and at the defects of the interlayer and external surfaces (Thue *et al.*, 2018). Once clays were grafted with organosilane, their hydrophilic surface becomes organophillic and can be easily dispersed in low-polarity compounds including polymers (Kurniawan *et al.*, 2014).

Silane coupling agents are a family of organosilicon monomers with the general structure of $R–SiX_3$ where: R refer to the organo-functional group and X refer to methoxy or ethoxy groups that were attached to silicon atom, an example of such agents is [3-(2-aminoethyl amino) propyl] trimethoxy silane (Kurniawan *et al.*, 2014).

In this research, two simplest modifications process were selected (i) conditioning with sodium chloride solution, and (ii) intercalation with cationic surfactant, to prepare low-cost adsorbents for the removal of selected contaminants from synthetic water.

2.4. Applications of clay as adsorbents

Due to their variety of structural and surface properties, high chemical stability, large specific surface area and high adsorption capacity, many clay and clay minerals have been investigated and used for the removal of various contaminants. In the following part, the removal of: arsenite, methylene blue, crystal violet, Congo red, phenol and nitrate, with modified or raw clay is reviewed.

2.4.1. Removal of Arsenite

Arsenic is used in pigment industries, rat poisons, insecticides and pesticides, wood preservatives, bronzing and glass. In addition, arsenic paste was used to treat skin and breast cancer, while arsenic trioxide is used as a chemotherapeutic drug for treatment of leukemia (Bhowmick *et al.*, 2018). The common symptoms of chronic arsenic poisoning were first reported in West Bengal. Symptoms include gastrointestinal dysfunction, respiratory disease, liver and cardiovascular disease, neurotoxicity, diabetes mellitus, adverse hematological outcomes, negative pregnancy outcomes and infant mortality (Bentahar *et al.*, 2016), thus WHO has lowered the provisional guideline for arsenic in water to 10 $\mu g.L^{-1}$ (Antoine, Fung and Grant, 2017).

Arsenic in its inorganic forms, As(III) or As(V), were the most found in water supplies than its organic forms (Bentahar *et al.*, 2016). As(III) is more dangerous and more difficult to be removed from drinking water than pentavalent arsenate As(V) (Fowler *et al.*, 2015). Applications of natural clays or modified clays as adsorbents for the removal of arsenic ions, As(III) and As(V), from water have been studied extensively, however, the literature review showed that removal of the As(V) from water was more studied than As(III) (Lim, Shukor and Wasoh, 2014).

In 1988, natural China clay with specific surface area of 13.5 $m^2.g^{-1}$ was used to remove As(III) from aqueous solutions, the maximum removal capacity was found to be 0.023 $mg.g^{-1}$ at pH of 8 after 3 hours of contact time (Yadava, Tyagi and Singh, 1988). Sepiolite which is a non-swelling, lightweight and porous mineral with specific surface area of 300 $m^2.g^{-1}$ was used for the removal of As(III) from groundwater, the results of this study showed that when the adsorbent was coated with iron oxide, its maximum adsorption capacity had reached 0.309 $mg.g^{-1}$ (Öztel, Akbal and Altaş, 2015). When the natural laterite which is rich with iron (45% w/w) and its specific

surface area 18.05 $m^2.g^{-1}$ was used for the removal of As(III), the capacity q_e reached 0.42 $mg.g^{-1}$ (Maiti, DasGupta, *et al.*, 2007).

Ti-pillared montmorillonite (S_{BET} 164.6 $m^2.g^{-1}$ and average pore diameter 1.76-2.76 nm) had a maximum adsorption capacity of 16 $mg.g^{-1}$, when tested to remove As(III) from drinking water at optimum pH in the range between 4-10 (Na *et al.*, 2010). Adsorption of As(III) on natural siderate (iron(II) carbonate $FeCO_3$), achieved equilibrium after 24 hours with maximum adsorption capacity of 9.43 $mg.g^{-1}$ (Zhao, Guo and Zhou, 2014). Natural laterite (rock type rich in iron and aluminum) was used for the removal of As(III), the maximum efficiency reached about 98% when the initial concentration of As(III) was 1 $mg.L^{-1}$ and solid to liquid ratio of 4/100 (Maiti, DasGupta, *et al.*, 2007). When the clay contains about 10% iron (Vermiculite) the maximum adsorption capacity of As(III), (at pH 5 and 293 K), had reached 72.2 $mg.g^{-1}$ after 30 min of contact time (Saleh, Sar and Tuzen, 2016).

In other study, the maximum adsorption capacity of As(III) from water reached 75 $mg.g^{-1}$ when a natural clay, composed of 80% smectite and 20% illite, was used at 298 K and pH range between 3-9. The specific surface area of the clay was 158 $m^2.g^{-1}$, and 43% of porosity (Eloussaief *et al.*, 2014). The acid activated montmorillonite (swelling clay mineral type 2:1) with specific surface area of 140 $m^2.g^{-1}$ has a maximum adsorption capacity equal to 159.43 $mg.g^{-1}$ for As(III) at pH 5. However naturally montmorillonite having specific surface area of 32 $m^2.g^{-1}$ has a maximum adsorption capacity for As(III) equal to 10.34 $mg.g^{-1}$ (Zehhaf *et al.*, 2013). A synthesized and calcined 2:1 clay type was found to has a higher maximum adsorption capacity of 295 $mg.g^{-1}$ for As(III) removal from aqueous solutions (Ghorbanzadeh *et al.*, 2015), but the adsorption was slow, it took 20 hours to reach the equilibrium state.

The differences in the maximum adsorption capacities of natural clays could be attributed to the following parameters: iron content, specific surface area and average pore diameter (Ghorbanzadeh *et al.*, 2015). In addition, the competing ions strongly affected adsorption of arsenite onto clay.

2.4.2. Removal of Cationic Dyes

The cationic dyes are a class of dyes that are commonly used for many purposes due to their advantages such as ease of application, robustness, and good fastness to materials (Huang *et al.*, 2016). Methylene blue (MB), a kind of phenothiazine salt, **Figure 2-9a**, and crystal violet (CV), **Figure 2-9b**, are commonly selected as models for cationic dyes during exploring the removal of dyes from aqueous solutions. MB and CV dyes have wide application in textile industry, for cotton, silk, wool, wood and carbon nanomaterials. Furthermore, CV is used in biological staining and as a dermatological agent, and in veterinary medicine.

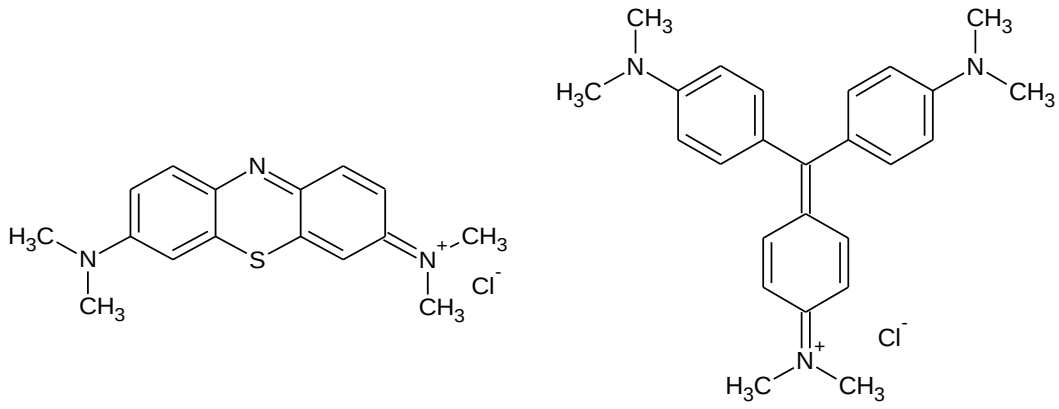

(a) (b)

Figure 2-9: The chemical structure of (a) MB dye, (b) CV dye

MB when contact with skin may cause discoloration, feeling of cold, redness or dryness (due to chronic exposure). Ingestion of this dye may cause gastrointestinal irritation, discoloration of oral mucosa, irritation of lips, mouth, and throat, paleness of complexion, lack of coordination or drowsiness (Anirudhan and Ramachandran, 2015), and can cause some

problems to the human health, such as: allergy, dermatitis, skin irritation, mutation, and cancer (Dotto *et al.*, 2016).

CV affects human health; high level ingestion causes nausea, vomiting and central nervous system depression (Anirudhan and Ramachandran, 2015). Further, it can cause eye burn and irritation to skin besides being hazardous to aquatic organisms (Khan, Khan and Shahjahan, 2015). In addition, it is linked with human bladder cancer and cancer in the digestive system of other animals (Miyah, Lahrichi and Idrissi, 2016).

For treatment of water contaminated with MB and CV, numerous low-cost adsorbents have been investigated. Among these adsorbents, clay and clay minerals have received great attention over last decade, encouraged by the availability of numerous modification methods to enhance the adsorption capacity of clay and clay minerals.

The determination of thermodynamic data: $\Delta G°$, $\Delta H°$ and $\Delta S°$, with a good accuracy is useful for the design of the adsorption unit, and for the successful implementation of adsorption technology. Thermodynamic data reported in previous studies for the adsorption of both cationic dyes, MB and CV, onto natural clay minerals were summarized in **Table 2-6**.

It's known that enthalpies of adsorption may be obtained from adsorption experiments at different temperatures or may be measured directly by using microcalorimetric technique. In case of MB-clay mineral aqueous solution and CV-clay mineral aqueous solution systems, thermodynamic data evaluated according to these two methods, are varied and sometimes contradictory regarding the nature of the adsorption phenomenon of the dye onto the clay mineral surface.

Generally, adsorption process is a less energy intensive unit operation and it is well known that the change in the free energy $|\Delta G|$ ranged between 0 – 20

$kJ.mol^{-1}$ for physical process and $|\Delta G|$ is ≥ 20 $kJ.mol^{-1}$ for chemical reactions (Gopinathan, Bhowal and Garlapati, 2017). In addition, earlier studies concluded that the enthalpy of the interaction clay-dye is endothermic process while the interaction dye-dye is an exothermic process at the adsorbent surface (Rytwo and Ruiz-Hitzky, 2003).

Numerous factors can affect the enthalpy of adsorption of cationic dyes onto natural clay minerals such as temperature, the structure of the adsorbent, the extent of hydration and their negatively charged layers. Its observed that the tested clay minerals uptake the cationic dyes with a maximum adsorption capacity in the range 10 to 370 $mg.g^{-1}$, moreover when raising the temperature, swelling effect is produced which facilitate the diffusion of dye into internal structure of the clay mineral. On the other side, an athermal process is reported for the adsorption of MB onto natural clay mineral (Hajjaji and Alami, 2009) or less influenced by raising the temperature (Elmoubarki *et al.*, 2015).

Table 2-6: Thermodynamic parameters for MB and CV adsorption onto different clay minerals

Clay mineral used	Nature	ΔG° kJ/mol	ΔH° kJ/mol	ΔS° J/mol.K	T range °C	References
MB						
Montmorillonite	Endo		+3.9		Cal.*	(Rytwo and Ruiz-Hitzky, 2003)
Kaolinite	Endo	-0.27 to -1.72	+14.11	+48.13	25-55	(Gopinathan, Bhowal and Garlapati, 2017)
Montmorillonite	Endo	-6.7 to -19.0	+145	+492	35-60	(Almeida *et al.*, 2009)
Bentonite	Endo	-17.0 to -19.4	+9.21	+92.2	10-35	(Hong *et al.*, 2009)
Smectite	No effect				15-35	(Hajjaji and Alami, 2009)
Sepiolite	Endo	--	+56.28	--	30-60	(Özdemir, Doğan and Alkan, 2006)
Illite associated with chlorite	Exo	+0.318 to 1.42	-7.5	-27.4	10-50	(Elmoubarki *et al.*, 2015)
Illite-kaolinite	Exo	-2.3 to -0.75	-13.6	-40.3	10-50	(Elmoubarki *et al.*, 2015)
Montmorillonite-nontronite	Exo		-7.99		20-40	(Gürses *et al.*, 2006)
Montmorillonite-nontronite	Endo		isosteric		40-60	(Gürses *et al.*, 2006)
CV						
Montmorillonite	Exo		-13.5		Cal. *	(Rytwo and Ruiz-Hitzky, 2003)
Kaolinite	Exo	-4.11 to -4.48	-0.235	+13.14	22-50	(Nandi *et al.*, 2008)
Pyrophyllite $Al_2(Si_4O_{10})(OH)_2$	Endo	-10.1 to -12.2	+9.28	+66.37	20-50	(Khan, Khan and Shahjahan, 2015)
Bentonite	Exo	-4.41 to -0.64	-83.81	-260.0	22-36	(Eren and Afsin, 2008)
Montmorillonite	Exo	-3.63 to -2.06	-18.97	-52.38	20-50	(Kumar, Sen and Bhattacharyya, 2016)
Sepiolite	Exo	-1.3 to -0.46	-18.79	-60.0	22-36	(Eren and Afsin, 2007)
Mixed (kaolinite-phyrophyllite)	Exo	-19.5 to -18.0	-25.59	-9.77	30-50	(Monash and Pugazhenthi, 2009)

*Cal. by direct calorimetric measurements

2.4.3. Removal of the Anionic Dye Congo Red

CR is typical example for anionic azo dyes, **Figure 2-10** shows it is chemical structure. Most of azo dyes are harmful to humans since they contain toxic aromatic or heterocyclic moieties in their molecular structures (Taamneh and Sharadqah, 2017). CR dye can be metabolized to benzidine, a known human carcinogen. Yet, the treatment of CR polluted wastewater can be complicated due to its complex aromatic structure, providing the dye physicochemical, thermal and optical stability, and resistance to biodegradation and photo degradation (Vimonses, Lei, Jin, Chris W.K. Chow, *et al.*, 2009).

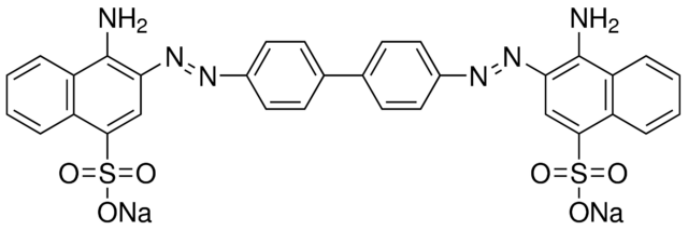

Figure 2-10: The chemical structure of CR dye

Usually, natural clays have low adsorption capacity towards anionic dyes, this can be attributed to the electrostatic repulsion between the negatively charged clay's surface and the anionic dyes molecules (Chen and Zhao, 2009**).** For example, the maximum amount of CR adsorbed at room temperature onto three Australian kaolins, varies between 5.58 and 6.89 $mg.g^{-1}$ (Vimonses, Lei, Jin, C. W K Chow, *et al.*, 2009), and the maximum adsorbed amount of CR onto the purified montmorillonite is 10.2 $mg.g^{-1}$. Hence, the clay surface must be modified to enhance their adsorption capacity. Many methods have been used to modify the clay surface such as calcination (Vimonses, Jin and Chow, 2010), acid treatment (Komadel, 2016) or functionalization with quaternary ammonium salts (organoclays) (Zhu, Wang and Xu, 2017; Kausar *et al.*, 2018).

Surface properties of leonardite, shale clay rich in humic and fulvic acids, change by carbonization at 900 °C causing an increase in the adsorption

capacity of this mineral to CR (Ausavasukhi, Kampoosaen and Kengnok, 2016). Acid treatment of Kaolinite and montmorillonite enhances their adsorption capacity of CR. The maximum absorption of this dye increases by 50% for kaolinite and by 15% for montmorillonite after acid treatment (Bhattacharyya, Gupta and Sarma, 2015).

Furthermore, organo-attapulgite showed high adsorption capacity (189.39 $mg.g^{-1}$) for CR removal from aqueous solution at room temperature (Chen and Zhao, 2009). Surfactant-modified montmorillonite displayed higher adsorption capacity (127 $mg.g^{-1}$) for CR than raw montmorillonite (Wang and Wang, 2008). The adsorption capacities of two organo-hectorites for CR are in the range between 180 and 200 $mg.g^{-1}$ at different temperatures, whereas the dye removal percentage never exceeds 10% for parent hectorite clay (Xia *et al.*, 2011). The effectiveness of organo-vermiculite to uptake CR dye from aqueous solution at 298 K is 73 times higher than that of parent vermiculate (Yu *et al.*, 2010). Similar results were also obtained for removal of CR from aqueous solution using organo-rectorite (Liu, Wang and Wang, 2010).

A summary of selected adsorption studies using surfactant modified clay for CR removal were presented in **Table 2-7**.

This summary revealed that organo-clays showed higher efficiencies for CR removal from aqueous solution than raw clays. The dye uptake process usually obeyed the pseudo-second-order kinetic expression and was best described by the Langmuir isotherm model. Moreover, thermodynamic studies showed that CR adsorption on organo-clay was endothermic and spontaneous in nature. But few studies were focused on using natural clay minerals mixture to remove anionic dyes from wastewater.

Table 2-7: Organoclays used for Congo red adsorption from aqueous solution

Organoclay	q_{max} (mg/g)	Isotherm study	Kinetic study	References
Cetyl trimethyl ammonium bromide-modified Bentonite	210	Langmuir	PSO	(Youssef AM and Al-Awadhi MM, 2013)
Cetyl trimethyl ammonium bromide-modified Kaolin	24.46	Langmuir	PSO	(Zenasni *et al.*, 2014)
Cetyl trimethyl ammonium bromide-modified Montmorillonite	351.00	Langmuir	PSO	(Liu, Wang and Wang, 2010)
Cetyl trimethyl ammonium bromide-modified Rectorite	153.85	Langmuir	PSO	(Liu, Wang and Wang, 2010)
Hexadecyl trimethyl ammonium bromide–modified Attapulgite	189.39	Langmuir	PSO	(Chen and Zhao, 2009)
Hexadecyl trimethyl ammonium bromide–modified Bentonite	16.04	Langmuir	PSO	(Fosso-Kankeu, Waanders and Fourie, 2016)
Hexadecyl trimethyl ammonium bromide–modified Vermiculite	192.31	Langmuir	PSO	(Fosso-Kankeu, Waanders and Fourie, 2016)
Dodecyl trimethyl ammonium bromide–modified Montmorillonite	83.60	----	-------	(Wang and Wang, 2008)
1,3-bis(dodecyl dimethyl ammonio)-2-hydroxypropane dichloride–modified Montmorillonite	192.57	Langmuir	PSO	(Gu *et al.*, 2014)

2.4.4. Removal of Phenol

Adsorption of organic compounds by clay or clay minerals has been broadly studied in recent years (Bazrafshan *et al.*, 2016). But its observed that raw clay minerals have low adsorption capacities towards hydrophobic organic compounds, because of the negative charges and hydrophilic appearances of its surface. To shift the surface characteristics of the clay minerals to hydrophobic, and to improve sorption capability to organics, clay minerals commonly modified with organic compounds, mostly cationic surfactants, to produce organoclay (Hamdaoui *et al.*, 2018). Organoclays are considered as an alternative material for activated carbon, moreover they are low-cost and have fast sorbent efficiency. For example, montmorillonite and hectorite were modified with thiamine (vitamin B) and supposed to be applied for phenol removal from drinking water (Ben Moshe and Rytwo, 2018).

In **Table 2-8**, previous literatures for the adsorption capacities of phenol from water using varied organoclays, were reported. Its observed that the adsorption capacity of the organoclays greatly depended on the types and dosages of the surfactants. In addition, increased phenol uptake can be achieved by decreasing the initial phenol concentration, and decreasing of contact time (Issabayeva *et al.*, 2017). More significant, it was assumed that the π-π polar interaction between the aromatic ring in phenols was the main adsorption driving force (Park, Godwin A Ayoko, *et al.*, 2013).

Table 2-8: Raw or organ-clays used for phenol adsorption from aqueous solutions

Raw or modified clay mineral	q_{max} ($mg.g^{-1}$)	Equilibrium conditions Dose ($g.L^{-1}$), pH, time(min)	References
Hexadecyl trimethyl ammonium modified bentonite	---	5, 6.5, 30	(Mirmohamadsadeghi *et al.*, 2012)
Kaolinite	1.71	8, 7.5, 40	(Numbonui Ghogomu *et al.*, 2015)
Metakaolinite	5.82	8, 7.5, 40	(Numbonui Ghogomu *et al.*, 2015)
Hexadecyl trimethyl ammonium chloride modified smectite	8.28	20, 9, 60	(Carvalho *et al.*, 2012)
Hexadecyl trimethyl ammonium bromide modified montmorillonite	9.90	5, 5, 24 H	(Ma *et al.*, 2016)
Pyrophyllite raw	11.49	2, 6.5, 25	(El Gaidoumi *et al.*, 2015)
Pyrophyllite HCl activated	13.7	2, 6.5, 25	(El Gaidoumi *et al.*, 2015)
Hexadecyl dimethyl (3-sulphonatopropyl) ammonium modified montmorillonite	13.76	5, 5, 24 H	(Ma *et al.*, 2016)
hexadecyl- trimethyl ammonium bromide modified bentonite	13.97	10, 6, 48 H	(Ma *et al.*, 2016)
aromatic-containing gemini surfactant modified montmorillonite	14.3	1, 10, 60	(Yang *et al.*, 2015)
Algerian montmorillonite	18.86	1, 5, 5.5 H	(Djebbar *et al.*, 2012)
Hexadecyl trimethyl ammonium bromide modified Rhassoul	25	4, --, 4 H	(Hamdaoui *et al.*, 2018)
Benzyl hexadecyl dimethyl ammonium modified bentonite	28.57	10, 6, 48 H	(Díaz-Nava, Olguín and Solache-Ríos, 2012)

2.4.5. Removal of Nitrate

Surfactant modified clays were studied widely for removal of anionic contaminants from water. Hexadecyl pyridinium chloride modified montmorillonite was used for nitrate removal. Results showed that the nitrate uptakes by this organoclay could be described well using the Langmuir isotherm while their uptake kinetics fitted well to the pseudo-second order model (Bagherifam *et al.*, 2014). However (Loganathan, Vigneswaran and Kandasamy, 2013), after reviewing the removal of nitrate from water using surface modification of adsorbents, they concluded that aluminosilicates' ability to adsorb nitrate is negligible. Even after surface modification with surfactant to provide positive surface charges, modified clay didn't show noticeable nitrate adsorption capacity. Moreover, the adsorption capacity for nitrate were found to be decreased in the presence of other anions (Loganathan, Vigneswaran and Kandasamy, 2013).

The results of the investigations of local materials as low-cost adsorbents in devolving countries, as seen in the previous survey, vary in general. The variations in the results can be attributed to the diverse processes used during searching for the appropriate materials. Moreover, the pervious review so far realize that each material has its characteristic physical and chemical properties such as porosity, surface area and physical strength, as well as inherent advantages and disadvantages.

In spite the number of published researches still there is an increasing demand for searching cheap and more feasible low-cost adsorbents to treat the massive quantum of pollutants in the water and wastewater, hence the purpose of this study.

CHAPTER THREE

3. MATERIALS AND METHODS

3.1. Materials

3.1.1. Clay Samples

Raw Morocco clay samples were obtained from Almarwani for Spices Company, Saudi Arabia, and raw Sudanese clay samples were collected from White Nile beach, Jebal Aulia area, Khartoum, Sudan. **Figure 3-1** shows the approximate location where raw Nile clay samples were collected.

Figure 3-1: Approximate location where raw Nile Clay were collected

3.1.2. Chemicals

All standard chemicals used in the present work are of analytical grade except otherwise stated. All chemicals were used without further purification.

NaCl and $CH_3COONa.3H_2O$ were obtained from S D Fine-cheme. Ltd, Mumbai, India. NaOH and H_2O_2 were obtained from Panreac, Spain. Glacial acetic acid, HCl (37%) and HNO_3 (70%), didecyl dimethyl ammonium

bromide surfactant, (Mol. wt. 406.5 g.mol^{-1}), were obtained from Sigma-Aldrich, USA.

Adsorbates that were studied include: methylene blue (C.I.52015, chemical formula $C_{16}H_{18}ClN_3S$, Mol. wt. 319.9 g.mol^{-1}, λ_{max} 664 nm), crystal violet (C.I.42555, chemical formula $C_{25}H_{30}N_3Cl$, Mol. wt. 408.0 g.mol^{-1}, λ_{max} 590 nm), Congo red (C.I.22120, chemical formula $C_{32}H_{22}N_6Na_2O_6S_2$, Mol. wt. 696.7 g.mol^{-1}, λ_{max} 498 nm), and, C_6H_5OH, (Mot. wt. 94.1 g.mol^{-1}, λ_{max} 270 nm) were obtained from S D Fine-cheme. Ltd, Mumbai, India. $NaAsO_2$, (Mot. wt. 129.9 g.mol^{-1}), and $NaNO_3$, (Mol. wt. 84.99 g.mol^{-1}) were obtained from Panreac, Spain.

3.1.3. Adsorbates

All adsorbates stock solutions of higher concentrations were prepared using double distilled and deionized water, then the required adsorbate concentrations were prepared by appropriate dilution with double distilled water and deionized water.

3.2. Methods

3.2.1. Adsorbents Pretreatment

The raw clay samples were suspended in distilled water with continuous stirring to remove soluble salts and impurities, after settlement, suspended materials were collected using a wet sieving technique. Then, the solid materials were dried at 60 °C for 24 hours, crushed with a mortar and pestle, sieved and the particles larger than 2 μm were removed. The fine particle clays were treated with hydrogen peroxide to oxidize organic matter (Środoń, 2013). Finally, the obtained materials were dried, crushed, grounded and sieved to fine textures, which were labelled as: “raw Nile and raw Morocco clays”.

3.2.2. Preparation of Na-Clays

The raw natural clay samples were converted into their sodium forms by ion exchange process with NaCl solution (Anirudhan and Ramachandran, 2015). 25 g of each of the raw clay samples were suspended in 500 mL 1M NaCl solution, and agitated, at room temperature, for 12 hours using mechanical stirrer, Heidolph instruments type RZR 1, Germany. Morocco suspended clay was separated by centrifugation for 10 min at 5000 rpm using EBA 20 centrifuge Hettich Type, Germany. Where, Nile suspended clay was separated by pump filtration using Whatman No. (1) filter paper. Then, a new NaCl solution is used for another 12 hours. The process was repeated 5 times. Excess chloride ions were washed out repeatedly with deionized water till no chloride ions were detected in the supernatant as tested by a simple $AgNO_3$ test. The obtained Na-clays were dried in an oven for 72 hours at 60 ^oC, grounded using a pestle and mortar, and sieved to obtain fine textures which were labeled as Na-MO and Na-NI clay. The procedure was shown schematically in **Figure 3-2.**

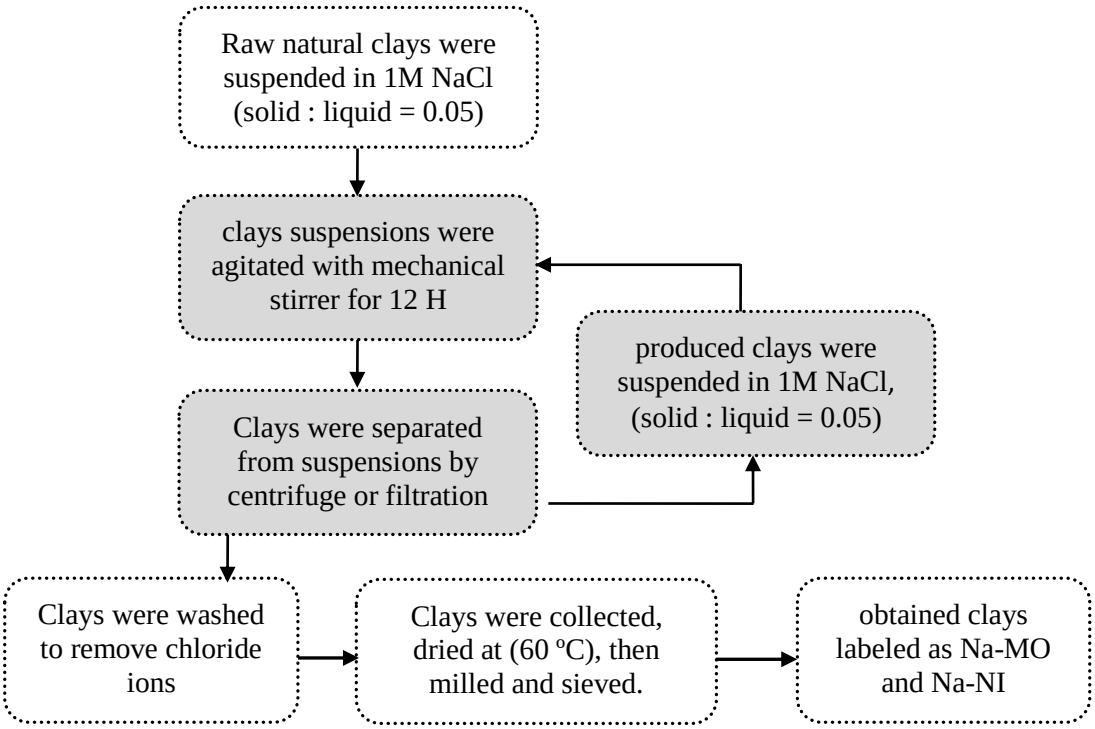

Figure 3-2: Procedure for the preparation process of Na-clays

3.2.3. Preparation of the Organo-Clays

Each of Na-MO and Na-NI clays were changed into their corresponding organo-clay form by treating with the cationic surfactant didecyl dimethyl ammonium bromide, (see **Figure 3-3**), according to Park method (Park, Godwin A. Ayoko, *et al.*, 2013).

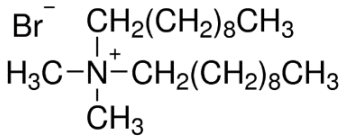

Figure 3-3: The structure of didecyl dimethyl ammonium bromide

Ten grams of each Na-MO and Na-NI clay were suspended in 400 ml of double distilled water and stirred for an hour at 70 °C in a water bath. 1 g of the surfactant was dissolved in 100 mL deionized water. The surfactant solution was added dropwise, using a dropping funnel, to the suspension while stirring using a magnetic stirrer at 70 °C. The resulting suspensions were mixed further for 12 hours. Then the suspended solid was filtered under vacuum, using Whatman No. (1) filter paper, washed several times with deionized water till no bromide ions were detected in the filtrate when tested with $AgNO_3$ solution. The obtained materials were dried at 70 °C for 72 hours, grounded using a pestle and mortar, sieved and labeled as Surf-MO and Surf-NI clays (Park, Godwin A. Ayoko, *et al.*, 2013; Sun *et al.*, 2017).

3.2.4. Adsorbents Characterization

The four prepared adsorbents; Na-NI, Na-MO, Surf-NI, and Surf-MO, were characterized with the following techniques as summarized in **Figure 3-4**.

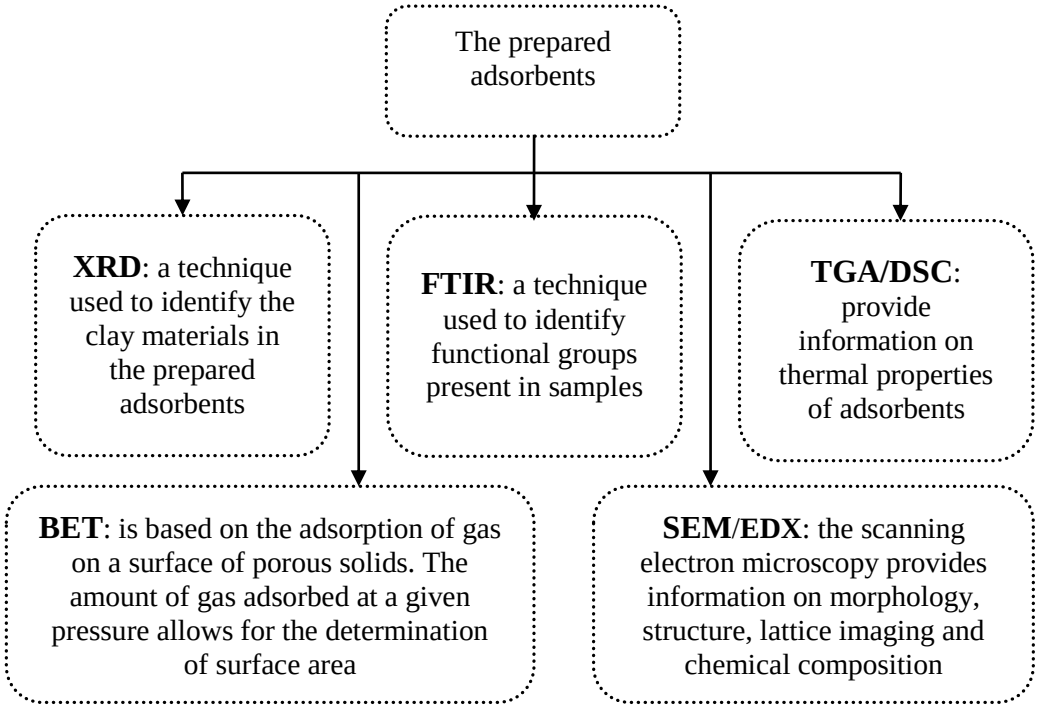

Figure 3-4: Characterization methods for the adsorbents

a) Specific Surface Area Measurements

The specific surface areas and pore size distribution of the adsorbents were estimated by nitrogen adsorption–desorption method at 77 K with the application of the Brunauer–Emmet–Teller (BET) equation on a Micromeritics ASAP2000 apparatus. The samples were degassed at 373 K prior to BET measurements for 1 hour.

b) X-Ray Diffraction Analysis

To identify the clay minerals, present in the 4 modified clay samples, XRD measurements were carried out by a powder X-ray diffractometer (Phillips Xpert-pro) between 10° and 80° 2θ using Cu K_α (λ=1.5406 Å) radiation at 40 kV. 20 mA and Ni filter. The identification of clay minerals was done by using standard techniques. Reflections data treatment were performed using the XPert highScore Plus software, version 2.0.

c) Fourier Transform Infrared Analysis

Fourier transform infrared spectra in the region 4000-400 cm^{-1} were used to study the 4 prepared adsorbents using Thermo Scientific spectrometer with

deuterated triglycine sulfate (DTGS) detector and a KBr splitter. The KBr pressed disc technique (1 mg of adsorbent sample and 200 mg of KBr) was used. Spectra manipulations were performed using the OMNIC software version 8.3.103 (Thermo Instruments Corp.).

d) Transmission and Scanning Electron Microscopy

The surface morphology of the adsorbents was examined using scanning electron microscopy type JEOL JED2200 series coupled with an energy dispersive X-ray detector (SEM-EDX), before and after modification. The corresponding SEM micrographs were obtained at an accelerating voltage of 15 kV (Hitachi SE 900) at several magnifications. The morphological observations were done using a Hitachi scanning electron microscope (model S-2400).

Transmission electron microscope image analysis of the adsorbent without and with a surfactant are examined on a TEM (JEOL JEM 1400 series) at 120 kV.

e) Thermal Analysis

Thermogravimetric analysis (TGA/DTG) was done with a SETRAM type 124 TG/DTA instrument using aluminium as inert reference material. The temperature was increased from room temperature to 900 °C at the regular increment of 10 °C.min^{-1} in the air atmosphere. Moreover, raw samples and the prepared adsorbents were studied before and after modification using differential scanning calorimetric under air atmosphere using DSC-60-Shimadzu. The heating rate was 2 deg.min^{-1}.

f) Loss on Ignition Experiments

Loss on Ignition test for each clay sample was determined by heating about 1 g of the clay sample at 1000 °C for 2 hours in a Nabertherm LE060K1BN, compact muffle furnace, single-phase, 1100 °C maximum temperature,

Germany. The loss on ignition was calculated in percentage from the loss in weight on ignition (Struijk, Rocha and Detellier, 2017).

g) The Point of Zero Charge Measurements

The pH point of zero charge (pH_{pzc}) of the four adsorbents was determined by solid addition method (Rao and Kashifuddin, 2016). Double distilled water was boiled for 20 min to remove the dissolved CO_2. This water was used to prepare 0.01M NaCl solution, then this solution was divided into 7 capped reagents bottles and the initial pH of each bottle is adjusted to the required pH level (4, 5, 6, 7, 8, 9 and10) by adding 0.1 M HNO_3 or 0.1 M NaOH solutions. 25 mL of sodium chloride solution from each bottle was transferred into a corresponding 50 mL conical flask, and the initial pH (pH_i) was recorded accurately. Then, 0.0250 g of the adsorbent were added to each flask and the flasks were agitated at 30˚C, using shaker incubator model LSI-100B from KWF Sci-Tech & development Co. China, after 24 hours the final pH (pH_f) of the supernatant liquid was recorded. Then (ΔpH) the difference, between the initial pH (pH_i) and final pH (pH_f) values were plotted against pH_i, the point of intersection of the resulting curve with abscissa, at which $\Delta pH = 0$, gave the pH_{pzc} (Bentahar *et al.*, 2015; Pawar *et al.*, 2016).

3.2.5. Adsorption Studies

The four prepared adsorbents, Na-NI, Na-MO, Surf-NI, and Surf-MO, were studied to explore their adsorption efficiency for the removal of six selected pollutants from synthetic aqueous solutions, using batch method. Na-MO clay was used for the removal of MB dye, CV dye, and As(III). Whereas, Surf-NI and Surf-MO clay were used for the removal of CR dye, nitrate, and phenol.

Batch experiments were carried out to investigate the effect of: (i) initial pH of the adsorbate solution, (ii) contact time, (iii) the dose of adsorbent, (iv)

the initial adsorbate concentration, and (v) the temperature; on the adsorption capacity of the prepared adsorbents.

a) pH Effect

The effect of the initial pH of the adsorbate solution on the amount adsorbed was studied over a range of pH from 2 to 11. In these experiments, 25 mL of adsorbate solutions with recognized initial concentration were transferred into sets of 100 mL Erlenmeyer flasks. Then, the pH of the solutions was adjusted to the required value by adding drops of 1M NaOH or 1M HCl or HNO_3, and the pH of the adsorbate solutions was measured using pH-Meter model: JENWAY 3510 UK. Then after, pre-weighed samples of the adsorbent were added to the flasks, capped with para film. The capped flasks were shaken in a shaker incubator model LSI-100B from KWF Sci-Tech and development Co. China, at a fixed temperature for 3 hours. Then, the flasks were removed from the shaker and the suspensions were centrifuged at 4000 rpm for 10 min., using a Hettich EBA 20 centrifuge, Germany. The remained adsorbates concentrations in the supernatant were determined.

b) Dosages Effect

The dosages effect investigations were carried out in a batch process using different quantities of the adsorbent. For each experiment, 25 mL of adsorbate solutions with recognized initial concentration and the pre-determined pH, were transferred into sets of 100 mL Erlenmeyer flasks. Then, different pre-weighed samples of the adsorbent were added to the flasks, capped with para film. The capped flasks were shaken in a shaker incubator model LSI-100B from KWF Sci-Tech and development Co. China, at a fixed temperature for 3 hours. The flasks were removed from the shaker and the suspensions were centrifuged at 4000 rpm for 10 min., using a Hettich EBA 20 centrifuge, Germany. The remained adsorbates concentrations in the supernatant were determined.

c) Contact Time Effect

For each experiment, pre-weighed samples of the adsorbent were added to sets of 100 mL Erlenmeyer flasks. Then, 25 mL of adsorbate solution with a known concentration and pre-determined pH, were transferred into the flasks. The flasks were capped with para film and shaken in a shaker incubator model LSI-100B from KWF Sci-Tech and development Co. China, at a fixed temperature. Flasks were removed form shaker after certain intervals of time, and the solutions were centrifuged at 4000 rpm for 10 min., using a Hettich EBA 20 centrifuge, Germany. The remained adsorbate concentrations in the supernatant were determined.

d) Temperature and Initial Concentration Effects

The adsorption isotherm experiments were carried out at three different temperatures using batch method. For each experiment, 5 adsorbate solutions with varied initial concentrations were prepared, the pH of these solutions was adjusted to the pre-determined optimum pH. Then, 25 mL of each solution were transferred into 5 Erlenmeyer flasks, containing pre-weighed adsorbent samples. Then, the flasks were capped with para film, and shaken in a shaker incubator model LSI-100B from KWF Sci-Tech and development Co. China, at the required temperature for 3 hours. The flasks were removed from the shaker, the suspension was centrifuged at 4000 rpm for 10 min., using a Hettich EBA 20 centrifuge, Germany. The remained adsorbate concentrations in the supernatant were determined.

e) Methods for the Determination of Remained Adsorbate

MB, CV, CR, and phenol were determined at their equivalent λ_{max}. using ultraviolet-visible spectrophotometer UV-Vis (Perkin Elmer instrument), model Lambda 25.

The remained As(III) was determined using inductively coupled plasma mass spectroscopy (ICP-MS) (Perkin Elmer instrument), with a 30-second uptake and stabilizing time, a 10-second probe rinse of samples and analytical standards, a pump speed of 0.5 rpm, a sample depth of 10 mm, and a sample gas flow of 1.07 $L.min^{-1}$. the instrument were calibrated using standard diluted As(III) solutions.

Nitrate was determined with Metron ion chromatography instrument with conductivity detector. The instrument was calibrated using multi anion standard method, using 3.6 mM Na_2CO_3 (0.77g in 2 liter) as eluent at flow rate 0.800 $mL.min^{-1}$, pressure 11.75 MPa, temperature 45.0 °C and data manipulation was conducted using MagIC Net software version 3.2.

3.3. Calculations

3.3.1. Adsorption Capacity

Th adsorption capacity ($mg.g^{-1}$) at equilibrium, q_e, or at each time interval, q_t, was calculated according to **Equation** (1):

$$q_e = (C_0 - C_e)\frac{V}{m} \quad \text{..... (1)}$$

where: C_0 and C_e are the concentrations of the adsorbate ($mg.L^{-1}$) at initial and the equilibrium state, respectively, V is the volume of the solution (L), and m is the dry weight of the adsorbent (g).

3.3.2. Adsorption Kinetics

Kinetic modeling not only allows estimation of sorption rates but also leads to suitable rate expressions characteristic of possible reaction mechanisms. In this respect, the three common kinetic models, the pseudo-first-order model (PFO), the pseudo-second-order model (PSO), and the intraparticle diffusion model were investigated.

a) First Order Lagergren Rate Equation

The first order rate equation was firstly presented by Lagergren for the adsorption of oxalic acid and malonic acid onto charcoal (Largitte and Pasquier, 2016; Tran *et al.*, 2017). The equation can be expressed correctly in nonlinear, **Equation** (2), and linear forms, **Equations** (3) or (4).

$$q_t = q_e(1 - e^{-k_1 t}) \quad \text{..... (2)}$$

$$\ln(q_e - q_t) = -k_1 t + \ln(q_e) \quad \text{..... (3)}$$

$$\log(q_e - q_t) = \frac{-k_1}{2.303} t + \log(q_e) \quad \text{..... (4)}$$

where: q_e and q_t are the amounts of adsorbate uptake per mass of adsorbent at equilibrium and at any time t (min), respectively; and k_1 (min^{-1}) is the rate constant of the PFO equation. A straight line of log (q_e - q_t) versus t suggests the applicability of this model, hence k_1 and q_e can be determined.

b) Pseudo Second Order Rate Equation

This model predicts the behavior over the whole range of adsorption and agrees with an adsorption mechanism being the rate controlling step. The pseudo second-order kinetic rate equation is expressed as in **Equation**s (5) and (6) for nonlinear and linear form, respectively.

$$q_t = \frac{q_e^2 k_2 t}{1 + k_2 q_e t} \quad \text{..... (5)}$$

$$\frac{t}{q_t} = \left(\frac{1}{q_e}\right) t + \frac{1}{k_2 q_e^2} \quad \text{..... (6)}$$

where: k_2, is the rate constant of PSO adsorption ($g.mg^{-1}.min^{-1}$). If second-order kinetics are applicable, the plot of t/q_t against t of **Equation** (6) should give a linear relationship, from which q_e and k_2 can be determined from the slope and intercept of the plot.

c) Intraparticle Diffusion Rate Equation

The intraparticle diffusion kinetic model based on the theory proposed by Weber and Morris (1963). The theory stated that the adsorbate uptake, q_t varies proportionally with the square root of the contact time, √t rather than t, as shown in **Equation (7**):

$$q_e = k_{id} x\sqrt{t} + C \quad \ldots\ldots\ldots\ldots\ldots\ldots\ldots\ldots\ldots\ldots\ldots\ldots\ldots\ldots\ldots\ldots\ldots\ldots\ldots\ldots (7)$$

where: k_{id} ($mg.g^{-1}.min^{-1/2}$) is the intra-particle diffusion rate constant and C is a constant related to the thickness of the boundary layer. If intraparticle diffusion occurs, then q_t versus √t will be linear, and the value of the k_{id} can be calculated from the slope (Nicoleta Popa, 2015).

3.3.3. Adsorption Isotherms Models

Adsorption isotherm is generally used to describe the distribution of adsorbate between the liquid phase and the solid phase at a constant temperature under given conditions, such as pH, dosage, contact time and particle size of adsorbent (Tran, You and Chao, 2016). Langmuir and Freundlich isotherm models are commonly used.

a) Langmuir Model

The theoretical Langmuir equation, which was originally applied to the adsorption of gases on a solid surface, was developed using the following assumptions: (i) a fixed number of accessible sites are available on the adsorbent surface and all active sites have the same energy; (ii) adsorption is reversible; (iii) once an adsorbate occupies a site, no further adsorption can occur on that site; and (iv) there is no interaction between adsorbate species. The nonlinear form of the Langmuir model is shown by **Equation (8)** and its common linearized form is shown in **Equation (9)** (Tran *et al.*, 2017).

$$q_e = \frac{Q^0_{max} K_L C_e}{1 + K_L C_e} \quad \ldots\ldots\ldots\ldots\ldots\ldots\ldots\ldots\ldots\ldots\ldots\ldots\ldots\ldots\ldots\ldots\ldots\ldots\ldots\ldots (8)$$

$$\frac{C_e}{q_e} = \left(\frac{1}{Q^0_{max}}\right) C_e + \frac{1}{Q^0_{max} K_L} \quad \text{..... (9)}$$

where: Q_{max} ($mg.g^{-1}$) is the maximum saturated monolayer adsorption capacity of an adsorbent, C_e ($mg.L^{-1}$) is the adsorbate concentration at equilibrium, q_e ($mg.g^{-1}$) is the amount of adsorbate uptake at equilibrium, and K_L ($L.mg^{-1}$) is a constant related to the affinity between an adsorbent and adsorbate and it is related to the energy of adsorption via Arrhenius equation.

The term separation factor, R_L, (dimensionless) was originally introduced by Hall et al. (Hai, 2017) to note the essential characteristics and the feasibility of a Langmuir isotherm. The factor is defined as **Equation** (10).

$$R_L = \frac{1}{1+K_L C_0} \quad \text{..... (10)}$$

where: K_L is the Langmuir constant, and C_0 ($mg.L^{-1}$) is the initial adsorbate concentration. The value of R_L shows the shape of the isotherms to be either unfavorable ($R_L>1$), linear ($R_L=1$), favorable ($0< R_L<1$), irreversible ($R_L =0$).

b) Freundlich Model

The Freundlich equation is one of the earliest empirical equations used to describe adsorption characteristics for heterogeneous surfaces. The model considers monomolecular layer coverage of solute by the adsorbent. Moreover, it assumes that the sorbent has a heterogeneous valance distribution and then has different affinity for adsorption (Hai, 2017). The nonlinear and linear forms of the Freundlich equation can be expressed as shown in **Equation**s (11) and (12), respectively.

$$q_e = K_F C_e^{1/n} \quad \text{..... (11)}$$

$$\log q_e = \frac{1}{n} \log C_e + \log K_F \quad \text{..... (12)}$$

where: q_e ($mg.g^{-1}$) is the amount of adsorbate uptake onto adsorbent at equilibrium, C_e ($mg.L^{-1}$) is the adsorbate concentration remained at

equilibrium, K_F ($mg.g^{-1}$)($L.mg^{-1})^{1/n}$ is the Freundlich constant related to the adsorption capacity, and 1/n (dimensionless; 0 < n < 10) is the Freundlich intensity parameter, which indicates the magnitude of the adsorption driving force or the surface heterogeneity (Hai, 2017). The parameters of the Freundlich equation can be obtained from the intercept and slope of the straight line of the plot log (q_e) versus log (C_e).

3.3.4. Adsorption Thermodynamics

Thermodynamic parameters, including the Gibbs energy change (ΔG°), the enthalpy change (ΔH°), and the entropy change (ΔS°), were crucial to establish the adsorption mechanisms (chemical or physical) (Hai, 2017). These parameters can be calculated from the adsorption experiments carried out at different temperatures. The ΔG° ($J.mol^{-1}$) is calculated by **Equation** (13).

$$\Delta G^0 = -RTlnK^0 \quad \text{..... (13)}$$

where K^0 is the standard equilibrium constant which is a dimensionless parameter, ΔG^0 is the standard Gibbs energy change, R is the gas constant (8.3144 $J.mol^{-1}.K^{-1}$) and T is the temperature (K). standard equilibrium constant, K^0 is related to the constant ($k_d = q_e/C_e$), the standard equilibrium constant could be calculated as **Equation** (14) (Zhou and Zhou, 2014).

$$K^0 = \frac{q_e}{C_e} \times M_{adsorbate} \times C^0 \quad \text{..... (14)}$$

where: M is the molecular mass of adsorbate, C^0 is the concentration of the solution in the chosen standard state (C^0 = 1 $mol.L^{-1}$). Then, ΔH^0 and ΔS^0 are determined through the slope and intercept of the well-known van't Hoff equation (**Equation** 15), respectively.

$$\ln K^0 = \frac{-\Delta H^0}{R} x \frac{1}{T} + \frac{\Delta S^0}{R} \quad \text{..... (15)}$$

then,

$$\Delta S^0 = \frac{\Delta H^0 - \Delta G^0}{T} \quad \text{..... (16)}$$

CHAPTER FOUR

4. RESULTS AND DISCUSSION

4.1. Characterization of the Adsorbents

4.1.1. X-Ray Diffraction Analysis

XRD analysis is regularly used for identification of clay minerals since the diffraction pattern usually contains a lot of characteristic features such as peak position, intensity shape and breadth. By matching these data with some standard tables of XRD data, it is often possible to identify different types of clay minerals (Środoń, 2013).

The XRD patterns of Na-MO and Surf-MO samples were shown in **Figure 4-1(a and b)**, and the 2θ˚ positions, d-spacing values along with their relative intensities of main clay minerals, were summarized in **Table 4-1**.

The diffraction patterns of Na-MO sample, **Figure 4-1(a)**, presented the characteristic illite reflections peaks at 2θ° angles of 8.51°, 29.47° and 60.05° equivalent to d-spacing d_{001} 10.39 Å, d_{003} 3.03 Å and d_{060} 1.54 Å, respectively (Ismadji, Soetaredjo and Ayucitra, 2015c). Besides, illite-quartz mixed minerals were manifested by the strong reflection at 2θ° angle of 26.68° related to d-spacing value of 3.34 Å (Shaban, Sayed, *et al.*, 2018). The sample also showed the characteristic diffraction peaks of kaolinite at 2θ° angles of 12.38°, 20.91° and 25.04°, which were linked to the d-spacing values at d_{001}7.15 Å, d_{110} 4.25 Å and d_{002} 3.56 Å, respectively. Other peaks were detected for kaolinite at 2θ° angles of 19.83° (4.47 Å), 34.77° (2.57 Å), and 50.18° (1.81 Å).

The XRD pattern of Surf-MO sample, **Figure 4-1(b)**, showed no change on the basal spacing due to the insertion of the surfactant into the interlayer

space of the Na-MO sample. Similar observations were reported in the literature (Bhattacharyya and Gupta, 2006).

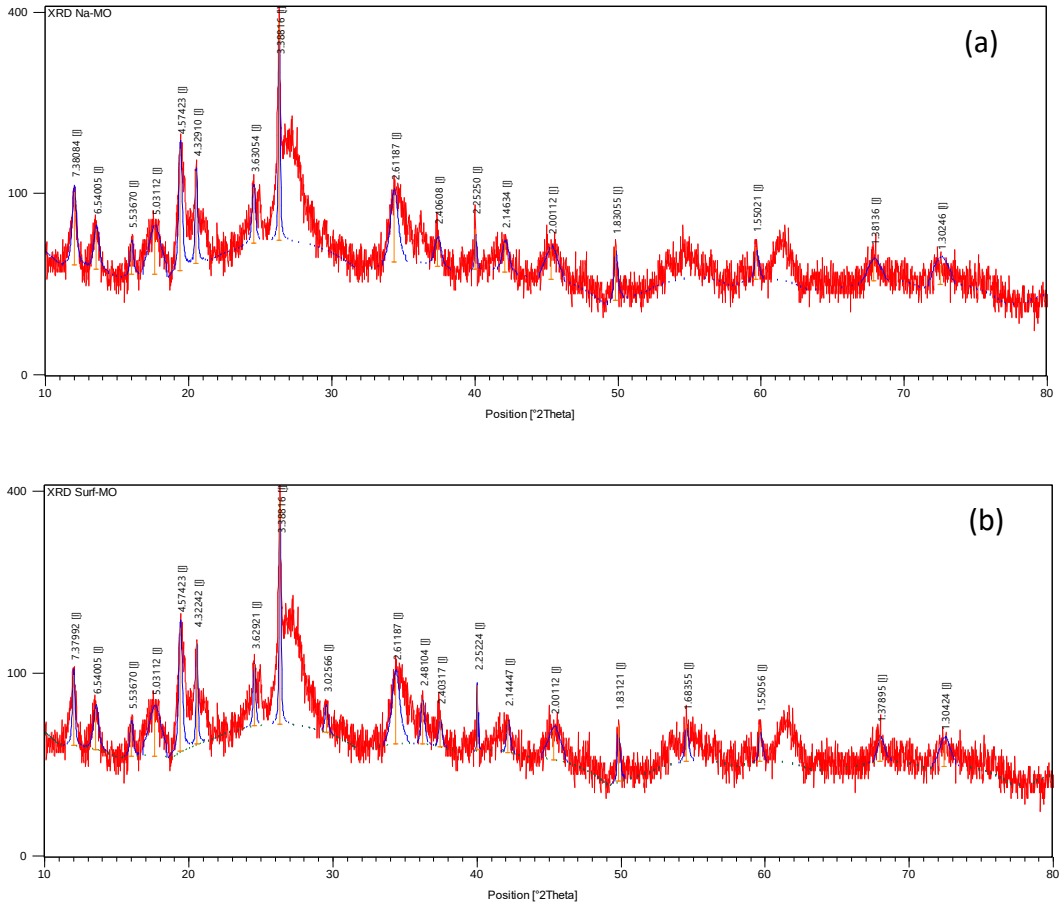

Figure 4-1: XRD patterns of (a) Na-MO and (b) Surf-MO samples

Table 4-1: The XRD data for Na-MO and Surf-MO samples

Na-MO sample			Surf-MO sample		
Position [°2Θ]	d-spacing [Å]	Rel. Int. [%]	Position [°2Θ]	d-spacing [Å]	Rel. Int. [%]
11.9911	7.38084	19.83	11.9926	7.37992	18.80
13.5395	6.54005	9.43	13.5395	6.54005	9.41
16.0079	5.53670	6.78	16.0079	5.53670	7.00
17.6287	5.03112	10.26	17.6287	5.03112	10.39
19.4058	4.57423	37.79	19.4058	4.57423	37.52
20.5162	4.32910	27.22	20.5482	4.32242	30.38
24.5200	3.63054	16.71	24.5291	3.62921	18.10
26.3044	3.38816	100.00	26.3044	3.38816	100.00
34.3351	2.61187	18.37	34.3351	2.61187	18.41
37.3757	2.40608	6.31	37.4226	2.40317	6.14
40.0291	2.25250	9.50	39.9994	2.25224	16.48

Likewise, **Figure 4-2 (a and b)** presented the XRD patterns of Na-NI and Surf-NI samples, respectively. Also, the 2θ˚ positions, d-spacing values along with their relative intensities for the identified clay minerals were summarized in **Table 4-2.**

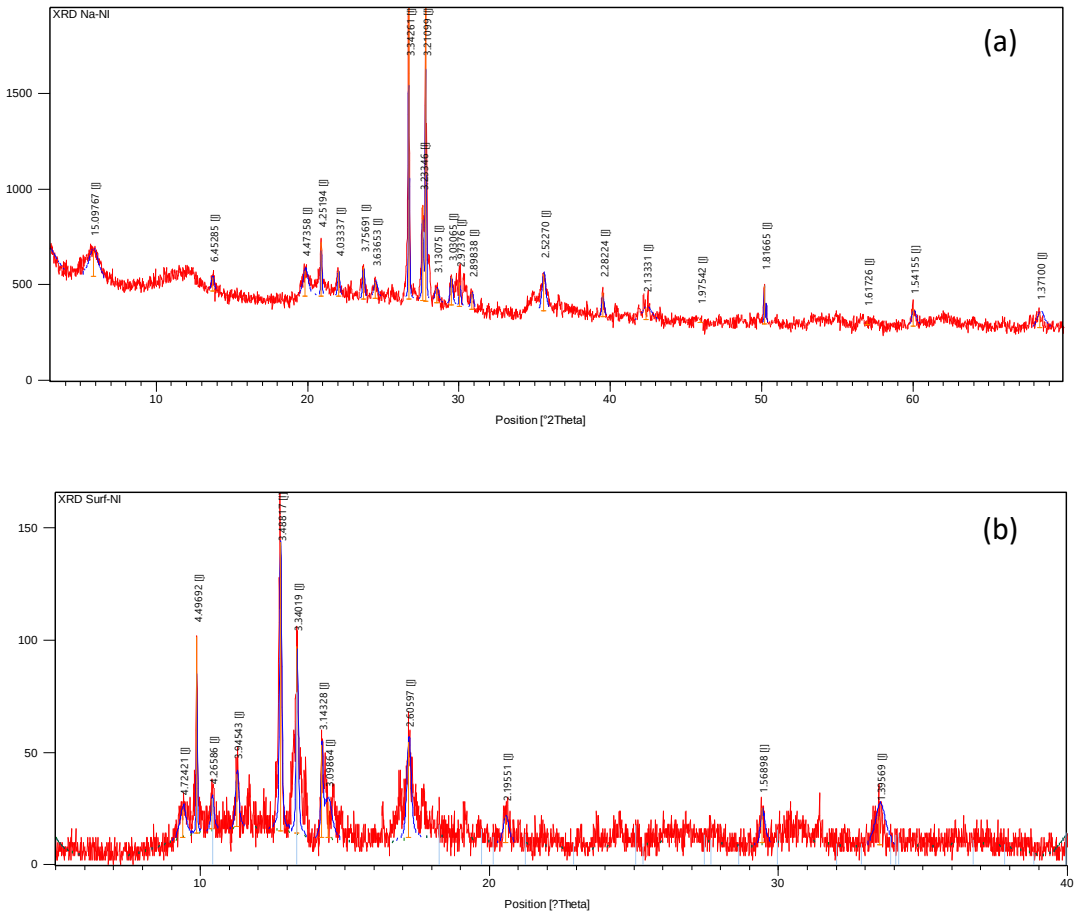

Figure 4-2: XRD patterns of (a) Na-NI, and (b) Surf-NI clay samples

XRD results for Na-NI clay, **Figure 4-2(a)**, indicated that the structure of this clay was complex and heterogeneous. The diffractogram exhibited the characteristic smectite reflections at 2θ° angles of 5.85° and 29.47° linked to the d-spacing values at d_{001} 15.10 Å and d_{003} 3.03 Å, respectively. Other smectite reflections were observed at 2θ° angles of 19.84°, 23.68°, and 60.01°, which were assigned to the d-spacing values at 4.47 Å, 3.75 Å and 1.54 Å. Illite reflections peaks were detected at 2θ° angles of 13.72° and 29.47° linked to d-spacing at d_{002} 6.45 Å and d_{003} 3.03 Å. Also, illite-quartz

mixed minerals exhibited strong reflection peaks at 2θ° angle of 26.67° at d-spacing value of 3.34 Å (Unuabonah *et al.*, 2008; Shaban, Sayed, *et al.*, 2018). While quartz was detected at 2θ° angles of 20.89°, 35.59°, 50.18°, 56.93° equivalent to d-spacing values of d_{101} 4.25 Å, d_{110} 2.52 Å, d_{112} 1.82 Å and d_{103} 1.62 Å, respectively (Bentahar *et al.*, 2017). These results were supported with many studies on Nile sediments (Elgabaly and Khadr 1962; Fayed and Hassan 1970; Weir, Ormerod, and El Mansey 1975).

The XRD pattern of Surf-NI sample as shown in **Figure 4-2** (**b**), were comparable to its Na-NI sample, but there was slight increase in d-spacing values (2-5%) after surfactant modification, as shown in **Table 4-2**. This confirms the success of the intercalation of the cationic surfactant in the clay gallery (Wang, Wang and Wang, 2013).

Table 4-2: The XRD data for Na-NI and Surf-NI samples

Na-NI sample			**Surf-NI sample**			**%**
Position [°2Θ]	d-spacing [Å]	Rel. Int. [%]	Position [°2Θ]	d-spacing [Å]	Rel. Int. [%]	d-spacing increase
19.8468	4.47358	8.64	18.7840	4.72421	9.71	5.65
20.8927	4.25194	18.10	19.7427	4.49692	67.97	5.76
23.6830	3.75691	10.64	22.5362	3.94543	18.14	5.02
26.6694	3.34261	99.62	25.5373	3.48817	100.00	4.35
27.7841	3.21099	100.00	26.6891	3.34019	64.80	4.02
29.4737	3.03065	9.44	28.8129	3.09864	12.57	2.24
35.5885	2.52270	12.64	34.4153	2.60597	33.24	3.30

The results of XRD analysis of all samples revealed that the Morocco clay samples were naturally composed of illite, kaolonite, and quartz whereas the Nile clay samples were composed of smcitite, illite and quartz.

4.1.2. Fourier Transform Infrared Spectroscopy

Infrared measurements are commonly used as a complementary technique of XRD and other methods for identification of clay minerals. FTIR spectra for the Na-MO and Surf-MO samples were shown in **Figure 4-3 (a** and **b)**, while the spectra for the Na-NI and Surf-NI samples were presented in **Figure 4-4**

(a and **b)**. The main infrared, FTIR, bands of the four clay samples were listed in **Table 4-2**.

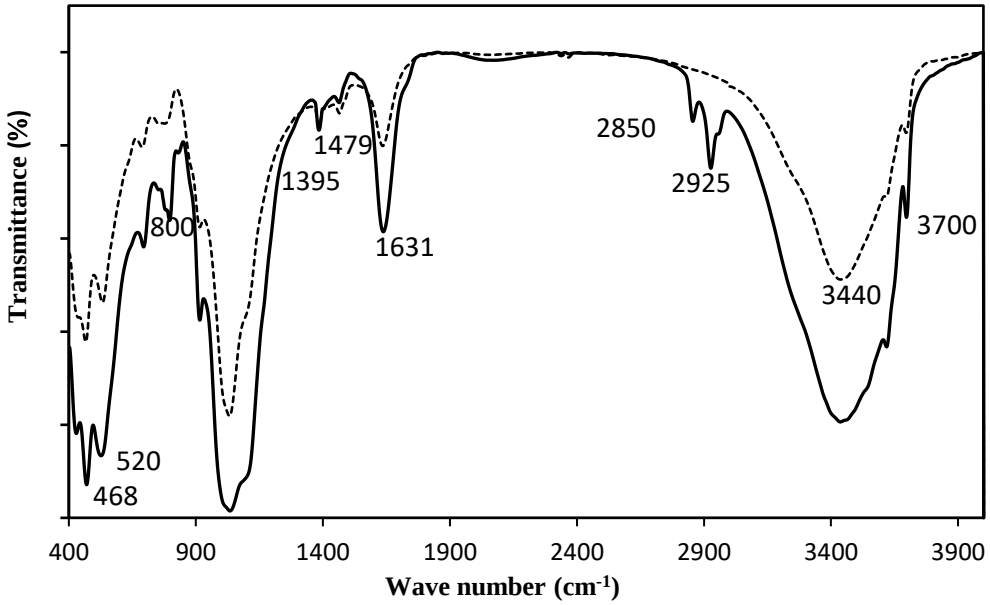

Figure 4-3: FTIR spectrum of the Na-MO (...), and Surf-MO (—) samples

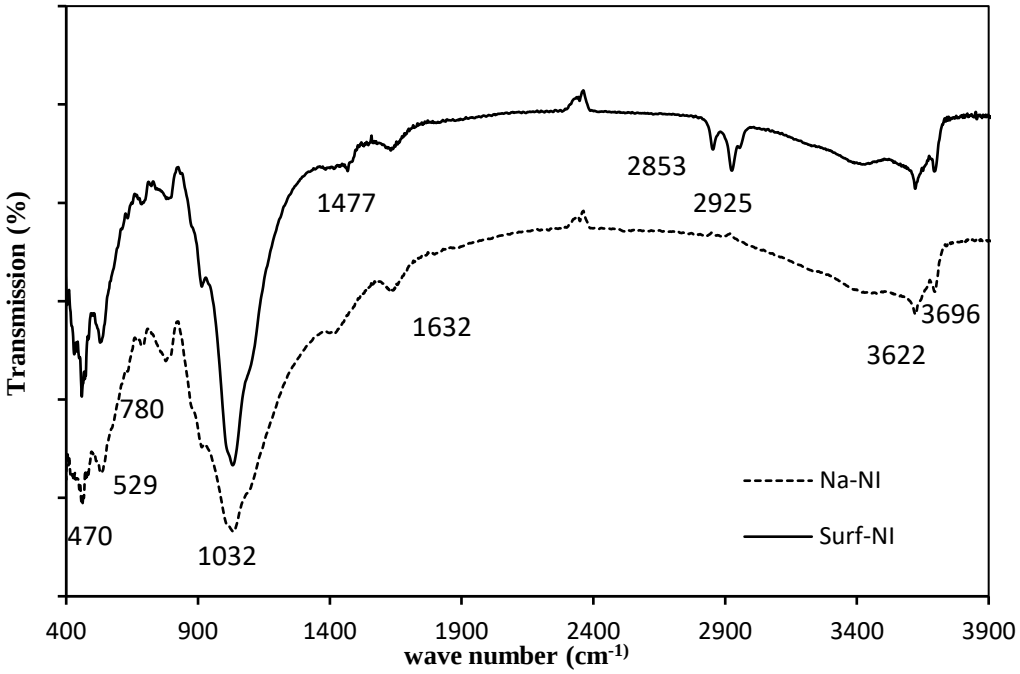

Figure 4-4: FTIR spectrum of the Na-NI (...), and Surf-NI (—) samples

The FTIR spectrums of Na-MO and Na-NI samples, **Figure 4-3 (a)** and **Figure 4-4 (a)**, respectively, showed the presence of many minerals. For illite or smectite, the band at 3620 cm^{-1} was attributed to the stretching

vibration of structural −OH in the 2:1 layer (Madejova and Komadel 2001; Pleşa Chicinaş et al. 2018), while the broader band at 3420 cm^{-1} was assigned to the adsorbed water on interlayers of illite-kaolinite mixture (Sun *et al.*, 2017). Quartz Si–O bending vibrations bands were detected in Na-MO and Na-NI samples at (467, 520 cm^{-1}) and (466, 533 cm^{-1}), respectively (Zhang *et al.*, 2015). Additionally, the Si–O–Si bending vibration band were observed in all samples around 1032 cm^{-1}. In other hand kaolinite Si–O stretching vibration was evidenced in Na-MO clay at (686, 798 cm^{-1}) (Pleşa Chicinaş *et al.*, 2018). A terminal hydroxyl group (Si-OH, Al-OH) was observed around 3695 cm^{-1} along with the bending vibration of water appeared between 1630-1653 cm^{-1} for both clay samples (Bentahar *et al.*, 2016; Pleşa Chicinaş *et al.*, 2018).

Table 4-3: The main bands in the FTIR spectra of the prepared adsorbents

IR bands (cm^{-1})	Na-MO	Surf-MO	Na-NI	Surf-NI
O-H stretching region: 3620-3700	3618, 3697	3620, 3700	3622, 3696	3621, 3694
Si-O stretching region: 1000-1120	1032	1031	1033	1032
O-H bending region: 910 - 940	912	914	915	914
Si-O bending region: 400 - 550	406, 417, 424, 468	466, 532	408, 421, 428, 450	430, 440, 459, 471
CH_2 and CH_3 stretching region	-	2850, 2925	-	2853, 2925
Adsorbed water	3440	3440	-	-

In the other hand, many peaks from the FTIR spectrums of Surf-MO and Surf-NI, as shown in **Figure 4-3(b)** and **Figure 4-4(b)** confirm the success of intercalation process. (i) the two absorptions bands around 2925 cm^{-1} and 2850 cm^{-1} that were ascribed to asymmetrical and symmetrical stretching vibration of CH_3 and CH_2 groups, (ii) the weak band around 1477 cm^{-1} that was attributed for C-H bending vibration of the CH_2 group (Wang, Wang and Wang, 2013; Hamdaoui *et al.*, 2018), (iii) the band around 780 cm^{-1} that was assigned to the mode of vibration of deformation out of the plane of the CH_2 group (Ltifi *et al.*, 2018). (iv) the week band observed around 1395 cm^{-1} which was ascribed to the C-N group of the surfactant (Ltifi *et al.*, 2018).

4.1.3. Energy Dispersive X-ray Spectroscopy

Energy dispersive x-ray spectroscopy (EDS) provides elemental analysis through the measurement of x-ray energy emitted from a sample.

Results of elemental analysis with EDX for Na-NI, Surf-NI, Na-MO and Surf-MO samples, were reported in **Table 4-4**.

Table 4-4: EDX results of the Na-NI, Surf-NI, Na-MO and Surf-MO samples

Element	Na-NI	Surf-NI	Na-MO	Surf-MO
	Weight%	Weight%	Weight%	Weight%
C	18.85	17.78	36.53	43.46
O	54.46	53.09	50.01	36.18
Na	1.26	0.66	0.17	0
Mg	0.9	1.28	0.77	1.46
Al	4.52	5.27	2.72	4.37
Si	11.52	13.19	7.28	10.76
K	0.51	0.5	0.54	0.74
Ca	1.74	1.47	0	0
Ti	0.89	0.87	0.33	0
Fe	4.45	5.21	1.07	3.03
Cu	0.55	0.41	0.37	0
Zn	0.35	0.26	0.23	0
	100	99.99	100.02	100

All samples showed very high peaks of oxygen, silicon and aluminum, as well as magnesium, iron, potassium and sodium, all of which were typical of the elemental composition of aluminium silicate minerals, in addition to traces amounts of zinc, copper and titanium. However calcium was not observed in Morocco clay samples but found in the Nile clay samples.

The carbon content of surf-MO sample was increased from 17.78% to 43.46% after surfactant intercalation, suggesting that the treatment was realized with success. Although the carbon content of surf-NI sample was decreased from 18.85% to 17.78% which accompanied with a decrease in calcium content from 1.74% to 1.47%, this can be ascribed to the removal of impurities of dolomite clay minerals during the intercalation process. This

observation can be supported by disappearing of dolomite peaks form the XRD pattern of Surf-NI sample. Additionally, the intercalation process caused the elimination of Na, Ti, Cu and Zn from Surf-MO sample, hence their mass % were decreased.

4.1.4. Scanning Electron Microscope

The goal of the SEM image observations was to display if there were any morphological changes after the modification of the clay samples. The SEM images of the Na-MO sample were shown in **Figure 4-5(a)** where a perfect clivage can be observed. While **Figure 4-5(b)** revealed that the surface morphology appeared to possess an irregular texture and porous cavities which can be considered as available sites for adsorption.

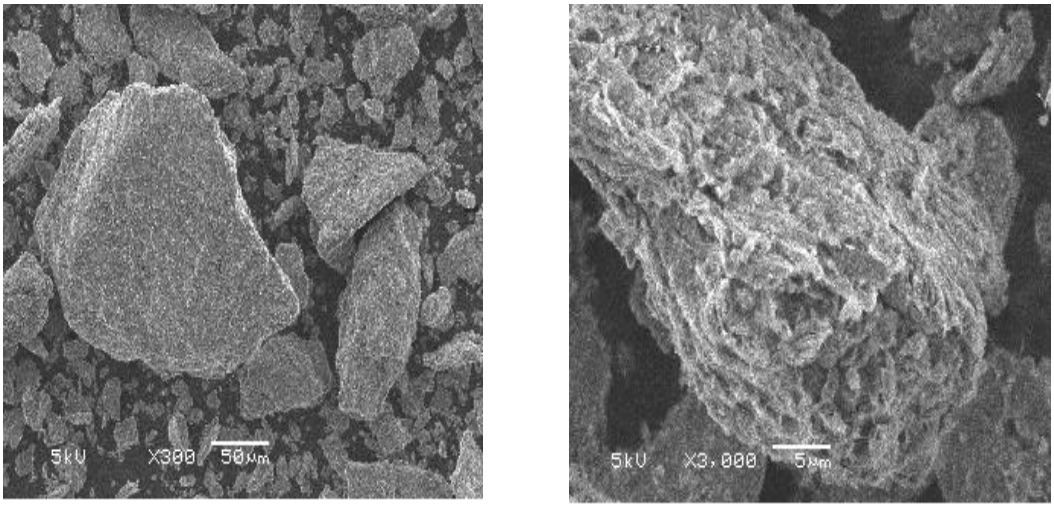

(a) **(b)**

Figure 4-5: SEM images of Na-MO sample

TEM images of Na-MO and Surf-MO samples were shown in Figure 4-6, where a typical and well-ordered arrangements of clay mineral platelets were detected, and the stacks of multilayers become more dispersive after modification with the surfactant. It can also be seen that the distance from layer to layer is much larger and more apparent in the organoclay samples compared to the Na-clay samples. A similar bahavior has been reported in the literature (Wang and Wang, 2008).

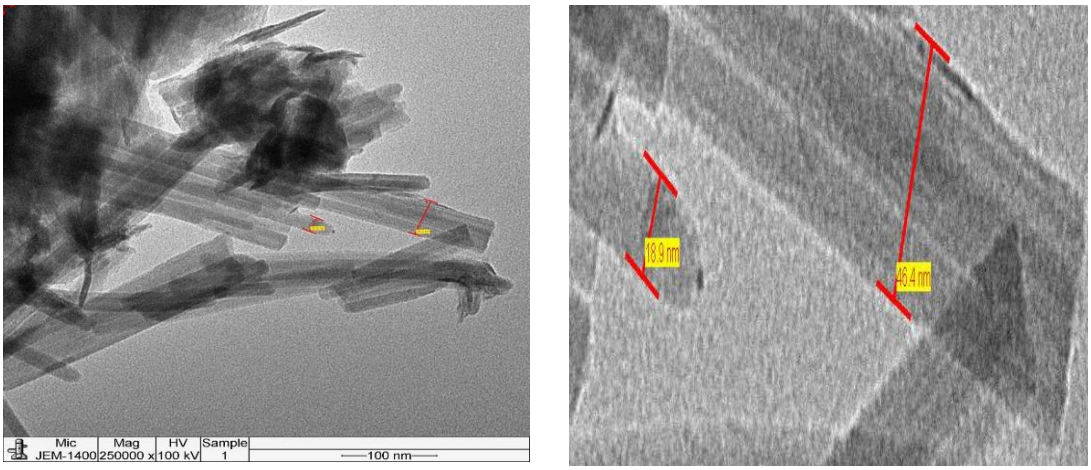

(a)

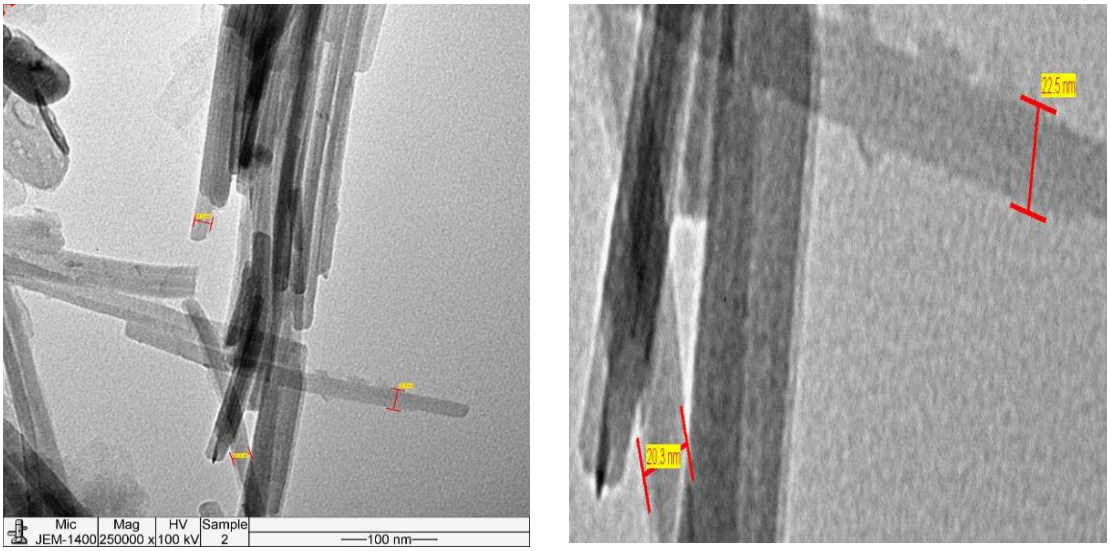

(b)

Figure 4-6: TEM images of (a) Na-MO, and (b) Surf-MO samples**.**

The surface morphology of the Na-NI and Surf-NI samples were shown in **Figure 4-7 (a and b)**, respectively. It can be obviously seen from both figures that the clay had porous structure. Besides, the form of Surf-NI, after modification was changed to an ultrafine thin ‘corn flake’ like crystal with cottony appearance. This maybe occurred due to the intercalation of the surfactant (Anirudhan and Ramachandran, 2015).

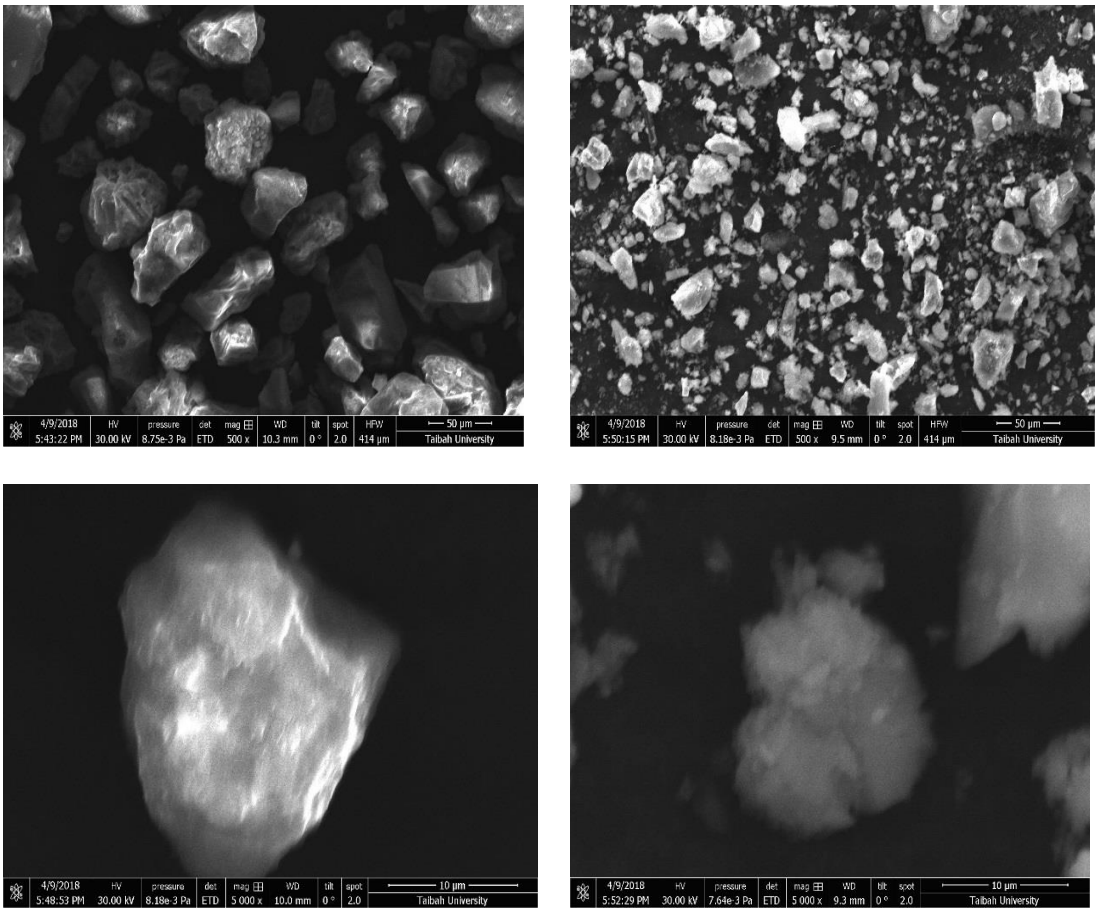

(a) **(b)**

Figure 4-7: SEM image of the (a) Na-NI, and (b) Surf-NI samples

4.1.5. Thermal Analysis

Thermal analysis is an additional useful tool for the characterization of clay. The technique determines water loss and phase changes upon heating the clay by the related thermal effects. Differential scaning calorimetry, DSC, curves for Na-MO and Na-NI samples were shown in **Figure 4-8**, whereas the thermal gravimetry analysis, TGA, curves for Surf-MO and Surf-NI samples were shown in **Figure 4-9**.

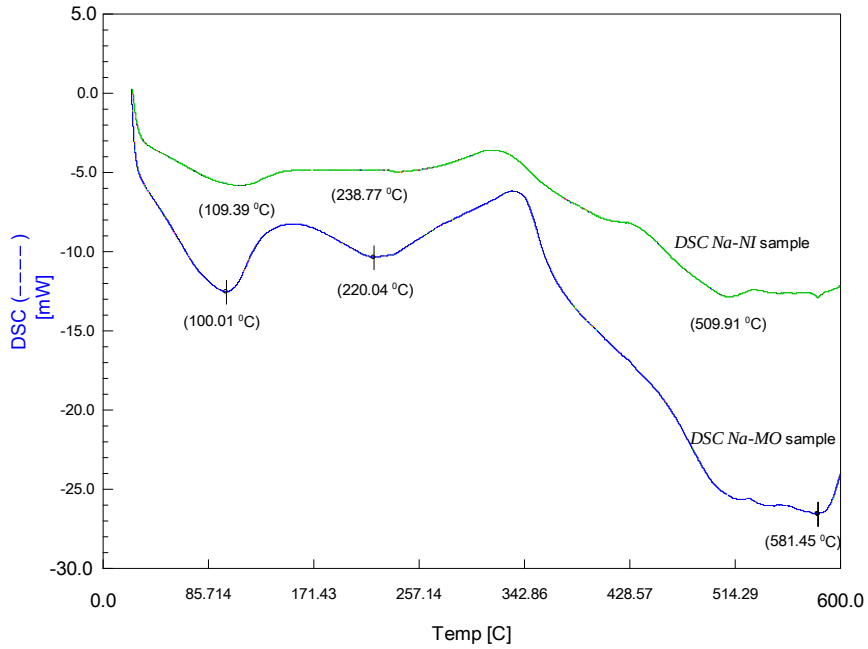

Figure 4-8: DSC thermogram for Na-MO and Na-NI samples

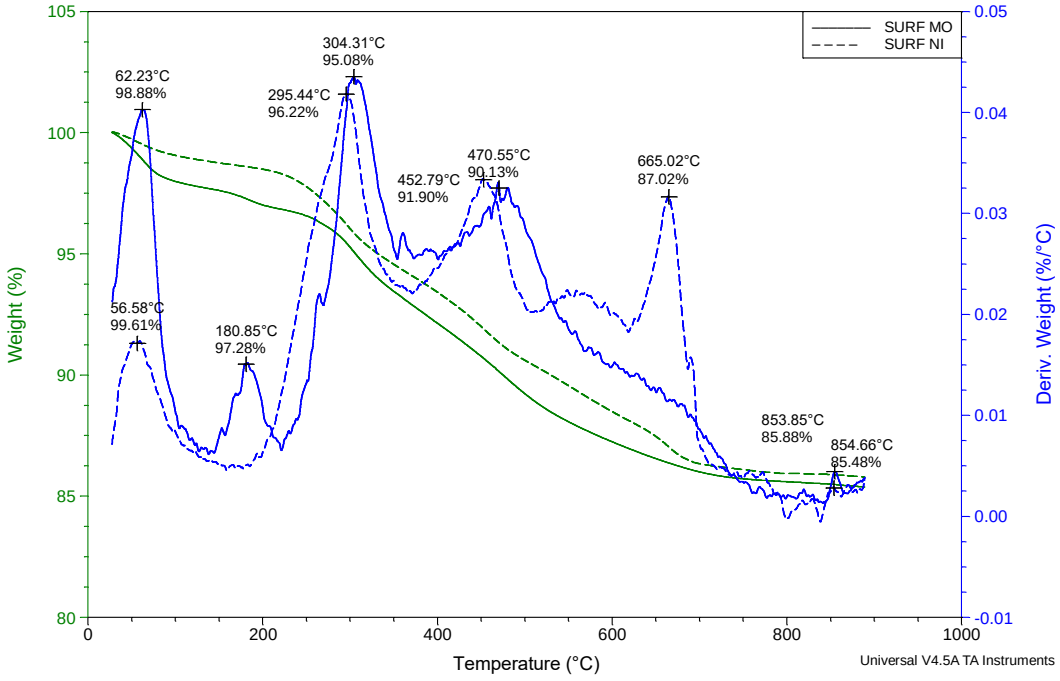

Figure 4-9: TG-DTA thermogram for Surf-MO and Surf-NI samples

The DSC thermograms for both Na-clay samples exhibited at least three endothermic peaks. The first peak was detected around 100 °C and 109 °C for Na-MO and Na-NI samples, respectively. This peak can be ascribed to the removal of physically bound water in pores and on the surfaces. The

second peak was a large exothermic peak, observed around 220 °C and 238 °C for Na-MO and Na-NI samples, respectively. This peak can be assigned to the interlayer water's phase change, since lossing of such water is more gradual and may persist continously to temperature. A broad endothermic band between 500-600 °C for both samples can atrributed to dehydroxylation of the samples and transformation of α quartz to β quartz (Kurniawan *et al.*, 2014).

The thermogravimetric (TG) and differential thermogravimetric analysis (DTA) of both Surf-MO and Surf-NI samples, showed several losses of mass according to the temperature. The first (1.12% and 0.4%) mass loss was observed beloow 100 °C for Surf-MO and Surf-NI, respectivley. This can be assigned to the loss of moisture from the samples. Surf-MO sample showed 2.78% mass loss around 180 °C, due to removal of water molecules associated with interparticle and interlayer surfaces (Ma *et al.*, 2016), but Surf-NI sample lack mass loss in this region, which proves the abcense of interlayer water. Both organoclay samples showed about 5% mass loss at around 300 °C due to the surrfactant decmposition, whereas their equivalent Na-clays lack phase changes in this region. This confirms the success of surfactant intercalation process. Moreover, both organocaly samples showed about 10% mass loss between 450-750 °C related to dehydroxylation processes and transformation of α quartz to β quartz (Kurniawan *et al.*, 2014).

Surf-NI sample showed two step mass loss at 452 °C and 695 °C, while Surf-MO sample showed only one peak at 471 °C. The account for this observation was, in dioctahedral structures of semctite, cations occupy either two cis sites, or one cis and one trans sites. Dehydroxylation process of cis vacant smectite observed at higher temperature than trans vacant smectite (Arbaoui and Boucherit, 2014).

4.1.6. Loss on Ignition

Results of loss on ignition (LOI) experiment were given in **Table 4-5**. Both raw clays showed high LOI (11.85% and 14.74%), while sodium enriched clays having considerably less LO1 (4.27% and 7.90%). The results of measurement of LOI infer that both raw clays contain much more occluded matter like organic matter, CO_2, water trapped in the pores and the edges, etc., compared to other clays.

Table 4-5: Loss on ignition

Morocco Samples		**The Nile samples**	
Sample	% Loss	Sample	% Loss
raw MO	14.74	raw Nile	11.85
Na-MO	7.90	Na-NI	4.27
Surf-MO	11.97	Surf-NI	14.45

4.1.7. Surface Area and Texture Analysis

The surface area and porosity of an adsorbent are important parameters in studying its adsorption capacity as well as its adsorption performance. The nitrogen adsorption-desorption isotherms on Na-MO, Surf-MO, Na-NI and Surf-MO samples were showed in **Figure 4-10** and **Figure 4-11**.

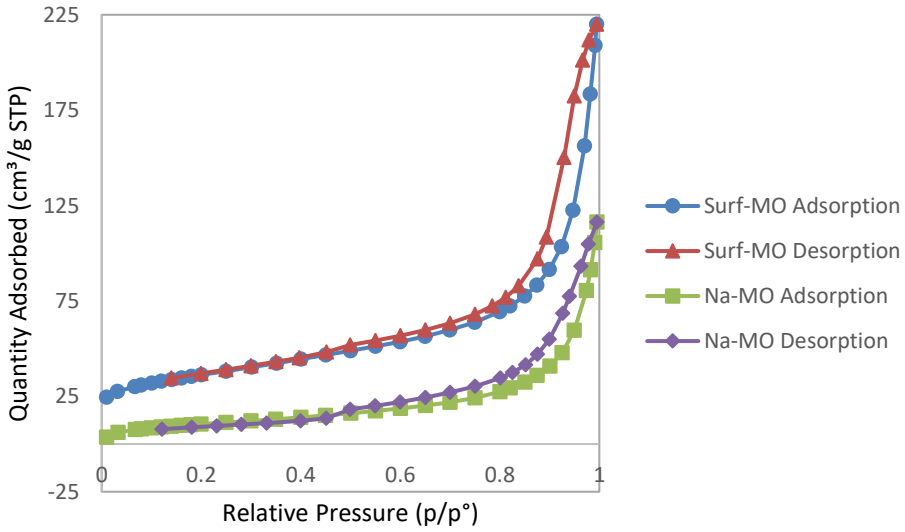

Figure 4-10: N_2 adsorption-desorption isotherms of Na-MO and Surf-MO

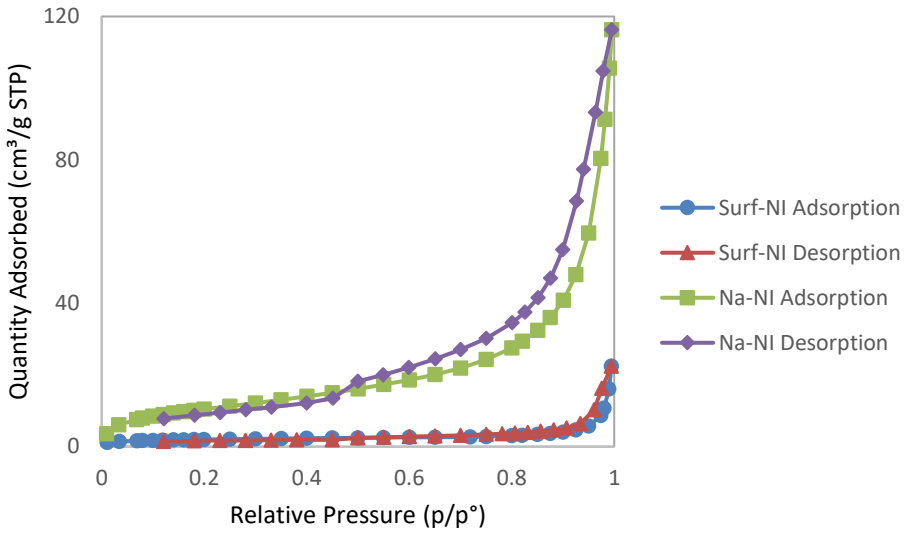

Figure 4-11: N_2 adsorption-desorption isotherms of Na-NI and Surf-NI

The adsorption-desorption isotherms of all samples were of the type IV, which is characteristic of mesoporous solids. Adsorption proceeds through multilayer adsorption followed by capillary condensation. The distinctive features of this type are its hysteresis loop which is linked with capillary condensation taking place in mesopores, and the limiting uptake over a range of high relative pressure (P/P_0). The BET results shown above indicated that these natural adsorbents were mesoporous because of their hysteresis loops type H3, that started above 0.4, which were specified for non-rigid aggregates of plate-like particles (Thommes *et al.*, 2015).

Comparison between textural properties of Na-clays and Surf-clays samples determined from nitrogen adsorption-desorption isotherms and from the point of zero charge experiments were reported in **Table 4-6**.

Table 4-6: The textural properties of the prepared adsorbents

Property	Na-MO	Surf-MO	Na-NI	Surf-NI
S_{BET} (m^2/g)	128	39	23	11
Total pore volume (cm^3/g)	0.320	0.181	0.097	0.042
BET average pore size (Å)	75.6	125.8	92.4	100.9
The point of zero charge	7.0	7.2	7.8	7.8

The decrease of the surface area of Surf-MO and Surf-NI from 128 to 39 and 23 to 11 $m^2.g^{-1}$, respectively can be atrributed to the large number of active sites satisfied by surfactant molecules and the reduction of the accessible internal surface for nitrogen gas. However, the Surf-clay exibits a larger pore size than their corrosponding Na-clays. The same behavior was observed for the organified rectorite (Liu, Wang and Wang, 2010).

4.2. Adsorption of Arsenite onto Na-MO

The prepared Na-MO adsorbent was applied for the removal of arsenite from artificial polluted water through batch mode، making use of different variables like dose, agitation time، temperature, initial concentration of arsenite (III) ions and pH. Experiments were carried out so that the effect of any one variable was studied, keeping all others constant.

4.2.1. Initial Concentration Effect

The effect of initial concentration was studied using varied concentrations of As(III) solutions at pH of 8, agitated with 20 $g.L^{-1}$ Na-MO for 3 hours at 30 °C. Results were shown in **Figure 4-12.**

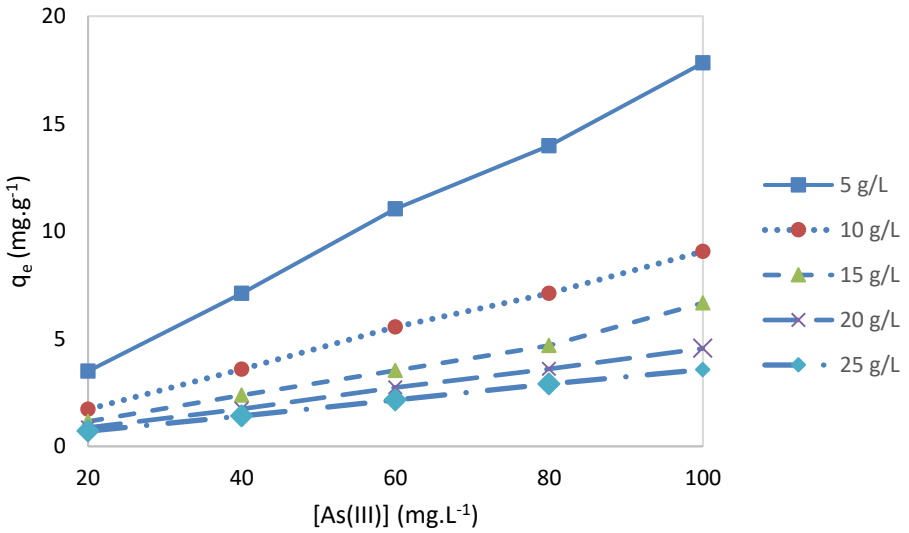

Figure 4-12: Initial concentration effect on As(III) adsorption onto Na-MO adsorbent. Conditions: pH of 8, 30 °C, 3 hours, 20 $g.L^{-1}$ adsorbent dose

The figure showed that the adsorption capacity was gradually increased as the initial concentration of As(III) increased. It can be proposed that any increase in the initial concentration leads to an increase in mass gradient between the solution and adsorbent, and thus acts as a driving force for the transfer of As(III) molecules from bulk solution to the particle surface.

4.2.2. Dosage Effect

The influence of adsorbent dose in equilibrium uptake was studied at different As(III) initial concentrations (20, 40, 60, 80 and 100 $mg.L^{-1}$) agitated with different dosages (5, 10, 15, 20 and 25 $g.L^{-1}$) at 30 °C for 3 hours. The results were shown in **Figure 4-13**.

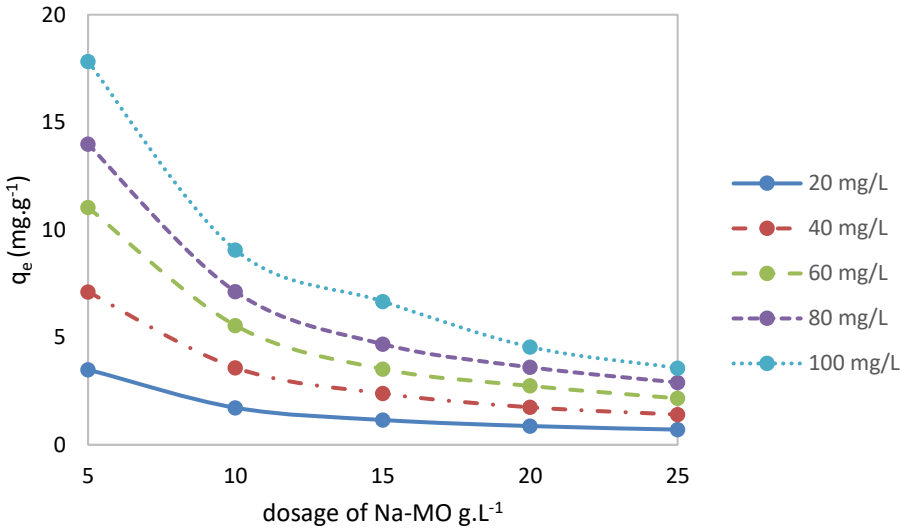

Figure 4-13: Adsorbent dose effect on the adsorption of As(III) onto Na-MO adsorbent. Conditions: pH of 8, 30 °C, 3 hours, conc. (20-100 $mg.L^{-1}$)

The results showed that the adsorption capacity, q_e, decreased with the increase in adsorbent dose, however the % removal increased as the dose increased. This is possibly due to the creation of particles aggregation which reduces the specific surface area and leads to an increase in the diffusional path (Sari and Tuzen, 2014). The second probable is due the reduction of the number of unsaturated sites (Yu, Zhao and Vance, 2001). Furthermore, as

the amount of clay is increased, the pH of the medium increases, which affects the surface boundary and the arsenite speciation, see **Figure (4-17).**

4.2.3. Contact Time Effect

The effect of contact time on the adsorption of As(III) were carried out at 30 °C, using 20 $g.L^{-1}$ of Na-MO adsorbent dose and varied the As(III) concentrations between 20 to 100 $mg.L^{-1}$ at normal pH. Results were illustrated in **Figure 4-15**.

It was observed that the rate of metal uptake increased rapidly at the beginning and decline throughout the time. After 2 hours, the reaction approaches equilibrium.

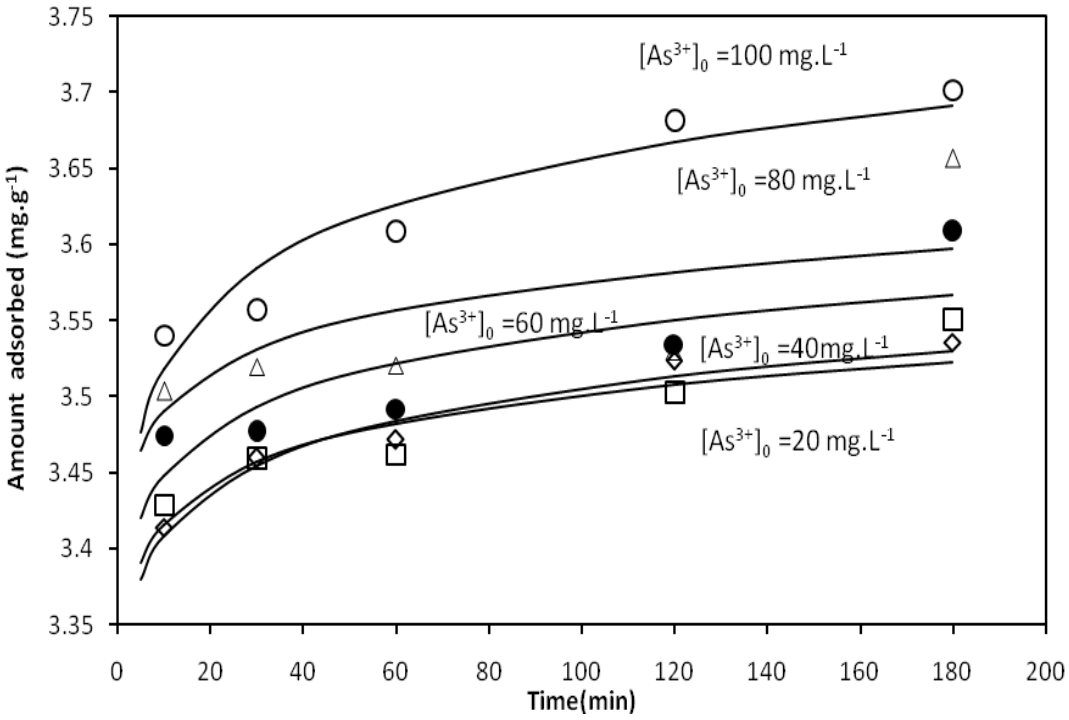

Figure 4-14: Contact time effect on the adsorption of As(III) onto Na-MO. Conditions: initial conc. (20-100 $mg.L^{-1}$), pH of 8, 30 °C, dose of 20 $g.L^{-1}$

4.2.4. Adsorption Isotherm Studies

Isotherm studies for As(III) adsorption onto Na-MO adsorbent, were performed using 20 $mg.L^{-1}$ As(III) solution at normal pH agitated for 3 hours with varied dosages (5 to 25 $g.L^{-1}$) at 30 °C. Then the data was fitted to the

Langmuir and Freundlich isotherms models to describe the mechanism of the adsorption process of As(III) onto Na-MO.

Both the Langmuir and Freundlich nonlinear forms, **Equations (7)** and **(10)**, with two adjustable parameters were numerically solved using the solver program of Microsoft excel with Newton method (Hossain, Ngo and Guo, 2013).

The mean square error (MSE, objective function) used for data analysis, was based on the relative deviation between experimental value, $q_{e,exp}$ and theoretical value, $q_{e,model.}$ It was calculated from **Equation (17)**:

$$MSE = \sum_{i=1}^{N} \left(\frac{q_{e.exp} - q_{e.model}}{q_{e.exp}} \right)^2 \quad \ldots\ldots\ldots\ldots\ldots\ldots (17)$$

The root mean square error (RMSE, percentage deviation) function was calculated for the different models using **Equation (18)**:

$$\%RMSE = \sqrt{\frac{1}{N-m} \sum_{i=1}^{N} \left(\frac{q_{e.exp} - q_{e.model}}{q_{e.exp}} \right)^2} \times 100 \quad \ldots\ldots\ldots (18)$$

where: *N* is the number of experimental points and *m* is the number of identified parameters. **Equation (18)** indicates the performance of the best fit between the experimental and predicted curves.

A comparison between the experimental amount of As(III) adsorbed per unit weight of clay and the simulated data using Langmuir or Freundlich isotherms is shown in **Figure 4-15**.

The parameters (q_{max}, K_L , K_F and n) and root mean square deviation for each S/L ratio were calculated and summarized in **Table 4-7**.

The results revealed that Freundlich model fitted As(III) adsorption data, at different dosages, better than Langmuir isotherm model, this fact was confirmed with the small RMSE values of Freundlich model compared with

Langmuir model. When n > 1, a repulsive forces between sorbed molecules is exist (Ghorbanzadeh *et al.*, 2015). But the values of n as reported in **Table 4-7** were less than unity, hence there were no repulsive forces and adsorption is favorable. This might be due to the heterogeneous distribution of active sites on the clay surface as suggested by Freundlich.

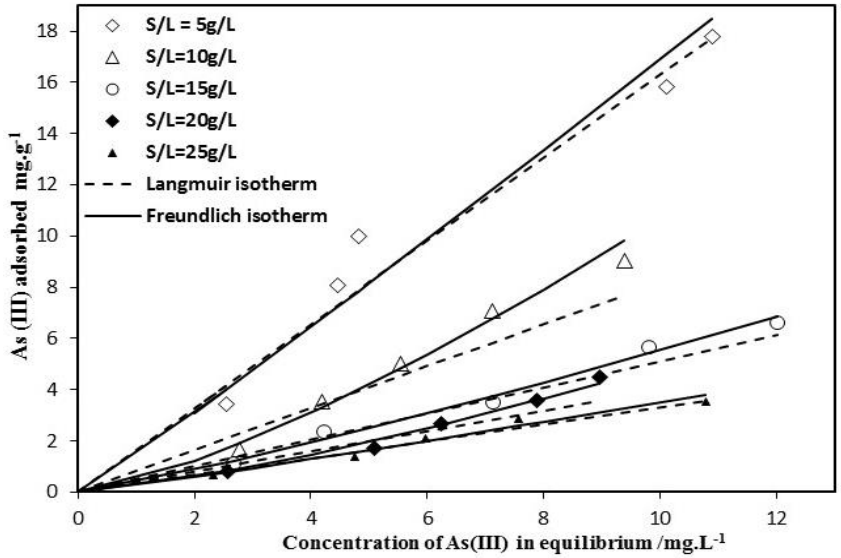

Figure 4-15: Equilibrium isotherms for the adsorption of As(III) onto Na-MO. Conditions: dose (S/L) 5–25 $g.L^{-1}$, 308 K, $[As(III)]_0$ = 20 $mg.L^{-1}$, pH of 8

Table 4-7: Isotherm parameters for As(III) adsorption onto MO-Na

Dose ($g.L^{-1}$)	Langmuir			Freundlich		
	q_{max} ($mg.g^{-1}$)	K_L ($L.mg^{-1}$)x10^5	RMSE	n	*K_F	RMSE
5	233.1	704	0.18	0.948	1.492	0.17
10	233.1	353	0.24	0.737	0.472	0.09
15	233.2	220	0.15	0.873	0.397	0.09
20	233.3	171	0.21	0.757	0.235	0.11
25	233.2	142	0.12	0.914	0.283	0.10

*K_F ($mg.g^{-1}$).($L.mg^{-1}$)$^{1/n}$

4.2.5. Adsorption Kinetics Studies

In the literature, different models were used to investigate the kinetics of adsorbent-adsorbate interactions. The kinetics of the adsorption of As(III) from aqueous solutions using different types of clay were well described by a pseudo-second order kinetic model (Maiti, DasGupta, *et al.*, 2007; Zehhaf

et al., 2013; Ren *et al.*, 2014; Zhao, Guo and Zhou, 2014; Öztel, Akbal and Altaş, 2015). This model assumes that the limiting step is the surface reaction. But the model is unable to give other important adsorption parameters such as mass transfer coefficient or effective pore diffusivity coefficient. For example (Zehhaf *et al.*, 2013) studied As(III) adsorption onto natural swelling clays (S_{BET} 25-140 m^2/g), they attributed the change of basal spacing d_{001} before and after adsorption to the diffusion of As(III) and As(V) into the inter-layers of clay. Thus, they proposed that the adsorption mechanism could be studied using intraparticle diffusion model (Bektaş, Aydın and Öncel, 2011).

Here, the pseudo-second order model and the intraparticle model based on Weber-Morris equation were tested. When plotting q_e vs. $\sqrt{t}$, straight-line were gained, indicating the possibility of intraparticle transfer as a rate limiting step, as displayed in **Figure 4-16**. The fitted constants for the intraparticle diffusion and pseudo-second order models were calculated and shown in **Table 4-8**.

The results showed that the adsorption of As (III) onto Na-MO adsorbent fitted well with the intraparticle model due to the low RMSE at different dosages. K_{id} lays between (1.1-1.8) $x10^{-2}$ $mg.g^{-1}.min^{-1/2}$.

Table 4-8: Kinetic parameters for As(III) adsorption onto Na-MO at different doses. Conditions: initial As(III) conc. (20-100 $mg.L^{-1}$), pH 8, 30 °C, 3 hours

	Pseudo-second order			**Intra particle diffusion**		
doses $g.L^{-1}$	k_2 $g.mg^{-1}.min^{-1}$	q_e $mg.\ g^{-1}$	RMSE	k_{id} $mg.\ g^{-1}.min^{-1/2}$	Intercept $mg.\ g^{-1}$	RMSE
5	0.364	3.55	0.021	0.01198	3.38	0.003
10	0.284	3.55	0.033	0.01107	3.39	0.004
15	0.211	3.62	0.046	0.01259	3.41	0.007
20	0.184	3.64	0.056	0.01191	3.44	0.012
25	0.227	3.73	0.034	0.01720	3.47	0.004

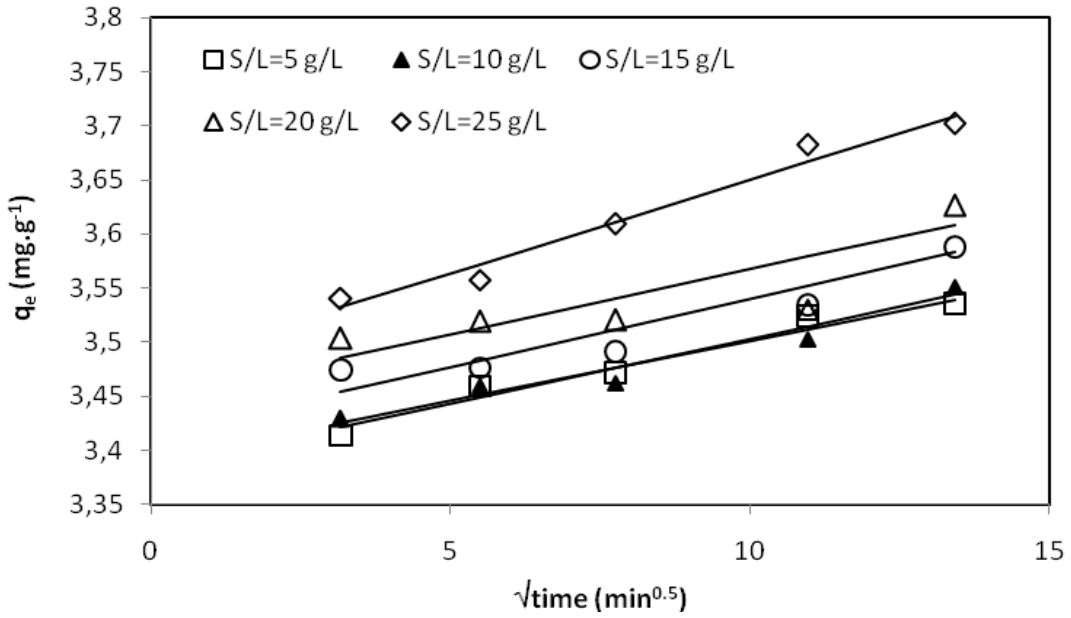

Figure 4-16: Intraparticle diffusion model at different As(III) doses. Conditions: (initial As(III) conc. (20-100 mg.L^{-1}), pH of 8, 30 °C, 3 hours)**.**

4.2.6. Adsorption Thermodynamic Studies

The thermodynamic parameters for the adsorption of As(III) onto Na-MO sample were determined at different temperatures (20-50 °C) using 20 mg.L^{-1} As(III) solution, at normal pH agitated with 5 g.L^{-1} adsorbent dose for 3 hours. The parameters were calculated and reported in **Table 4-9.**

The negative ΔG° values stated that the adsorption is thermodynamically favorable and spontaneous. The negative ΔH° value indicated that arsenite adsorption onto Na-MO adsorbent is exothermic process.

Table 4-9: Thermodynamic constants for the adsorption of arsenite on Na-MO: Conditions: 20 mg.L^{-1} As(III) solution, at normal pH, 5 g.L^{-1} dose, 3 hours.

T (K)	**ΔG°** (kJ.mol^{-1})	**ΔH°** (kJ.mol^{-1})	**ΔS°** (J.mol^{-1}.K^{-1})
298	-9.3	-4.588	15.8
308	-9.8		16.8
318	-10.2		17.6
328	-10.7		18.7

However, the positive ΔS° values indicating an increase in the randomness at the interface clay-arsenite solution and showing the high affinity of the

adsorbent for As(III). Furthermore, it suggests some structural changes in the arsenic types. For example, in natural water, the major arsenite species are H_3AsO_3, $H_2AsO_3^-$ and $HAsO_3^{2-}$ (Öztel, Akbal and Altaş, 2015). In acidic medium, As(III) adsorption is not favorable (Anjum *et al.*, 2011). The speciation of As(III) as function of the solution pH were shown in **Figure 4-17** as reported by (Chibban *et al.*, 2012).

In the pH range 0-9, the adsorbed species is mainly the H_3AsO_3 whereas at pH range 10-11, the anionic form $H_2AsO_3^-$ dominates. All experimental work of this study were conducted in this range, thus the interaction of arsenite species on clay surface can be described schematically as follows (Maiti, Dasgupta, *et al.*, 2007):

$$\equiv MOH + H_3AsO_3 \rightarrow \equiv MH_2AsO_3 + H_2O \quad \ldots\ldots\ldots\ldots\ldots\ldots\ldots\ldots (18)$$

$$2\equiv MOH + H_3AsO_3 \rightarrow [\equiv MHAsO_3M\equiv] + 2H_2O \quad \ldots\ldots\ldots\ldots\ldots\ldots (19)$$

$$\equiv MOH_2^+ + H_2AsO_3^- \rightarrow \equiv MH_2AsO_3 + H_2O \quad \ldots\ldots\ldots\ldots\ldots\ldots\ldots (20)$$

Where ≡MOH represents a reactive surface hydroxyl and M represents Si or Al/Fe. **Equation (18)** represents monodentate ligand exchange and **Equation (19)** represents the bidentate step. Whereas, **Equation (20)** depicts the reaction at the protonated surface. All reaction products and stoichiometry are identified by (Maiti, Dasgupta, *et al.*, 2007), using X-ray spectroscopy (XAS).

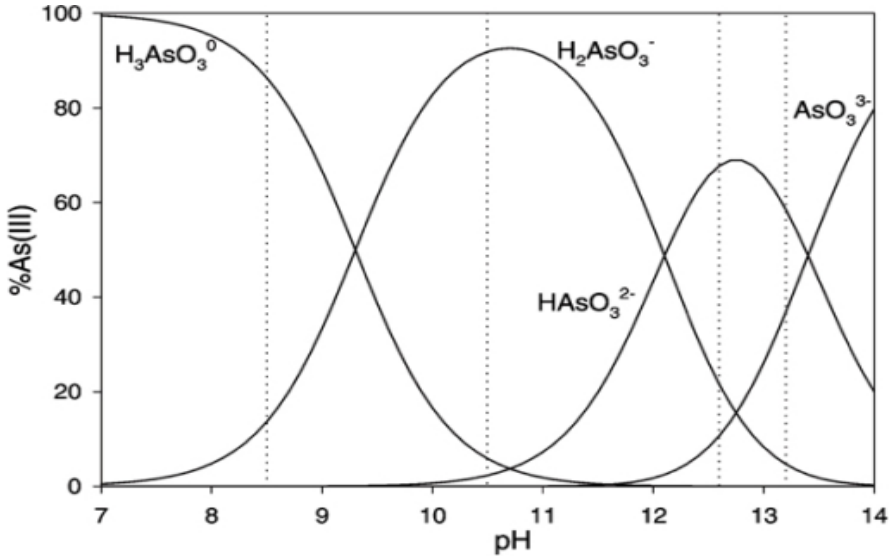

Figure 4-17: Distribution of As(III) as function of pH (Chibban *et al.*, 2012)

4.3. Adsorption of Cationic Dyes onto Na-MO

The applicability of Na-MO sample for the removal of MB and CV dyes from aqueous solutions was investigated using batch mode experiments. The results were shown and discussed in the following sections.

4.3.1. pH Effect

The adsorption behavior of MB and CV onto Na-MO clay was studied over a wide range of pH, using 100 $mg.L^{-1}$ initial dye concentration, agitated at 30 °C with 1.0 $g.L^{-1}$ Na-MO adsorbent dose for 3 hours. The results were shown in **Figure 4-18**.

There was an increase in the amount of dye adsorbed with increasing the pH value for both dyes. The lower adsorption of MB and CV at acidic pH is probably due to the presence of excess H^+ ions competing with the cationic dyes toward the adsorption sites. At higher pH (pH >7), the clay surface will be more negatively charged, giving rise to more easily association between the cationic dye and the adsorbent surface.

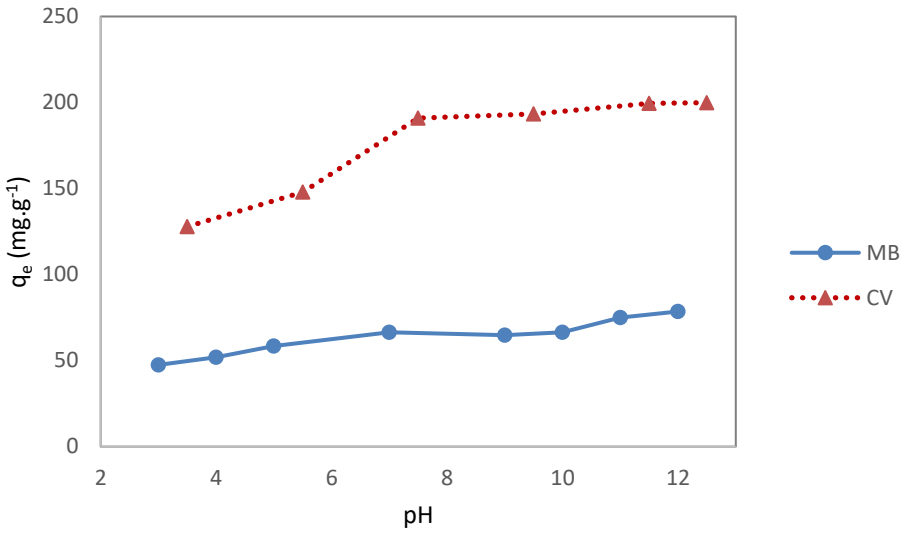

Figure 4-18: pH effect on adsorption of MB and CV onto Na-MO. Conditions: initial concentration 100 mg.L^{-1}, dose 1 g.L^{-1}, 3 hours, 30 °C.

4.3.2. Dosage Effect

The effect of adsorbent dosage on adsorption of MB and CV onto Na-MO was studied, using 100 mg.L^{-1} CV and 80 mg.L^{-1} MB initial concentration at their normal pH, 7.5 and 7 for CV and MB, respectively. agitated with varied adsorbent dose (0.5-2.0) g.L^{-1} at 30 °C for 3 hours. The results were shown in **Figure 4-19**.

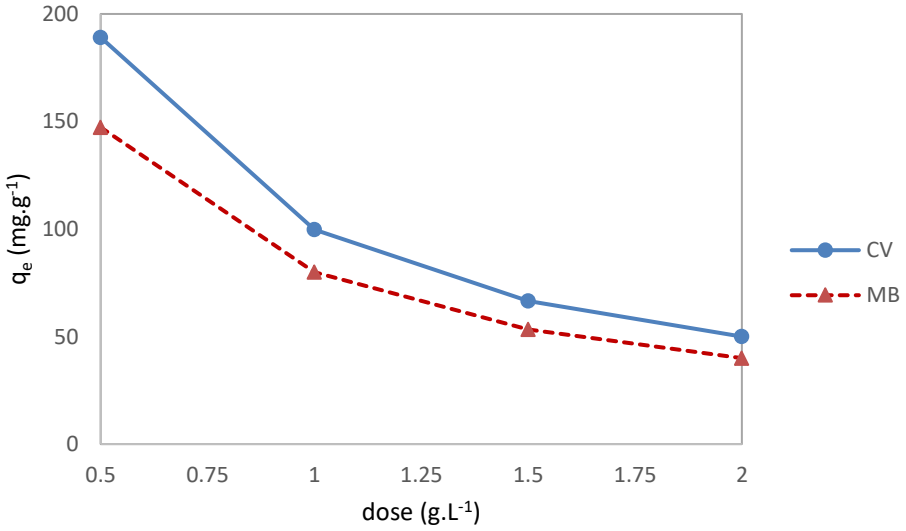

Figure 4-19: Dose effect on adsorption of MB and CV onto Na-MO. Conditions: [MB] 80 mg.L^{-1}, [CV] 100 mg.L^{-1}, 3 hours, 30 °C, normal pH

The amount of adsorbed dye decreases gradually, from 189 to 50 $mg.g^{-1}$ for CV and from 147 to 40 $mg.g^{-1}$for MB, with the increase in adsorbent dose. This can be attributed to the increase in the number of active sites as the adsorbent material dosage increased, so in the following experiments, 1.0 $g.L^{-1}$ was selected as optimum adsorbent dose.

4.3.3. Contact Time Effect

Contact time effect on the adsorption of MB and CV dyes onto Na-MO, was studied, using 100 $mg.L^{-1}$ initial dye concentration at normal pH, stirred with 1.0 $g.L^{-1}$ of Na-MO dose at 30 °C for different periods. The results were showed in **Figure 4-20**.

It appears that a rapid initial uptake occurs, with equilibrium reached in less than 50 min. For both MB and CV, the adsorption is very rapid in the first 5 minutes and then becomes slower until equilibrium is reached. The rapid initial increase in the amount of adsorbed dye may be due to the increase in the number of vacant sites available at the beginning.

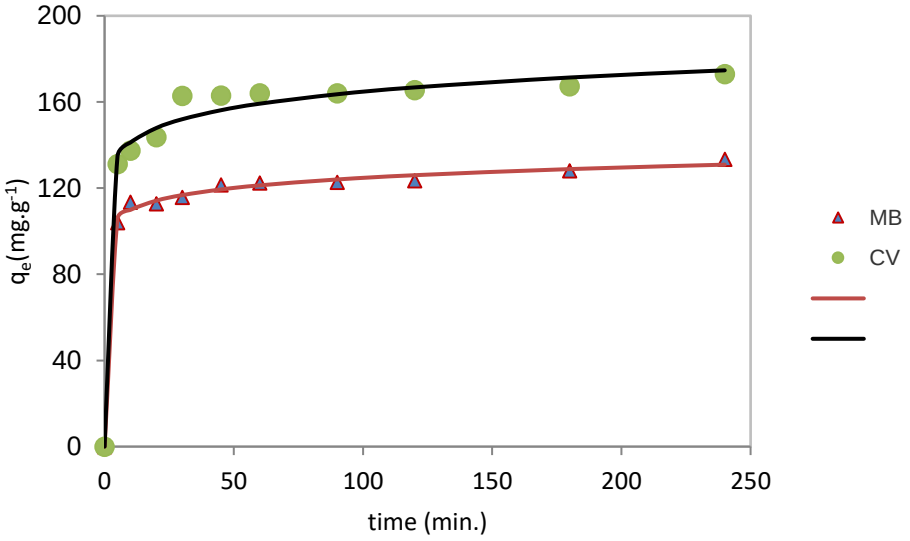

Figure 4-20: Contact time effect on adsorption of MB and CV onto Na-MO: Conditions: initial conc. 100 $mg.L^{-1}$, dose 1.0 $g.L^{-1}$, 30 °C, normal pH

4.3.4. Initial Concentration and Temperature Effect

The initial concentration and temperature effect on the adsorption of both dyes, MB and CV, onto Na-MO, was studied, using different initial dye concentrations (100-300) $mg.L^{-1}$ at their normal pH, stirred with 1.0 $g.L^{-1}$ of adsorbent at varied temperature (20-50) °C for 3 hours. The results for MB and CV were illustrated in **Figure 4-21(A)** and **(B)**, respectively.

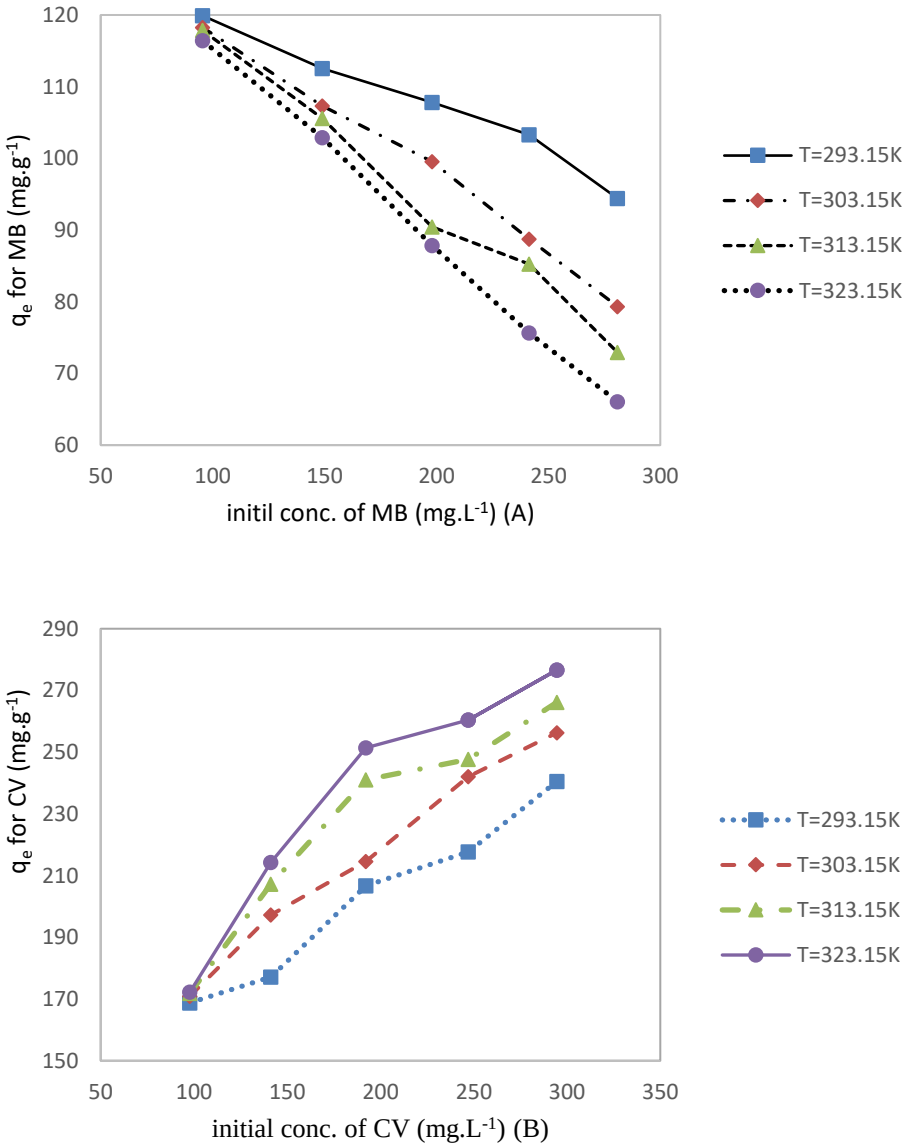

Figure 4-21: Initial conc. and temp. effect on the MB and CV adsorption onto Na-MO (a) MB and (b) CV. Conditions: 3 hours, normal pH, 1 $g.L^{-1}$ dose.

It is observed that the q_e for MB decreases with the increase in solution concentration and temperature, therefore, adsorption of MB onto Na-MO adsorbent is not favored at high concentrations and temperatures. While the q_e for CV increases with the increase in solution concentration and temperature, thus it is favored at high concentration and temperatures.

The difference behavior between these isotherms is probably due to the different adsorption mechanisms of the two monovalent cationic dyes. Two studies (Rytwo, Nir and Margulies, 1995; Rytwo *et al.*, 1998) from literature concluded that the interactions between CV molecules and natural clay differ in certain aspects from those between MB and clay due to the amount of charged complexes formed between two dye molecules (monomer, dimmer or trimer).

The aggregation of MB molecules in solution also reduces its adsorption on the clay. But, at low temperature, there is a competition between MB molecules and water molecules in the inter-lamellar spaces of clay and it is well known that the adsorption of water molecules on a solid is higher at lower adsorption temperature.

4.3.5. Adsorption Isotherm Studies

The isotherms data were analysed with the linear forms of the Lanmguir and Freundlich models. Equilibrium adsorption data were well described by the Langmuir model for both dyes, MB and CV, with a high correlation coefficient (R^2), as shown in **Table 4-10**. Similar behavior was observed by (Al-Futaisi, Jamrah and Al-Hanai, 2007).

The results of **Table 4-10** also showed that an increase in temperature promoted a decrease in the maximum adsorption of MB. The Langmuir monolayer capacity, q_{max}, was found to be 62.5 $mg.g^{-1}$ at 50°C. (Özdemir, Doğan and Alkan, 2006; Elmoubarki *et al.*, 2015) reported similar result.

Table 4-10: Isotherm parameters for the adsorption of MB and CV onto Na-MO

Dye	T (K)	Langmuir			Freundlich		
		q_{max} ($mg.g^{-1}$)	K_L ($L.mg^{-1}$)	R^2	n	$*K_F$	R^2
MB	293	100.0	-0.0649	0.99	-5.7	494.2	0.88
	303	76.9	-0.0425	0.98	-3.1	1075.9	0.93
	313	71.4	-0.0375	0.98	-2.7	1314.1	0.95
	323	62.5	0.0320	0.97	-2.1	2024.5	0.97
CV	293	330.0	0.0492	0.98	3.95	150.3	0.98
	303	330.0	0.0612	0.99	5.12	214.2	0.96
	313	330.0	0.0857	0.99	5.88	1314.1	0.96
	323	330.0	0.0789	0.98	6.06	2024.5	0.96

$*K_F$ $(mg.g^{-1}).(L.\ mg^{-1})^{1/n}$

For the CV adsorption, it appears that the q_{max} is temperature independent. The parameters K_L, n and K_F are also in the same order of magnitude to those reported in literature (Al-Futaisi, Jamrah and Al-Hanai, 2007; Gao *et al.*, 2016; Kumar, Sen and Bhattacharyya, 2016). Calculated constants values for Langmuir (K_L) and Freundlich (n) can be interpreted as the free energy of adsorption and the adsorption intensity respectively. The high values of K_F reflect a high adsorption capacity of the Na-MO adsorbent.

4.3.6. Adsorption Thermodynamics Studies

The thermodynamic behavior of the adsorption of MB and CV dyes onto Na-MO sample were investigated, using different initial concentrations at their normal pH, agitated with 1.0 $g.L^{-1}$ of adsorbent at varied temperature (20-50) °C for 3 hours. The calculated thermodynamic parameters were listed in **Table 4-11**.

The enthalpy of MB adsorption, + 6.5 $kJ.mol^{-1}$, was endothermic and in the same order of magnitude to those reported by (Rytwo and Ruiz-Hitzky, 2003; Hong *et al.*, 2009; Gopinathan, Bhowal and Garlapati, 2017). The negative ΔS° value for MB adsorption suggested a decrease in randomness at the interface between the solid and the solution. However, the positive ΔS° value for CV attributed to an increase in chaos of the system due to CV

adsorption of and showed the high affinity of Na-MO adsorbent for CV molecules. Also, the negative ΔH°value, -9.8 kJ.mol^{-1}, showed an exothermic adsorption process for CV species. Besides, the ΔG° values for both dyes were < 20 kJ.mol^{-1} (between -9.25 and +7.44 kJ.mol^{-1}) showed that the adsorption of MB and CV were physical process in nature.

Table 4-11: Thermodynamic constants for the adsorption of MB and CV onto Na-MO adsorbent. Conditions: (3 hours, normal pH, 1.0 g.L^{-1} dose).

Dye	T (K)	**ΔG°** (kJ.mol^{-1})	**ΔH°** (kJ.mol^{-1})	**ΔS°** (J.mol^{-1}.K^{-1})
MB	293.15	+ 6.75	+ 6.5	- 23.0
	303.15	+ 6.98		
	313.15	+ 7.20		
	323.15	+ 7.44		
CV	293.15	- 8.31	- 9.8	+ 28.5
	303.15	- 8.63		
	313.15	- 8.90		
	323.15	- 9.25		

4.4. Adsorption of Anionic Dye Congo Red

Batch experiments were applied to investigate the adsorption capacities of the three adsorbents, Na-MO, Surf-MO and Surf-NI, for CR removal. The results were illustrated and discussed in the following sections.

4.4.1. pH Effect

The pH effect on the adsorption capacity of the three adsorbents for CR was done using 150 mg.L^{-1} CR solution adjusted to different pH values then agitated with 0.6 g.L^{-1} adsorbent dose at 30 °C for 3 hours. The results were shown in **Figure 4-22**.

The figure showed that the highest adsorption capacities were observed at lower pH. i.e. on pH 5, q_e for Na-MO, Surf-MO and Surf-NI were 67, 80 and 125 mg.g^{-1}, respectively. Moreover, when the pH was increased from pH 7 to 11, slight decrease in amount of CR adsorbed, q_e, were observed. The minor decrease may be attributed to the high repulsion between acidic CR

molecules and the hydroxide ion at the surface of clay, especially at a higher pH value. Similar trends were reported by (Hu *et al.*, 2010).

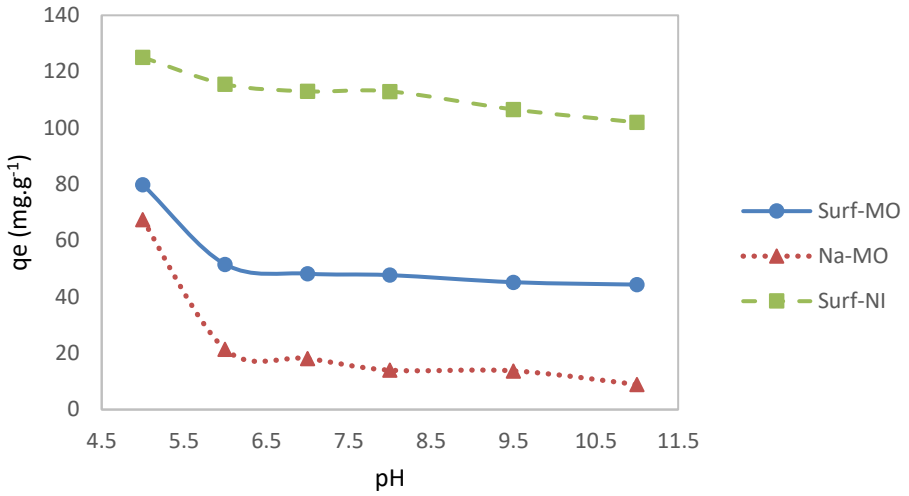

Figure 4-22: pH effect on CR adsorption onto Surf-Clays and Na-MO. Conditions: [CR]=150 mg.L^{-1}, dose 0.6 g.L^{-1}, 30 °C, 3 hours

4.4.2. Dosage Effect

The dosage effect studies on the adsorption capacity of CR onto the three adsorbents, were done by agitating varied dose of each adsorbent between 0.2 to 2.2 g.L^{-1}, with 150 mg.L^{-1} CR solution adjusted to pH of 6 at 30 °C for 180 min. The results were illustrated in **Figure 4-23**.

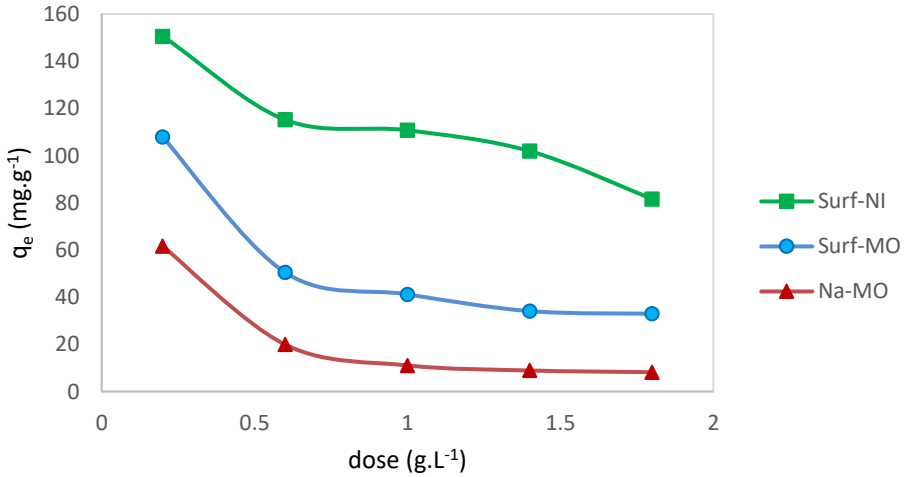

Figure 4-23: Dose effect on CR adsorption onto Surf-Clays and Na-MO Conditions: [CR]=150 mg.L^{-1}, pH 6, 30 °C, 3 hours.

This figure indicated that the adsorption capacity, q_e, for CR adsorbed onto the adsorbents, Na-MO, Surf-MO and Surf-NI, was rapidly decreaed by increasing the dosage from 0.2 to 0.6 $g.L^{-1}$. Thenafter, slight dcrease was observed, because of the increase in the number of active sites as the adsorbent dose increased. Meanwhile the % removal of CR was increased as the dosages increase. (the Plot was not shown here).

4.4.3. Contact Time Effect

The contact time effect studies on the adsorption capacity of CR onto the three adsorbents, were carried out by varying the time from 5 to 240 min., using 150 $mg.L^{-1}$ CR solution with pH adjusted to 6 and 0.6 $g.L^{-1}$ of adsorbent dose at 30 °C. The results were shown in **Figure 4-24**.

The figure illustrated that the amount of anionic dye CR adsorbed onto all studied adsorbent was enhanced rapidly during the first 50 minutes of contact between the adsorbate and the adsorbent, then the rate slowed down gradually until the equilibrium was reached at less than 120 minutes.

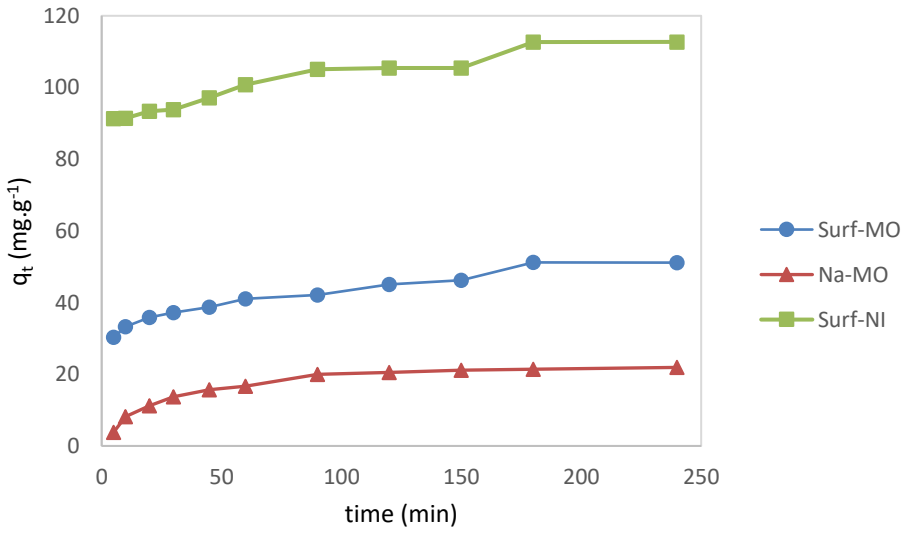

Figure 4-24: Time effect on CR adsorption onto Surf-Clays and Na-MO: Conditions: dose 0.6 $g.L^{-1}$, [CR]=150 $mg.L^{-1}$, pH 6, temp. 30 °C

4.4.4. Adsorption Kinetics Studies

The pseudo-first-order and pseudo-second-order models were used to fit the data of the contact time effects studies. Illustrations of the kinetic data according to the two models were given in **Figure 4-25** and **Figure 4-26,** respectively.

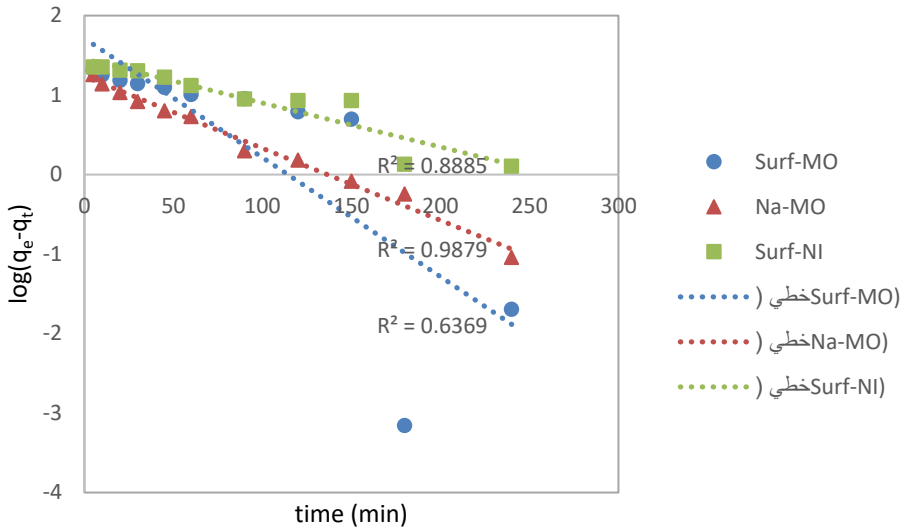

Figure 4-25: PFO kinetic plots for CR adsorption on Surf-Clays and Na-MO. Conditions: dose 0.6 g.L^{-1}, pH 6, 3 hours, 30 °C

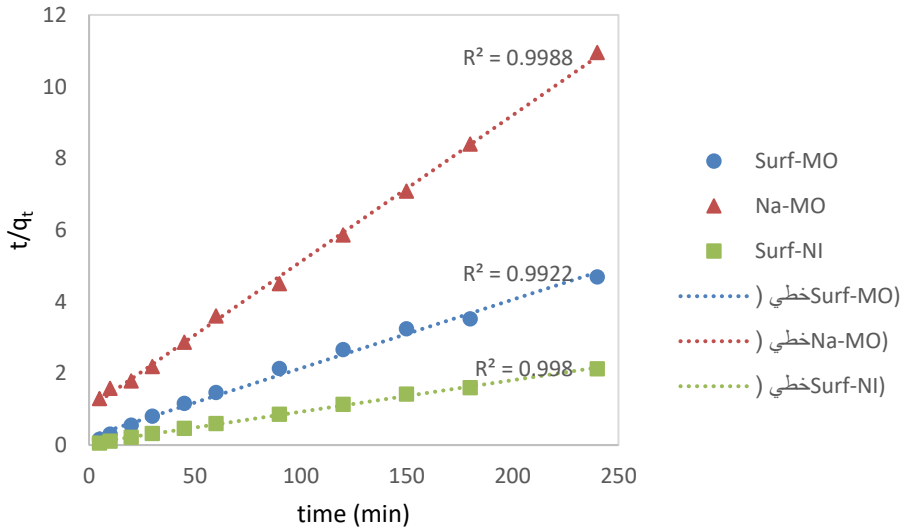

Figure 4-26: PSO kinetic plots for CR adsorption on Surf-Clays and Na-MO. Conditions: dose 0.6 g.L^{-1}, pH 6, 3 hours, 30 °C

The kinetics parameters for both models were listed in **Table 4-12**.

A higher R^2 value (>0.99) denoted better model fitting, therefore the pseudo-second-order model was the suitable approach for predicting the adsorption kinetics of CR onto Surf-NI, Surf-MO and Na-MO.

Table 4-12: Kinetic parameters of CR adsorption onto Surf-clays and Na-MO

adsorbent		Pseudo-first order			Pseudo-second order		
	q_e(exp)	q_e(cal.) ($mg.g^{-1}$)	K_1 $x10^{-2}$ (min^{-1})	R^2	q_e(cal.)	*K_2 $x10^{-3}$	R^2
Surf-MO	51.20	51.63	3.4545	0.6369	52.36	1.588	0.9922
Na-MO	21.91	17.23	2.0957	0.9879	24.51	1.616	0.9988
Surf-NI	112.7	28.38	1.2667	0.8885	113.64	1.610	0.9980

*K_2: $g.(mg.min)^{-1}$

4.4.5. Adsorption Isotherm Studies

To investigate the interaction between CR dye and Surf-NI, Surf-MO and Na-MO, Langmuir model and Freundlich model were tested to fit the experimental data. The Langmuir isotherm assumes that the adsorption of CR occurs in a monolayer, while the Freundlich isotherm assumes that the adsorption occurs in multilayers on heterogeneous surface and proceeds in a reversible way.

Langmuir and Freundlich isotherms parameters; the maximum adsorption capacity, q_{max}, Langmuir adsorption constant K_L, the Freundlich constant, K_F and the adsorption intensity factor n, were evaluated and summarized in **Table 4-13**.

Table 4-13: Isotherm parameters for CR adsorption onto Surf-clays and Na-MO

Adsorbent	Langmuir			Freundlich		
	q_{max} ($mg.g^{-1}$)	K_L ($L.mg^{-1}$)	R^2	n	*K_F	R^2
Na-MO	5.8	-0.010	0.9955	5.60	2.05	0.9988
Surf-MO	83.3	0.011	0.9955	2.88	8.33	0.9680
Surf-NI	91.7	-0.0526	0.9990	10.5	170.1	0.9447

*K_F $(mg.g^{-1}).(L.mg^{-1})^{1/n}$

Based on the correlation coefficient values, it was possible to conclude that the Langmuir model (R^2 > 0.99) was better fit the experimental data than the

Freundlich isotherm, so CR adsorption onto all adsorbents was a monolayer formation. In case of Surf-MO, the q_{max} calculated from the Langmuir isotherm is equal to 83 $mg.g^{-1}$ at 293 K which was equal to the experimental value. The maximum adsorption capacity of Na-MO for the removal of CR was comparable to that reported for CR adsorption onto pure Kaolin (Bentahar *et al.*, 2017).

4.4.6. Adsorption Thermodynamic Studies

Thermodynamic parameters; (ΔG°), (ΔH°) and (ΔS°), help to evaluate the effect of temperature on the adsorption of CR onto Na-MO, Surf-MO and Surf-NI, hence provide comprehensive information about the inherent energy changes associated with the adsorption process. Tests were done at varied temperatures using 0.6 $g.L^{-1}$adsorbent dose, and 150 $mg.L^{-1}$ CR solution at pH 6 for 4 hours. Then, ln K_c vs. 1/T were plotted and showed in **Figure 4-27**, and the thermodynamic parameters were computed and listed in **Table 4-14**.

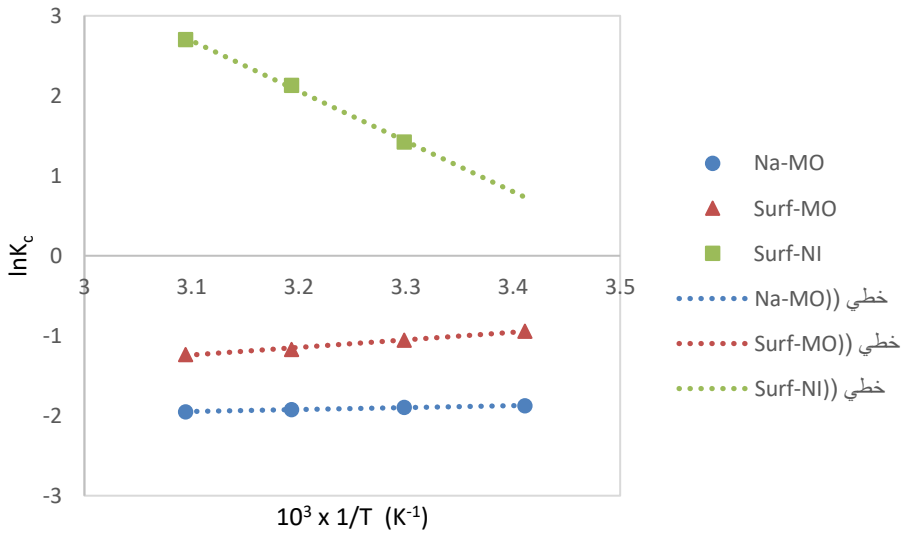

Figure 4-27: Ln K_c vs 1/T for CR adsorption on Surf-clays and Na-MO Conditions: [CR] 150 $mg.L^{-1}$, 3 hours, pH 6 and dose 0.6 $g.L^{-1}$.

Table 4-14: Thermodynamic parameters for CR adsorption onto Surf-Clays and Na-MO

adsorbent	ΔS° ($J.mol^{-1}.K^{-1}$)	ΔH° ($kJ.mol^{-1}$)	ΔG° ($kJ.mol^{-1}$)			
			293	303	313	323
Na-MO	-22.5	-2.1	4.56	4.78	5.01	5.23
Surf-MO	-34.7	-7.9	2.30	2.65	2.99	3.34
Surf-NI	184.4	15.8	-	-40.05	-41.37	-42.70

The values of ΔG˚ for the adsorption of CR onto Na-MO and Surf-MO, were found to be positive at various temperatures, while both of ΔH˚ and ΔS˚ were found to be negative. Therefore, the positive values of ΔG˚ and the negative value of ΔH˚ indicate the adsorption is nonspontaneous and exothermic, and negative ΔS˚ value of the adsorption process indicates a decrease of the randomness at the adsorbent-adsorbate interface during the adsorption (Te, Wichitsathian and Yossapol, 2015). These values are in the order of magnitude with those reported for CR adsorption onto natural serpentine (Shaban, Abukhadra, *et al.*, 2018).

In the other hand, the values of ΔG˚ was found to be negative for the adsorption of CR onto Surf-NI, indicates the adsorption is spontaneous. Whereas both of ΔH˚ and ΔS˚ were found to be positive. The positive of ΔH˚ indicates the adsorption is endothermic, and positive ΔS˚ indicates an increase of the randomness at the adsorbent-adsorbate interface.

4.5. Adsorption of Phenol onto Surf-Clays

Batch experiments were done to investigate the efficiency of Surf-MO and Surf-NI adsorbents for phenol removal from aqueous solutions, the results were presented and discussed in the following sections.

4.5.1. pH Effect

The pH of an aqueous solution strongly affects the clay surface charge and the ionization degree of the adsorbate. To evaluate the pH effect on the adsorption of phenol onto both Surf-clays, experiments were carried out

using 0.6 g.L^{-1} adsorbents dose, 155.5 mg.L^{-1} initial phenol concentration for 3 hours at 30 ˚C. The solutions pH was varied between 3.5-9.5. The results were shown in **Figure 4-28**.

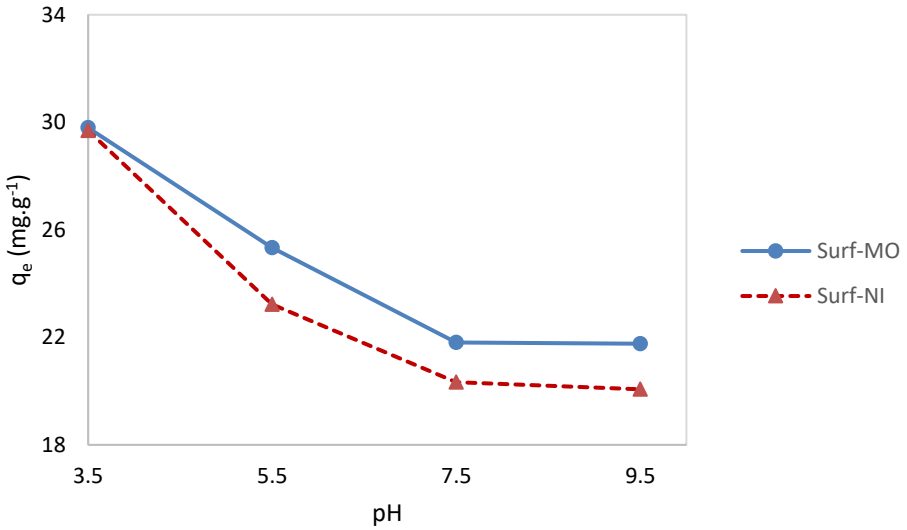

Figure 4-28: pH effect on phenol adsorption onto Surf-clays adsorbents

Conditions: [phenol] =155.5 mg.g^{-1}, dose 0.6 g.L^{-1}, 3 hours, 30 °C.

The results illustrated that the amount of the adsorbed phenol onto both Surf-clays was decreased as the pH of the solution increased. Because by raising the pH, the ionization degree of phenol and the quantity of hydroxyl ions increase, hence an electrostatic repulsion is formed between the negatively charged surface sites of the adsorbent and phenol ions. (Numbonui Ghogomu *et al.*, 2015; Alizadeh, Delnavaz and Shakeri, 2018) reported similar results**.** Thus 3.5 was set as the optimum pH.

4.5.2. Dosage effect

To select the optimum dose of Surf-clays for phenol removal, batch experiments were performed using varied adsorbents dose (0.6-2.2 g.L^{-1}) with initial phenol concentration of 155.5 mg.L^{-1} and pH 3.5, for 3 hours at 30 ˚C. The results were shown in **Figure 4-29**.

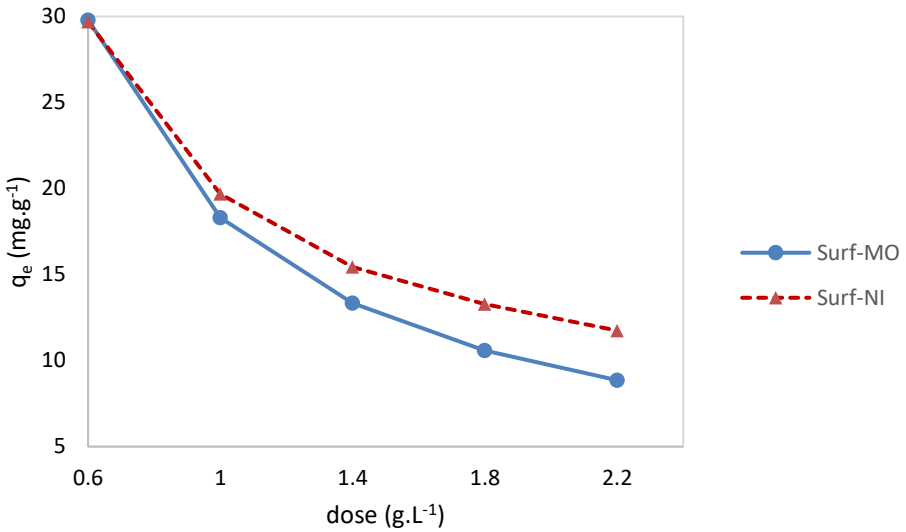

Figure 4-29: Dose effect on phenol adsorption onto Surf-clays adsorbents

Conditions: [phenol] =155.5 mg.g^{-1}, pH = 3.5, 3 H, Temp. = 30 °C.

The figure showed that the capacity, q_e, of adsorbed phenol decreased as the dose increased, in contrast to the % removal which increased as the dose increased (the plot was not shown). Similar results were reported (Ismail, Eltayeb and A, 2013). Thus, the selected optimal dose for phenol removal was set as 1.0 g.L^{-1}, because there were slightly difference in q_e values between the two adsorbents.

4.5.3. Contact Time Effect

The adsorption of phenol onto both organo-clays was studied as a function of contact time to determine the time required for equilibrium. For this, 155.5 mg.L^{-1} of phenol solutions at pH 3.5 were agitated with a dose of 1.0 g.L^{-1} at 30 ˚C. The results were shown in **Figure 4-30**.

The higher adsorption rates at the beginning were due to the availability of adsorption sites of the adsorbents, thus phenol ions were easily adsorbed on these sites. The equilibrium can be reached within 2 hours.

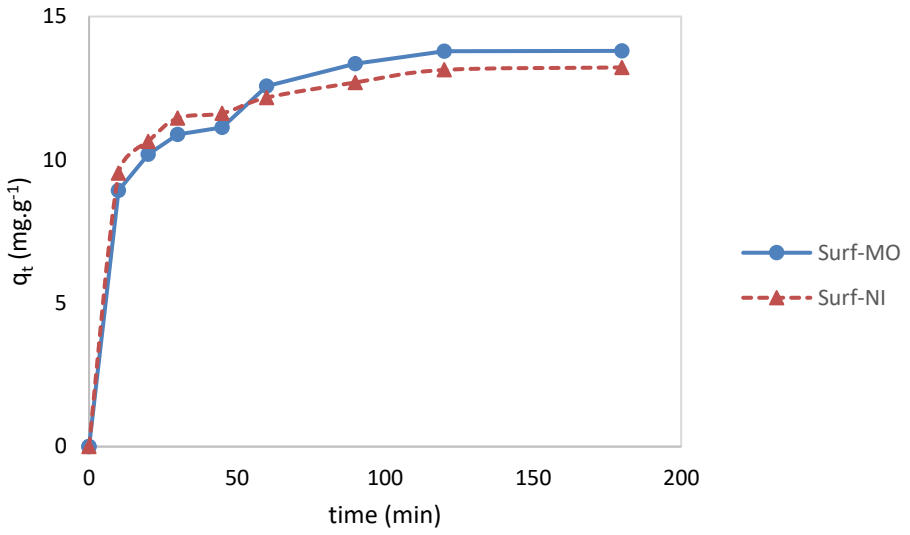

Figure 4-30: Contact time effect on phenol adsorption onto Surf-clays adsorbents. Conditions: [phenol] 155.5 mg.g^{-1}, pH 3.5, dose 1 g.L^{-1}, 30 °C**.**

4.5.4. Adsorption Kinetics Studies

To assess the kinetics of phenol– Surf-clays interactions, the pseudo-first-order and pseudo-second-order models were used to fit the experimental data of (**section 4.5.3**). The plots of log(q_e-q_t) vs. t and t/q_t vs. t for pseudo-first-order and pseudo-second-order models, respectively were shown in **Figure 4-31 (a** and **b).** Moreover, the linear correlation coefficient R^2, and the rate constants k_1 and k_2, as well as the calculated and experimental adsorption capacity, q_e and q_{exp}, respectively, were shown in **Table 4-15**.

The pseudo-second-order model was found to fit the adsorption data better than the pseudo-first-order model, due to the higher value of correlation coefficient (R^2>0.99) and the closer value of the calculated adsorption capacity to the experimental q_{exp} value. Similar results were reported by (Hamdaoui *et al.*, 2018).

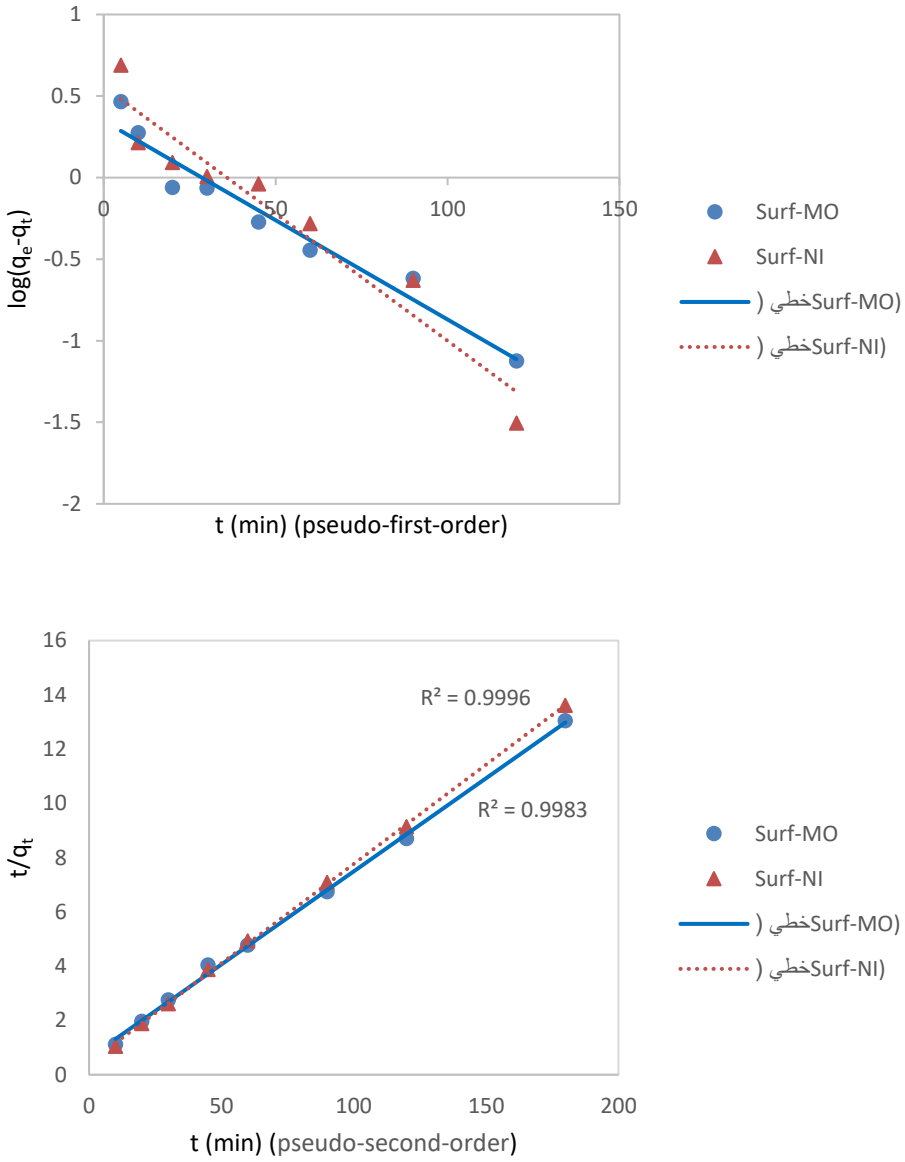

Figure 4-31: kinetic models for phenol adsorption onto Surf-clays

Conditions: [phenol] 155.5 $mg.g^{-1}$, pH 3.5, dose 1 $g.L^{-1}$, Temp. 30 °C.

Table 4-15: Kinetics models' parameters for phenol adsorption onto Surf-clays

adsorbent		Pseudo-first order			Pseudo-second order		
	q_e(exp)	q_e(cal.) ($mg.g^{-1}$)	K_1 x10^{-2} (min^{-1})	R^2	q_e(cal.)	K_2 x10^{-3}	R^2
Surf-MO	13.78	3.62	3.59268	0.9289	14.58	7.5	0.9983
Surf-NI	13.13	2.22	2.80966	0.9502	13.64	12.2	0.9983

*K_2: $g.(mg.min)^{-1}$

4.5.5. Adsorption Isotherm Studies

Langmuir and Freundlich models were used for evaluating the relationship between the amount of phenol adsorbed onto Surf-clays and its equilibrium concentration in aqueous solution. Results were shown in **Figure 4-32**, **Figure 4-33** and **Table 4-16**.

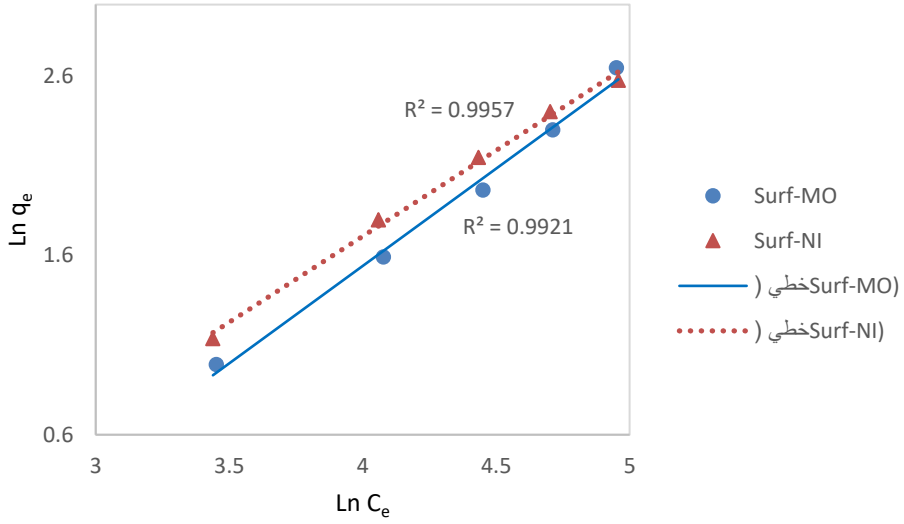

Figure 4-32: Freundlich plots for phenol adsorption onto Surf-clays. Conditions: [phenol] 35-155.5 mg.g^{-1}, pH 3.5, dose 1 g.L^{-1}, 3 hours, 30 °C

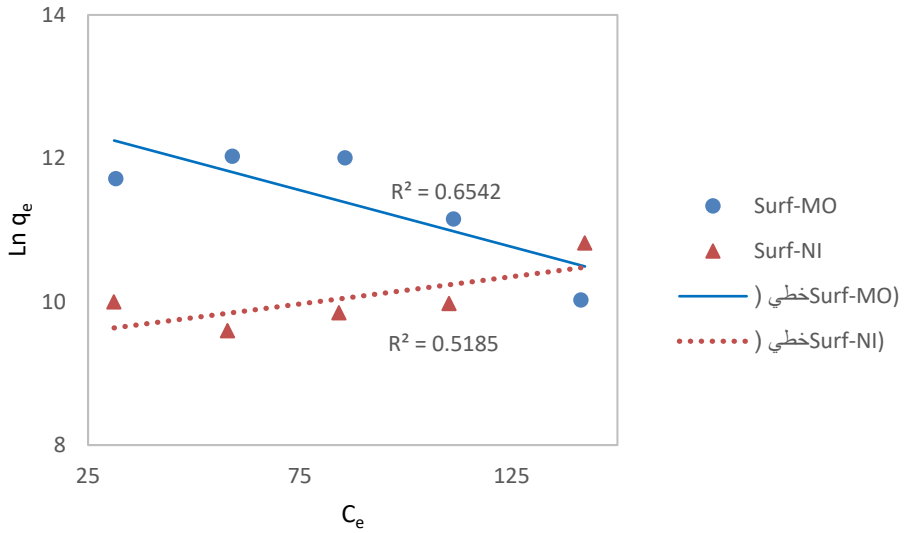

Figure 4-33: Langmuir plots for phenol adsorption onto Surf-clays Conditions: [phenol] 35-155.5 mg.g^{-1}, pH 3.5, dose 1 g.L^{-1}, 3 hours, 30 °C.

Table 4-16: Isotherm parameters for phenol adsorption onto Surf-clays

Adsorbent	Langmuir Model			Freundlich Model		
	q_{max}	K_L(L.mg^{-1})	R^2	1/n	*K_F	R^2
Surf-MO	-63.29	-0.0012	0.6542	0.96	0.1192	0.9957
Surf-NI	131.58	0.0008	0.5185	1.09	0.0605	0.9921

*K_F (mg.g^{-1}).(L. mg^{-1})$^{1/n}$

As seen from the **Table 4-16**, Freundlich model fits to experimental data for phenol adsorption better than the Langmuir model due to the higher linear correlation coefficient (R^2 >0.99) for both Surf-clays. Similar results were reported by (Nourmoradi *et al.*, 2016).

The Freundlich affinity index, 1/n values, were 0.96 and 1.09 for Surf-MO and Surf-NI, respectively. This parameter measures the adsorption intensity or the surface heterogeneity. The adsorption is favorable when 0<1/n<1, irreversible when 1/n=1 and unfavorable when 1/n>1 (Te, Wichitsathian and Yossapol, 2015). Thus, phenol sorption onto Surf-MO (0.96) is favorable compared to Surf-NI (1.09). Moreover, the values of the binding affinity constant, K_F, were 0.1192 and 0.0605 for Surf-MO and Surf-NI, respectively. This shows that the Surf-MO adsorbent is better for the uptake of phenol than Surf-NI adsorbent.

4.5.6. Adsorption Mechanism

The applicability of Freundlich isotherm suggests that different sites with several adsorption energies were involved because the model offers the multilayer adsorption phenomenon and assumes that the surfaces of the adsorbent are heterogeneous and includes different classes of adsorption sites with varied affinities.

The adsorption process of phenol onto both Surf-clays can be controlled by several mechanisms, such as electrostatic interaction between phenol and intercalated surfactant cations, hydrophobic interaction due to the organic

micelles resulting from surfactant intercalation, and the donor–acceptor complex formation between metal cations (Lewis acids) when coordinated with phenol (Lewis bases) in the aqueous solution. Hence, the adsorption system of phenol onto organoclays is likely to involve multilayer sorption (Park, Godwin A. Ayoko, *et al.*, 2013).

4.5.7. Adsorption Thermodynamic Studies

For better understanding the effect of temperature on phenol adsorption onto the Surf-clays, experiments were done at varied temperatures using 1.0 $g.L^{-1}$ adsorbent dose and 100 $mg.L^{-1}$ phenol concentration at pH 3.5 for 3 hours. The results were shown in **Figure 4-34**.The thermodynamic parameters, ΔG^0, ΔS^0 and ΔH^0 were calculated and listed in **Table 4-17**.

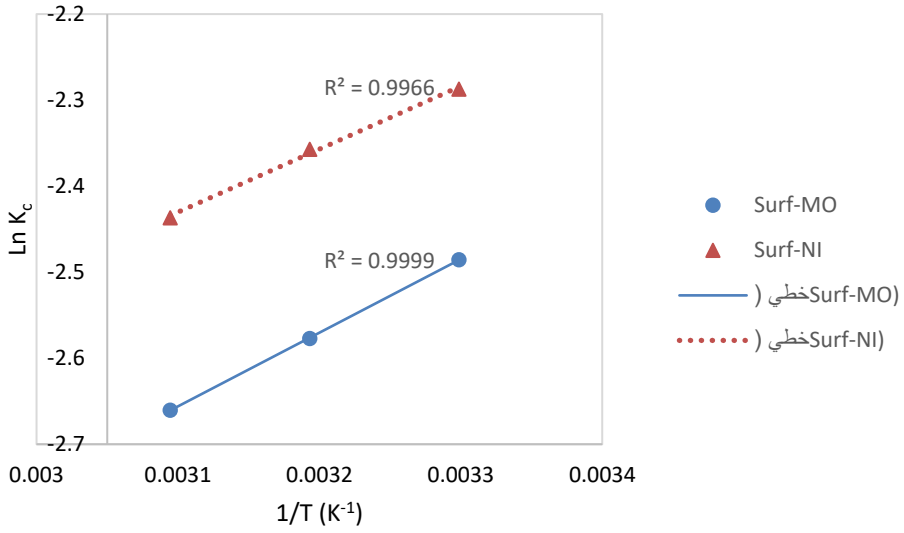

Figure 4-34: Plots of ln K_c vs. 1/T for phenol adsorption onto Surf-clays. Conditions: [phenol] 100 $mg.L^{-1}$, pH 3.5, dose 1 $g.L^{-1}$, (30, 40 and 50 °C).

Table 4-17: Thermodynamic parameters for phenol adsorption onto Surf-clays

adsorbent	ΔS° ($J.mol^{-1}.K^{-1}$)	ΔH° ($kJ.mol^{-1}$)	ΔG° ($kJ.mol^{-1}$)			R^2
			303 K	313 K	323 K	
Surf-MO	44.155	7.119	-6.269	-13.910	-14.360	0.9999
Surf-NI	39.078	6.088	-5.758	-6.149	-6.540	0.9966

The positive value of ΔH^0 for both adsorbents, suggested the endothermic nature for phenol adsorption onto both organo-clays. The positive ΔS^0 values indicated that the adsorption process was accompanied by reasonable increase in entropy and reflect the affinity of both organoclays towards phenol. Meanwhile, the negative values of ΔG^0 suggested the adsorption of phenol onto both organo-clays was a spontaneous process. Moreover, the ΔG^0 values less than -20 $kJ.mol^{-1}$ suggested physical sorption onto both organoclays. Treated Moroccan pyrophyllite showed comparable results (El Gaidoumi *et al.*, 2015).

4.6. Adsorption of Nitrate onto Surf-Clay

Batch experiments were done to investigate the efficiency of Surf-MO and Surf-NI for nitrate removal from aqueous solutions. Poor results were obtained for the removal of nitrate.

Poor results for nitrate removal agreed with (Loganathan, Vigneswaran and Kandasamy, 2013), conclusion after reviewing the removal of nitrate from water using surface modification of the adsorbents, they observed that clay's ability to remove nitrate is negligible. Even after surface modification with surfactant, to provide positive surface charges, they did not reveal noticeable nitrate adsorption capacity. Additionally, the adsorption capacity for nitrate were found to be decreased in the presence of other anions.

4.7. Conclusions and recommendations

4.7.1. Conclusions

Within the boundaries of this study, two natural clay samples were purified and enriched with sodium chloride to improve their adsorption properties. Mineralogical and textural analysis showed that Morocco clay sample was a non-swelling mesopores material composed of illite-kaolinite minerals mixture with specific surface area of 128 $m^2 \cdot g^{-1}$, while the Nile clay sample was swelling clay composed of smectite and illite minerals with specific surface area of 23 $m^2 \cdot g^{-1}$.

Both of Na-MO and Na-NI samples were successfully modified with the cationic surfactant didecyl dimethyl ammonium bromide. The process was confirmed with XRD, FTIR, thermal analysis and SEM/TEM of samples before and after modification.

Na-MO sample proved to be effective for As(III) removal from aqueous solutions via adsorption technique. It is established that both ligand exchange and ion exchange at the surface may be the mechanism of adsorption. The maximum adsorption capacity was calculated by fitting Langmuir equation to the adsorption isotherms and found to be 233.1 $mg \cdot g^{-1}$ and the Freundlich model was in good correlation with the adsorption isotherms data. The negative $\Delta G°$ and $\Delta H°$ values revealed that the adsorption was spontaneous and exothermic. Experimental data were fitted well by the intraparticle diffusion model.

Na-MO adsorbent also proved to be effective for removal of two cationic dyes, MB and CV, from synthetic wastewater. Langmuir model fitted well the adsorption data of both dyes. Moreover, the enthalpy of adsorption for MB was positive (6.5 $kJ.mol^{-1}$) signifying that the process is endothermic, whereas, the enthalpy of adsorption of CV was negative (-9.8 $kJ.mol^{-1}$)

proving that the process was exothermic. Physisorption was the dominant mechanism for adsorption of both monovalent cationic dyes onto Na-MO.

When comparing the adsorption performance of Na-MO, Surf-MO and Surf-NI for CR removal from aqueous solutions, both organoclays showed higher adsorption capacities than Na-MO adsorbent. CR adsorption data onto Na-MO was fitted well with Freundlich model, whereas Langmuir provided the better fit for both organoclays. The Langmuir maximum monolayer adsorption capacity was 5.8, 83.3 and 91.7 $mg.g^{-1}$ for Na-MO, Surf-MO and Surf-NI, respectively. Overall, the adsorption capacity of both organoclays was significantly improved by modification.

When comparing the adsorption performance of Surf-MO and Surf-NI for phenol removal, the two adsorbents showed relatively similar adsorption capacities under same conditions. The adsorption data of phenol onto both adsorbents was rapid and fitted well to pseudo-second order model. The thermodynamic studies showed that the adsorption was endothermic in nature and spontaneous process accompanied with reasonable increase in entropy which reflected the affinity of both organoclays towards phenol.

The results obtained in this work suggest that natural clays may provide the cost-reducing alternative for many contaminants removal from water and wastewater, and to solve real problems in some countries.

4.7.2. Recommendations

1) Further investigation emphasized on using both column and batch approach are needed to assess the adsorption capacities and removal efficiencies of natural clay towards chemical contaminants.
2) Natural clays from different Sudan states, may be evaluated for contaminants removal using fixed bed column to optimize different conditions such as breakthrough time, effect of flow rate, bed height initial concentration

3) Plant extracts can be tested, instead of surfactants, for coating clay to improve their adsorption capacities.
4) To improve the removal efficiency of the natural clays as low-cost and viable adsorbent for wastewater treatment, several modification techniques can be investigated and regeneration of used adsorbent materials is requirement.
5) Additional investigations should focus on unraveling the sorption mechanisms between chemical pollutants and sorbent components.
6) Mapping natural clay in the Sudan and determining the types and local usages is recommended.
7) Assessment of Nile clay as a supplement nutrient, namely for pregnant, is suggested, since several elements were detected in this clay such as K, Ca, Mg, Fe and Zn. This suggestion is supported with the behavior of many pregnant.

References

Abidi, N., Errais, E., Duplay, J., Berez, A., Jrad, A., Schäfer, G., Ghazi, M., Semhi, K. and Trabelsi-Ayadi, M. (**2015**) 'Treatment of dye-containing effluent by natural clay', *Journal of Cleaner Production*, 86, pp. 432–440.

Adegoke, K. A. and Bello, O. S. (**2015**) 'Dye sequestration using agricultural wastes as adsorbents', *Water Resources and Industry*. Elsevier, 12, pp. 8–24.

Ahmad, T. and Danish, M. (**2018**) 'Prospects of banana waste utilization in wastewater treatment : A review', *Journal of Environmental Management*. Elsevier Ltd, 206, pp. 330–348.

Ahmad, T., Danish, M., Rafatullah, M., Ghazali, A., Sulaiman, O., Hashim, R. and Ibrahim, M. N. M. (**2012**) 'The use of date palm as a potential adsorbent for wastewater treatment: A review', *Environmental Science and Pollution Research*, 19(5), pp. 1464–1484.

Al-Futaisi, A., Jamrah, A. and Al-Hanai, R. (**2007**) 'Aspects of cationic dye molecule adsorption to palygorskite', *Desalination*, 214(1–3), pp. 327–342.

Ali, R. M., Hamad, H. A., Hussein, M. M. and Malash, G. F. (**2016**) 'Potential of using green adsorbent of heavy metal removal from aqueous solutions: Adsorption kinetics, isotherm, thermodynamic, mechanism and economic analysis', *Ecological Engineering*. Elsevier B.V., 91, pp. 317–332.

Alizadeh, B., Delnavaz, M. and Shakeri, A. (**2018**) 'Removal of Cd(II) and phenol using novel cross-linked magnetic EDTA/chitosan/TiO2nanocomposite', *Carbohydrate Polymers*. Elsevier, 181(August 2017), pp. 675–683.

Almeida, C. A. P., Debacher, N. A., Downs, A. J., Cottet, L. and Mello, C. A. D. (**2009**) 'Removal of methylene blue from colored effluents by adsorption on montmorillonite clay', *Journal of Colloid and Interface Science*. Elsevier Inc., 332(1), pp. 46–53.

Anastopoulos, I. and Kyzas, G. Z. (**2014**) 'Agricultural peels for dye adsorption: A review of recent literature', *Journal of Molecular Liquids*. Elsevier B.V., 200(PB), pp. 381–389.

Anirudhan, T. S. and Ramachandran, M. (**2014**) 'Removal of 2,4,6-trichlorophenol from water and petroleum refinery industry effluents by surfactant-modified bentonite', *Journal of Water Process Engineering*. Elsevier Ltd, 1, pp. 46–53.

Anirudhan, T. S. and Ramachandran, M. (**2015**) 'Adsorptive removal of basic dyes from aqueous solutions by surfactant modified bentonite clay (organoclay): Kinetic and competitive adsorption isotherm', *Process Safety and Environmental Protection*. Institution of Chemical Engineers, 95, pp. 215–225.

Anjum, A. (**2017**) 'Adsorption Technology for Removal of Toxic Pollutants', in Rene, E. R., Sahinkaya, E., Lewis, A., and Lens, P. N. L. (eds) *Sustainable Heavy Metal Remediation, Environmental Chemistry for a Sustainable World*. Cham: Springer International Publishing (Environmental Chemistry for a Sustainable World), pp. 25–80.

Anjum, A., Lokeswari, P., Kaur, M. and Datta, M. (**2011**) 'Removal of As (III) from Aqueous Solutions Using Montmorillonite', *Journal of Analytical Sciences, Methods and Instrumentation*, 01(02), pp. 25–30..

Antoine, J. M. R., Fung, L. A. H. and Grant, C. N. (**2017**) 'Assessment of the potential health risks associated with the aluminium, arsenic, cadmium and lead

content in selected fruits and vegetables grown in Jamaica', *Toxicology Reports*. Elsevier, 4(February), pp. 181–187.
Arbaoui, F. and Boucherit, M. N. (**2014**) 'Comparison of two Algerian bentonites: Physico-chemical and retention capacity study', *Applied Clay Science*. Elsevier B.V., 91–92, pp. 6–11.
Attallah, M. F., Ahmed, I. M. and Hamed, M. M. (**2013**) 'Treatment of industrial wastewater containing Congo Red and Naphthol Green B using low-cost adsorbent', *Environmental Science and Pollution Research*, 20(2), pp. 1106–1116.
Ausavasukhi, A., Kampoosaen, C. and Kengnok, O. (**2016**) 'Adsorption characteristics of Congo red on carbonized leonardite', *Journal of Cleaner Production*. Elsevier Ltd, 134(Part B), pp. 506–514.
Auta, M. and Hameed, B. H. (**2012**) 'Modified mesoporous clay adsorbent for adsorption isotherm and kinetics of methylene blue', *Chemical Engineering Journal*. Elsevier B.V., 198–199, pp. 219–227.
Auta, M. and Hameed, B. H. (**2013**) 'Acid modified local clay beads as effective low-cost adsorbent for dynamic adsorption of methylene blue', *Journal of Industrial and Engineering Chemistry*, 19(4), pp. 1153–1161.
de Azevedo, A. C. N., Vaz, M. G., Gomes, R. F., Pereira, A. G. B., Fajardo, A. R. and Rodrigues, F. H. A. (**2017**) 'Starch/rice husk ash based superabsorbent composite: high methylene blue removal efficiency', *Iranian Polymer Journal (English Edition)*. Springer Berlin Heidelberg, 26(2), pp. 93–105.
Bagherifam, S., Komarneni, S., Lakzian, A., Fotovat, A., Khorasani, R., Huang, W., Ma, J., Hong, S., Cannon, F. S. and Wang, Y. (**2014**) 'Highly selective removal of nitrate and perchlorate by organoclay', *Applied Clay Science*. Elsevier B.V., 95, pp. 126–132.
Bazrafshan, E., Amirian, P., Mahvi, A. and Ansari-moghaddam, A. (**2016**) 'Application of adsorption process for phenolic compounds removal from aqueous environments: a systematic review', *Global NEST Journal*, 18(1), pp. 146–163.
Bektaş, N., Aydın, S. and Öncel, M. S. (**2011**) 'The Adsorption of Arsenic Ions Using Beidellite, Zeolite, and Sepiolite Clays: A Study of Kinetic, Equilibrium and Thermodynamics', *Separation Science and Technology*. Taylor & Francis, 46(6), pp. 1005–1016.
Bentahar, S., Dbik, A., Khomri, M. El, Messaoudi, N. El and Lacherai, A. (**2017**) 'Adsorption of methylene blue, crystal violet and congo red from binary and ternary systems with natural clay: Kinetic, isotherm, and thermodynamic', *Journal of Environmental Chemical Engineering*. Elsevier, 5(6), pp. 5921–5932.
Bentahar, S., Lacherai, A., Dbik, A., El, N. and El, M. (**2015**) 'Equilibrium , Isotherm , Kinetic and Thermodynamic Studies of Removal of Crystal Violet by Adsorption onto a Natural Clay', *Iranica Journal of Energy & Environment* 6(4), pp. 260–268.
Bentahar, Y., Hurel, C., Draoui, K., Khairoun, S. and Marmier, N. (**2016**) 'Adsorptive properties of Moroccan clays for the removal of arsenic(V) from aqueous solution', *Applied Clay Science*. Elsevier B.V., 119, pp. 385–392.
Bergaya, F. and Lagaly, G. (**2013**) 'General Introduction, Clays, Clay Minerals, and

Clay Science', in *Developments in Clay Science*. 1st ed. Elsevier Inc., pp. 1–19.
Bernhoft, R. A. (**2012**) 'Mercury toxicity and treatment: A review of the literature', *Journal of Environmental and Public Health*, (460508), pp. 1–10.
Bhatnagar, A. and Sillanpää, M. (**2011**) 'A review of emerging adsorbents for nitrate removal from water', *Chemical Engineering Journal*. Elsevier B.V., 168(2), pp. 493–504.
Bhattacharyya, K. G. and Gupta, S. Sen (**2006**) 'Kaolinite, montmorillonite, and their modified derivatives as adsorbents for removal of Cu(II) from aqueous solution', *Separation and Purification Technology*, 50(3), pp. 388–397.
Bhattacharyya, K. G., Gupta, S. Sen and Sarma, G. K. (**2015**) 'Kinetics, equilibrium isotherms and thermodynamics of adsorption of Congo red onto natural and acid-treated kaolinite and montmorillonite', *Desalination and Water Treatment*. Taylor & Francis, 53(2), pp. 530–542.
Bhowmick, S., Pramanik, S., Singh, P., Mondal, P., Chatterjee, D. and Nriagu, J. (**2018**) 'Arsenic in groundwater of West Bengal, India: A review of human health risks and assessment of possible intervention options', *Science of the Total Environment*. Elsevier B.V., 612, pp. 148–169.
Borah, L., Goswami, M. and Phukan, P. (**2015**) 'Adsorption of methylene blue and eosin yellow using porous carbon prepared from tea waste: Adsorption equilibrium, kinetics and thermodynamics study', *Journal of Environmental Chemical Engineering*, 3(2), pp. 1018–1028.
Bousba, S. and Meniai, A. H. (**2013**) 'Adsorption of 2-chlorophenol onto sewage sludge based adsorbent: Equilibrium and kinetic study', *Chemical Engineering Transactions*, 35(January), pp. 859–864.
Brigatti, M. F., Galán, E. and Theng, B. K. G. (**2013**) 'Structure and Mineralogy of Clay Minerals', in *Handbook of Clay Science*. Elsevier Ltd, pp. 21–81.
Burakov, A. E., Galunin, E. V, Burakova, I. V, Kucherova, A. E., Agarwal, S., Tkachev, A. G. and Gupta, V. K. (**2018**) 'Ecotoxicology and Environmental Safety Adsorption of heavy metals on conventional and nanostructured materials for wastewater treatment purposes : A review', *Ecotoxicology and Environmental Safety*. Elsevier Inc., 148(November 2017), pp. 702–712.
Carolin, C. F., Kumar, P. S., Saravanan, A., Joshiba, G. J. and Naushad, M. (**2017**) 'Efficient techniques for the removal of toxic heavy metals from aquatic environment : A review', *Journal of Environmental Chemical Engineering*, 5(May), pp. 2782–2799.
Carvalho, M. N., da Motta, M., Benachour, M., Sales, D. C. S. and Abreu, C. A. M. (**2012**) 'Evaluation of BTEX and phenol removal from aqueous solution by multi-solute adsorption onto smectite organoclay', *Journal of Hazardous Materials*. Elsevier B.V., 239–240, pp. 95–101.
Chen, H. and Zhao, J. (**2009**) 'Adsorption study for removal of Congo red anionic dye using organo-attapulgite', *Adsorption*, 15(4), pp. 381–389.
Chibban, M., Zerbet, M., Carja, G. and Sinan, F. (**2012**) 'Application of low-cost adsorbents for arsenic removal. A review', *Journal of Environmental Chemistry and Ecotoxicology*, 4(5), pp. 91–102.
Churchman, G. J., Gates, W. P., Theng, B. K. G. and Yuan, G. (**2006**) 'Chapter 11.1 Clays and Clay Minerals for Pollution Control', in Bergaya, F., Theng, B. K. G.,

and Lagaly, G. (eds) *Developments in Clay Science*, pp. 625–675.
Crini, Grégorio, Badot, P.-M. (**2010**) 'Sorption Processes and Pollution: Conventional and Non-conventional Sorbents for Pollutant Removal from Wastewaters'. Presses Univ. Franche-Comté, 2010, p. 489.
Dammak, N., Fakhfakh, N., Fourmentin, S. and Benzina, M. (**2013**) 'Natural clay as raw and modified material for efficient o-xylene abatement', *Journal of Environmental Chemical Engineering*. Elsevier B.V., 1(4), pp. 667–675.
Dell, J., Cristina, M. and Odorico, P. D. (**2018**) 'The Global Water Grabbing Syndrome', *Ecological Economics*. Elsevier B.V., 143, pp. 276–285.
Development, T. U. N. W. W. (**2017**) *Wastewater Facts and Figures; The untapped resource*. Perugia, Italy.
Díaz-Nava, M. C., Olguín, M. T. and Solache-Ríos, M. (**2012**) 'Adsorption of phenol onto surfactants modified bentonite', *Journal of Inclusion Phenomena and Macrocyclic Chemistry*, 74(1–4), pp. 67–75.
Distefano, T. and Kelly, S. (**2017**) 'Are we in deep water? Water scarcity and its limits to economic growth', *Ecological Economics*. Elsevier B.V., 142, pp. 130–147.
Djebbar, M., Djafri, F., Bouchekara, M. and Djafri, A. (2012) 'Adsorption of phenol on natural clay', *African J. of Pure and Applied Chemistry*, 6(2), pp. 15–25.
Dotto, G. L., Rodrigues, F. K., Tanabe, E. H., Fröhlich, R., Bertuol, D. A., Martins, T. R. and Foletto, E. L. (**2016**) 'Development of chitosan/bentonite hybrid composite to remove hazardous anionic and cationic dyes from colored effluents', *Journal of Environmental Chemical Engineering*. Elsevier B.V., 4(3), pp. 3230–3239.
Elgabaly, M. M. and Khadr, M. (**1962**) 'Clay Mineral Studies of Some Egyptian Desert and Nile Alluvial Soils', *Journal of Soil Science*, 13(2), pp. 333–342.
Elmoubarki, R., Mahjoubi, F. Z., Tounsadi, H., Moustadraf, J., Abdennouri, M., Zouhri, A., El Albani, A. and Barka, N. (**2015**) 'Adsorption of textile dyes on raw and decanted Moroccan clays: Kinetics, equilibrium and thermodynamics', *Water Resources and Industry*. Elsevier, 9, pp. 16–29.
Eloussaief, M., Bouaziz, S., Kallel, N. and Benzina, M. (**2014**) 'Valorization of El Haria clay in the removal of arsenic from aqueous solution', *Desalination and Water Treatment*. Taylor & Francis, 52(10–12), pp. 2220–2224.
Eren, E. and Afsin, B. (**2007**) 'Investigation of a basic dye adsorption from aqueous solution onto raw and pre-treated sepiolite surfaces', *Dyes and Pigments*, 73(2), pp. 162–167.
Eren, E. and Afsin, B. (**2008**) 'Investigation of a basic dye adsorption from aqueous solution onto raw and pre-treated bentonite surfaces', *Dyes and Pigments*, 76(1), pp. 220–225.
Ezzatahmadi, N., Ayoko, G. A., Millar, G. J., Speight, R., Yan, C., Li, J., Li, S., Zhu, J. and Xi, Y. (**2017**) 'Clay-supported nanoscale zero-valent iron composite materials for the remediation of contaminated aqueous solutions : A review', *Chemical Engineering Journal*. Elsevier B.V., 312, pp. 336–350.
Fayed, L. A. and Hassan, M. I. (**1970**) 'Identification and distribution of clay minerals in some sediments of the Nile Delta, U.A.R.', *International Journal of Rock Mechanics and Mining Sciences and*, 7(6), pp. 605–610.

Feng, N. C. and Guo, X. Y. (**2012**) 'Characterization of adsorptive capacity and mechanisms on adsorption of copper, lead and zinc by modified orange peel', *Transactions of Nonferrous Metals Society of China (English Edition)*. The Nonferrous Metals Society of China, 22(5), pp. 1224–1231.

Fomina, M. and Gadd, G. M. (**2014**) 'Biosorption: Current perspectives on concept, definition and application', *Bioresource Technology*. Elsevier Ltd, 160, pp. 3–14.

Fosso-Kankeu, E. and Mulaba-Bafubiandi, A. F. (**2014**) 'Implication of plants and microbial metalloproteins in the bioremediation of polluted waters: A review', *Physics and Chemistry of the Earth*. Elsevier Ltd, 67–69, pp. 242–252.

Fosso-Kankeu, E., Waanders, F. and Fourie, C. L. (**2016**) 'Adsorption of Congo Red by surfactant-impregnated bentonite clay', *Desalination and Water Treatment*. Taylor & Francis, 57(57), pp. 1–9.

Fowler, B. A., Selene, C.-H., Chou, Robert, J., Jones, Dexter, L., Sullivan Jr, W. and Chen, C.-J. (**2015**) 'Arsenic', in *Handbook on the Toxicology of Metals*. Fourth Edi. Elsevier, pp. 581–624.

El Gaidoumi, A., Chaouni Benabdallah, A., Lahrichi, A. and Kherbeche, A. (**2015**) 'Adsorption of phenol in aqueous medium by a raw and treated moroccan pyrophyllite', *Journal of Materials and Environmental Science*, 6(8), pp. 2247–2259.

Galán, E. and Ferrell, R. E. (**2013**) 'Genesis of Clay Minerals', in *Developments in Clay Science*. Elsevier Ltd, pp. 83–126.

Gao, W., Zhao, S., Wu, H., Deligeer, W. and Asuha, S. (**2016**) 'Direct acid activation of kaolinite and its effects on the adsorption of methylene blue', *Applied Clay Science*, 126, pp. 98–106.

Ghorbanzadeh, N., Jung, W., Halajnia, A., Lakzian, A., Kabra, A. N. and Jeon, B.-H. (**2015**) 'Removal of arsenate and arsenite from aqueous solution by adsorption on clay minerals', *Geosystem Engineering*. Taylor & Francis, 18(6), pp. 302–311.

De Gisi, S., Lofrano, G., Grassi, M. and Notarnicola, M. (**2016**) 'Characteristics and adsorption capacities of low-cost sorbents for wastewater treatment: A review', *Sustainable Materials and Technologies*. Elsevier B.V., 9, pp. 10–40.

Gopinathan, R., Bhowal, A. and Garlapati, C. (**2017**) 'Thermodynamic study of some basic dyes adsorption from aqueous solutions on activated carbon and new correlations', *The Journal of Chemical Thermodynamics*. Elsevier Ltd, 107(2437), pp. 182–188.

Gorzin, F. and Ghoreyshi, A. A. (**2013**) 'Synthesis of a new low-cost activated carbon from activated sludge for the removal of Cr (VI) from aqueous solution: Equilibrium, kinetics, thermodynamics and desorption studies', *Korean Journal of Chemical Engineering*, 30(8), pp. 1594–1602.

Gu, Z., Gao, M., Luo, Z., Xue, G., Lu, L. and Liu, Y. (**2014**) 'Gemini Surfactant Modified Montmorillonite as Highly Efficient Adsorbent for Anionic Dyes', *Separation Science and Technology*. Taylor & Francis, 49(18), pp. 2878–2889.

Guggenheim, S. and Martins, T. R. (**1995**) 'Definition of Clay and Clay Mineral: Joint Report of the AIPEA Nomenclature and CMS Nomenclature Committees', *Clays and Clay Minerals*, 43(2), pp. 255–256.

Gupta, V. K. and Suhas (**2009**) 'Application of low-cost adsorbents for dye removal - A review', *J. of Environmental Management*. Elsevier Ltd, 90(8), pp. 2313-2342.

Gürses, A., Doğar, Ç., Yalçin, M., Açikyildiz, M., Bayrak, R. and Karaca, S. (**2006**) 'The adsorption kinetics of the cationic dye, methylene blue, onto clay', *Journal of Hazardous Materials*, 131(1–3), pp. 217–228.

Hai, T. N. (**2017**) 'Comments on "Effect of Temperature on the Adsorption of Methylene Blue Dye onto Sulfuric Acid–Treated Orange Peel"', *Chemical Engineering Communications*. Taylor & Francis, 204(1), pp. 134–139.

Hai, Y., Li, X., Wu, H., Zhao, S., Deligeer, W. and Asuha, S. **(2015**) 'Modification of acid-activated kaolinite with TiO2 and its use for the removal of azo dyes', *Applied Clay Science*, 114(Supplement C), pp. 558–567.

Hajjaji, M. and Alami, A. (**2009**) 'Influence of operating conditions on methylene blue uptake by a smectite rich clay fraction', *Applied Clay Science*. Elsevier B.V., 44(1–2), pp. 127–129.

Hamdaoui, M., Hadri, M., Bencheqroun, Z., Draoui, K., Nawdali, M., Zaitan, H. and Barhoun, A. (**2018**) 'Improvement of phenol removal from aqueous medium by adsorption on organically functionalized Moroccan stevensite', *Materials and Environmental Sciences*, 9(4), pp. 1119–1128.

Hong, S., Wen, C., He, J., Gan, F. and Ho, Y. S. (**2009**) 'Adsorption thermodynamics of Methylene Blue onto bentonite', *Journal of Hazardous Materials*, 167(1–3), pp. 630–633.

Hossain, A., Ngo, H. H. and Guo, W. (**2013**) 'Introductory of Microsoft Excel SOLVER Function - Spreadsheet Method for Isotherm and Kinetics Modelling of Metals Biosorption in Water and Wastewater', *Journal of Water Sustainability*, 3(4), pp. 223–237.

Hossain, M. A., Ngo, H. H., Guo, W. S. and Setiadi, T. (**2012**) 'Adsorption and desorption of copper(II) ions onto garden grass', *Bioresource Technology*, 121(Supplement C), pp. 386–395.

Hu, Z., Chen, H., Ji, F. and Yuan, S. (**2010**) 'Removal of Congo Red from aqueous solution by cattail root', *Journal of Hazardous Materials*, 173(1–3), pp. 292–297.

Huang, J., Kankanamge, N. R., Chow, C., Welsh, D. T., Li, T. and Teasdale, P. R. (**2018**) 'Removing ammonium from water and wastewater using cost-effective adsorbents: A review', *Journal of Environmental Sciences*. Elsevier B.V., 63, pp. 174–197.

Huang, Q., Liu, M., Chen, J., Wang, K., Xu, D., Deng, F., Huang, H., Zhang, X. and Wei, Y. (**2016**) 'Enhanced removal capability of kaolin toward methylene blue by mussel-inspired functionalization', *Journal of Materials Science*. Springer US, 51(17), pp. 8116–8130.

Husein, D. Z. (**2013**) 'Adsorption and removal of mercury ions from aqueous solution using raw and chemically modified Egyptian mandarin peel', *Desalination and Water Treatment*. Taylor & Francis, 51(34–36), pp. 6761–6769.

Iqbal, M., Saeed, A. and Kalim, I. (**2009**) 'Characterization of Adsorptive Capacity and Investigation of Mechanism of Cu^{2+}, Ni^{2+} and Zn^{2+} Adsorption on Mango Peel Waste from Constituted Metal Solution and Genuine Electroplating Effluent', *Separation Science and Technology*. Taylor & Francis, 44(15), pp. 3770–3791.

Islam, M. A., Benhouria, A., Asif, M. and Hameed, B. H. (**2015**) 'Methylene blue adsorption on factory-rejected tea activated carbon prepared by conjunction of

hydrothermal carbonization and sodium hydroxide activation processes', *Journal of the Taiwan Institute of Chemical Engineers*, 52(Supplement C), pp. 57–64.
Islam, M. A., Tan, I. A. W., Benhouria, A., Asif, M. and Hameed, B. H. (**2015**) 'Mesoporous and adsorptive properties of palm date seed activated carbon prepared via sequential hydrothermal carbonization and sodium hydroxide activation', *Chemical Engineering Journal*, 270(Supplement C), pp. 187–195.
Ismadji, S., Soetaredjo, F. E. and Ayucitra, A. (**2015a**) 'Modification of Clay Minerals for Adsorption Purpose', in *Green Chemistry for Sustainability*, pp. 39–56.
Ismadji, S., Soetaredjo, F. E. and Ayucitra, A. (**2015b**) 'Natural Clay Minerals as Environmental Cleaning Agents', in *Green Chemistry for Sustainability*. Cham: Springer International Publishing (SpringerBriefs in Molecular Science), pp. 5–37.
Ismadji, S., Soetaredjo, F. E. and Ayucitra, A. (**2015c**) 'The Characterization of Clay Minerals and Adsorption Mechanism onto Clays', in *Clay Materials for Environmental Remediation*, pp. 93–112.
Ismadji, S., Soetaredjo, F. E. and Ayucitra, A. (**2015d**) 'The Equilibrium Studies in the Adsorption of Hazardous Substances Using Clay Minerals', in *Clay Materials for Environmental Remediation*. SpringerBr. Springer, pp. 57–91.
Ismadji, S., Soetaredjo, F. E. and Ayucitra, A. (**2015e**) 'The Kinetic Studies in the Adsorption of Hazardous Substances Using Clay Minerals', in *Green Chemistry for Sustainability*, pp. 113–124.
Ismail, M. A., Eltayeb, M. A. Z. and A, A. M. S. (**2013**) 'Elimination of Heavy Metals from Aqueous Solutions using Zeolite LTA Synthesized from Sudanese Clay', *Research journal of chemical sciences*, 3(5), pp. 93–98.
Issabayeva, G., Hang, S. Y., Wong, M. C. and Aroua, M. K. (**2017**) 'A review on the adsorption of phenols from wastewater onto diverse groups of adsorbents', *Reviews in Chemical Engineering*. pp. 1–19.
Jayaraj, R., Suthakaran, A., Amala, S., Anbarasi, C., Selvamathan, S. and Martin Deva Prasath, P. (**2012**) 'Competitive adsorption of dyes (crystal violet, methylene blue, malachite green) on chlor-alkali waste (slurry)', *Journal of Chemical and Pharmaceutical Research*, 4(2), pp. 1251–1258.
Jorfi, S., Ahmadi, M. J., Pourfadakari, S., Jaafarzadeh, N., Soltani, R. D. C. and Akbari, H. (**2017**) 'Adsorption of Cr(VI) by Natural Clinoptilolite Zeolite from Aqueous Solutions: Isotherms and Kinetics', *Polish Journal of Chemical Technology*, 19(3), pp. 106–114.
Kausar, A., Iqbal, M., Javed, A., Aftab, K., Nazli, Z.-H., Bhatti, H. N. and Nouren, S. (**2018**) 'Dyes adsorption using clay and modified clay: A review', *Journal of Molecular Liquids*. Elsevier B.V, 256, pp. 395–407.
Khan, T. A., Khan, E. A. and Shahjahan (**2015**) 'Removal of basic dyes from aqueous solution by adsorption onto binary iron-manganese oxide coated kaolinite: Non-linear isotherm and kinetics modeling', *Applied Clay Science*. Elsevier B.V., 107, pp. 70–77.
Khattri, S. D. and Singh, M. K. (**2009**) 'Removal of malachite green from dye wastewater using neem sawdust by adsorption', *Journal of Hazardous Materials*, 167(1–3), pp. 1089–1094.

Kim, I., Saif Ur Rehman, M. and Han, J.-I. (**2014**) 'Fermentable sugar recovery and adsorption potential of enzymatically hydrolyzed rice straw', *Journal of Cleaner Production*, 66(Supplement C), pp. 555–561.
Komadel, P. (**2016**) 'Acid activated clays: Materials in continuous demand', *Applied Clay Science*. Elsevier B.V., 131, pp. 84–99.
Kumar, G., Sen, S. and Bhattacharyya, K. G. (**2016**) 'Adsorption of Crystal violet on raw and acid-treated montmorillonite , K10 , in aqueous suspension', *Journal of Environmental Management*. Elsevier Ltd, 171, pp. 1–10.
Kurniawan, A., Ismadji, S., Soetaredjo, F. E. and Ayucitra, A. (**2014**) 'Chapter 11. Natural Clays/Clay Minerals and Modified Forms for Heavy Metals Removal', in *Heavy Metals In Water*. Cambridge: Royal Society of Chemistry, pp. 213–248.
Kyzas, G. and Kostoglou, M. (**2014**) 'Green Adsorbents for Wastewaters: A Critical Review', *Materials*, 7(1), pp. 333–364.
Largitte, L. and Pasquier, R. (**2016**) 'A review of the kinetics adsorption models and their application to the adsorption of lead by an activated carbon', *Chemical Engineering Research and Design*. Institution of Chemical Engineers, 109, pp. 495–504.
Li, W. W. and Yu, H. Q. (**2014**) 'Insight into the roles of microbial extracellular polymer substances in metal biosorption', *Bioresource Technology*. Elsevier Ltd, 160, pp. 15–23.
Lim, K., Shukor, M. and Wasoh, H. (**2014**) 'Physical, Chemical, and Biological Methods for the Removal of Arsenic Compounds.', *BioMed research international*, 2014, pp. 1–9.
Liu, D., Edraki, M. and Berry, L. (**2017**) 'Investigating the settling behaviour of saline tailing suspensions using kaolinite, bentonite, and illite clay minerals', *Powder Technology*. Elsevier B.V.
Liu, R.-L., Liu, Y., Zhou, X.-Y., Zhang, Z.-Q., Zhang, J. and Dang, F.-Q. (**2014**) 'Biomass-derived highly porous functional carbon fabricated by using a free-standing template for efficient removal of methylene blue', *Bioresource Technology*, 154(Supplement C), pp. 138–147.
Liu, Y., Wang, W. and Wang, A. (**2010**) 'Removal of congo red from aqueous solution by sorption on organified rectorite', *Clean - Soil, Air, Water*. WILEY-VCH Verlag, 38(7), pp. 670–677.
Loganathan, P., Vigneswaran, S. and Kandasamy, J. (**2013**) 'Enhanced removal of nitrate from water using surface modification of adsorbents - A review', *Journal of Environmental Management*. Elsevier Ltd, pp. 363–374.
Ltifi, I., Ayari, F., Ben, D., Chehimi, H. and Trabelsi, M. (**2018**) 'Physicochemical characteristics of organophilic clays prepared using two organo - modifiers : alkylammonium cation arrangement models', *Applied Water Science*. Springer Berlin Heidelberg.
Ma, L., Chen, Q., Zhu, J., Xi, Y., He, H., Zhu, R., Tao, Q. and Ayoko, G. A. (**2016**) 'Adsorption of phenol and Cu(II) onto cationic and zwitterionic surfactant modified montmorillonite in single and binary systems', *Chemical Engineering Journal*. Elsevier B.V., 283, pp. 880–888.
Madejova, J. and Komadel, P. (**2001**) 'Baseline Studies of the Clay Minerals Society Source Clays : Infrared Methods', *Clays and Clay Minerals*, 49(5), pp. 410–432.

Maiti, A., DasGupta, S., Basu, J. K. and De, S. (**2007**) 'Adsorption of arsenite using natural laterite as adsorbent', *Separation and Purification Technology*, 55(3), pp. 350–359.
Malik, R., Ramteke, D. S. and Wate, S. R. (**2007**) 'Adsorption of malachite green on groundnut shell waste based powdered activated carbon', *Waste Management*, 27(9), pp. 1129–1138.
Miandad, R., Kumar, R., Barakat, M. A., Basheer, C., Aburiazaiza, A. S., Nizami, A. S. and Rehan, M. (**2018**) 'Untapped conversion of plastic waste char into carbon-metal LDOs for the adsorption of Congo red', *Journal of Colloid and Interface Science*. Elsevier Inc., 511, pp. 402–410.
Mirmohamadsadeghi, S., Kaghazchi, T., Soleimani, M. and Asasian, N. (**2012**) 'An efficient method for clay modification and its application for phenol removal from wastewater', *Applied Clay Science*, 59–60, pp. 8–12.
Mishra, U., Paul, S. and Bandyopadhaya, M. (**2013**) 'Removal of zinc ions from wastewater using industrial waste sludge: A novel approach', *Environmental Progress & Sustainable Energy*. Wiley Online Library, 32(3), pp. 576–586.
Miyah, Y., Lahrichi, A. and Idrissi, M. (**2016**) 'Assessment of adsorption kinetics for removal potential of Crystal Violet dye from aqueous solutions using Moroccan pyrophyllite', *Journal of the Association of Arab Universities for Basic and Applied Sciences*. doi: 10.1016/j.jaubas.2016.06.001.
Mohd, F., Abu, H., Rozaimah, S. and Abdullah, S. (**2018**) 'An overview of the technology used to remove trihalomethane (THM), trihalomethane precursors , and trihalomethane formation potential (THMFP) from water and wastewater', *Journal of Industrial and Engineering Chemistry*. The Korean Society of Industrial and Engineering Chemistry, 57, pp. 1–14.
Monash, P. and Pugazhenthi, G. (**2009**) 'Removal of Crystal Violet Dye from Aqueous Solution Using Calcined and Uncalcined Mixed Clay Adsorbents', *Separation Science and Technology*, 45(1), pp. 94–104.
Mondal, N. K., Das, K., Das, B. and Sadhukhan, B. (**2016**) 'Effective utilization of calcareous soil towards the removal of methylene blue from aqueous solution', *Clean Technologies and Environmental Policy*. Springer Berlin Heidelberg, 18(3), pp. 867–881.
Montoya-Suarez, S., Colpas-Castillo, F., Meza-Fuentes, E., Rodríguez-Ruiz, J. and Fernandez-Maestre, R. (**2016**) 'Activated carbons from waste of oil-palm kernel shells, sawdust and tannery leather scraps and application to chromium(VI), phenol, and methylene blue dye adsorption', *Water Science and Technology*, 73(1), pp. 21–27.
Moore, D. M. (**1996**) 'Comment on: Definition of Clay and Clay Mineral: Joint Report of the Aipea Nomenclature and Cms Nomenclature Committees', *Clays and Clay Minerals*, 44(5), pp. 710–712.
Ben Moshe, S. and Rytwo, G. (**2018**) 'Thiamine-based organoclay for phenol removal from water', *Applied Clay Science*. Elsevier, 155(Jan.), pp. 50–56.
Mu, B. and Wang, A. (**2016**) 'Adsorption of dyes onto palygorskite and its composites : A review', *Biochemical Pharmacology*. Elsevier B.V., 4(1), pp. 1274–1294.
Mubarik, S., Saeed, A., Athar, M. M. and Iqbal, M. (**2016**) 'Characterization and

mechanism of the adsorptive removal of 2,4,6-trichlorophenol by biochar prepared from sugarcane baggase', *Journal of Industrial and Engineering Chemistry*. The Korean Society of Industrial and Engineering Chemistry, 33, pp. 115–121.

Na, P., Jia, X., Yuan, B., Li, Y., Na, J. and Wang, L. (**2010**) 'Arsenic adsorption on Ti-pillared montmorillonite', *Journal of Chemical Technology & Biotechnology*, 85(5), pp. 708–714.

Nandi, B. K., Goswami, A., Das, A. K., Mondal, B. and Purkait, M. K. (**2008**) 'Kinetic and Equilibrium Studies on the Adsorption of Crystal Violet Dye using Kaolin as an Adsorbent', *Separation Science and Technology*, 43(6), pp. 1382–1403.

Ngulube, T., Ray, J., Masindi, V. and Maity, A. (**2017**) 'An update on synthetic dyes adsorption onto clay based minerals : A state-of-art review', *Journal of Environmental Management*. Elsevier Ltd, 191, pp. 35–57.

Nguyen, T. A. H., Ngo, H. H., Guo, W. S., Zhang, J., Liang, S., Yue, Q. Y., Li, Q. and Nguyen, T. V (**2013**) 'Bioresource Technology Applicability of agricultural waste and by-products for adsorptive removal of heavy metals from wastewater', *Bioresource Technology*, 148, pp. 574–585.

Nicoleta Popa, M. V. (**2015**) 'Adsorption of Heavy Metals Cations onto Zeolite Material from Aqueous Solution', *Journal of Membrane Science & Technology*, 05(01), pp. 1–8.

Nourmoradi, H., Avazpour, M., Ghasemian, N., Heidari, M., Moradnejadi, K., Khodarahmi, F., Javaheri, M. and Moghadam, F. M. (**2016**) 'Surfactant modified montmorillonite as a low cost adsorbent for 4-chlorophenol: Equilibrium, kinetic and thermodynamic study', *Journal of the Taiwan Institute of Chemical Engineers*. Elsevier Ltd., 59, pp. 244–251.

Numbonui Ghogomu, J., Tsemo Noufame, D., Buleng Njoyim Tamungang, E., Ajifack, D., Nsami Ndi, J. and Mbadcam Ketcha, J. (**2015**) 'Adsorption of phenol from aqueous solutions onto natural and thermallymodified kaolinitic materials', *International J. of Biological and Chemical Sciences*, 8(5), p. 2325.

Omo-okoro, P. N., Daso, A. P. and Okonkwo, J. O. (**2017**) 'A review of the application of agricultural wastes as precursor materials for the adsorption of per- and polyfluoroalkyl substances: A focus on current approaches and methodologies', *Environmental Technology & Innovation*. Elsevier B.V. doi: 10.1016/j.eti.2017.11.005.

Organization, W. H. (**2017**) *Potable reuse: Guidance for producing safe drinking-water*. Geneva, Switzerland: World Health Organization.

Özdemir, Y., Doğan, M. and Alkan, M. (**2006**) 'Adsorption of cationic dyes from aqueous solutions by sepiolite', *Microporous and Mesoporous Materials*, 96(1–3), pp. 419–427.

Öztel, M. D., Akbal, F. and Altaş, L. (**2015**) 'Arsenite removal by adsorption onto iron oxide-coated pumice and sepiolite', *Environmental Earth Sciences*, 73(8), pp. 4461–4471.

de Paiva, L. B., Morales, A. R. and Valenzuela Díaz, F. R. (**2008**) 'Organoclays: Properties, preparation and applications', *Applied Clay Science*. Elsevier B.V., pp. 8–24.

Park, Y., Ayoko, G. A., Horváth, E., Kurdi, R., Kristof, J. and Frost, R. L. (**2013**) 'Structural characterisation and environmental application of organoclays for the removal of phenolic compounds', *Journal of Colloid and Interface Science*. Elsevier Inc., 393(1), pp. 319–334.

Park, Y., Ayoko, G. A., Kurdi, R., Horváth, E., Kristóf, J. and Frost, R. L. (**2013**) 'Adsorption of phenolic compounds by organoclays: Implications for the removal of organic pollutants from aqueous media', *Journal of Colloid and Interface Science*. Elsevier Inc., 406, pp. 196–208.

Pattnaik, B. K. and Equeenuddin, S. (**2016**) 'Potentially toxic metal contamination and enzyme activities in soil around chromite mines at Sukinda Ultramafic Complex , India', *Journal of Geochemical Exploration*. Elsevier B.V., 168, pp. 127–136.

Pavan, F. A., Camacho, E. S., Lima, E. C., Dotto, G. L., Branco, V. T. A. and Dias, S. L. P. (2014) 'Formosa papaya seed powder (FPSP): Preparation, characterization and application as an alternative adsorbent for the removal of crystal violet from aqueous phase', *Journal of Environmental Chemical Engineering*, 2(1), pp. 230–238.

Pawar, R. R., Lalhmunsiama, Bajaj, H. C. and Lee, S. M. (**2016**) 'Activated bentonite as a low-cost adsorbent for the removal of Cu(II) and Pb(II) from aqueous solutions: Batch and column studies', *Journal of Industrial and Engineering Chemistry*. The Korean Society of Industrial and Engineering Chemistry, 34, pp. 213–223.

Perrons, R. K. (**2013**) 'Assessing the damage caused by Deepwater Horizon: Not just another Exxon Valdez', *Marine Pollution Bulletin*. Elsevier Ltd, 71(1–2), pp. 20–22.

Pleşa Chicinaş, R., Bedelean, H., Stefan, R. and Măicăneanu, A. (**2018**) 'Ability of a montmorillonitic clay to interact with cationic and anionic dyes in aqueous solutions', *Journal of Molecular Structure*, 1154, pp. 187–195.

Rao, K., Mohapatra, M., Anand, S. and Venkateswarlu, P. (**2011**) 'Review on cadmium removal from aqueous solutions', *International Journal of Engineering, Science and Technology*, 2(7), pp. 81–103.

Rao, R. A. K. and Kashifuddin, M. (**2016**) 'Adsorption studies of Cd(II) on ball clay: Comparison with other natural clays', *Arabian Journal of Chemistry*. King Saud University, 9, pp. S1233–S1241.

Reeve, P. J. and Fallow, H. J. (**2018**) 'Natural and surfactant modi fi ed zeolites : A review of their applications for water remediation with a focus on surfactant desorption and toxicity towards microorganisms', *Journal of Environmental Management*, 205, pp. 253–61.

Ren, X., Zhang, Z., Luo, H., Hu, B., Dang, Z., Yang, C. and Li, L. (**2014**) 'Adsorption of arsenic on modi fi ed montmorillonite', *Applied Clay Science*, 98, pp. 17–23.

Rosales, E., Meijide, J., Pazos, M. and Sanromán, M. A. (**2017**) 'Bioresource Technology Challenges and recent advances in biochar as low-cost biosorbent : From batch assays to continuous-flow systems', *Bioresource Technology*. Elsevier Ltd, 246, pp. 176–192.

Ruiz-hitzky, E., Aranda, P. and Belver, C. (**2012**) 'Nanoarchitectures Based on Clay

Materials', in *Manipulation of nanoscale materials: an introduction to nanoarchitectonics*, pp. 87–111.
Rytwo, G., Nir, S. and Margulies, L. (**1995**) 'Interactions of Monovalent Organic Cations with Montmorillonite: Adsorption Studies and Model Calculations', *Soil Science Society of America Journal*, 59(2), pp. 554–564.
Rytwo, G., Nir, S., Margulies, L., Casal, B., Merino, J., Ruiz-hitzky, E. and Serratosa, J. M. (**1998**) 'Adsorption of Monovalent Organic Cations on Sepiolite: Experimental Results and Model Calculations', *Clays and Clay Minerals*, 46(3), pp. 340–348.
Rytwo, G. and Ruiz-Hitzky, E. (**2003**) 'Enthalpies of adsorption of methylene blue and crystal violet to montmorillonite', *Journal of Thermal Analysis and Calorimetry*, 71, pp. 751–759.
Saleh, A., Sar, A. and Tuzen, M. (**2016**) 'Chitosan-modified vermiculite for As(III) adsorption from aqueous solution : Equilibrium , thermodynamic and kinetic studies', *Journal of Molecular Liquids*, 219, pp. 937–945.
Santos, S. C. R., Oliveira, Á. F. M. and Boaventura, R. A. R. (**2016**) 'Bentonitic clay as adsorbent for the decolourisation of dyehouse effluents', *Journal of Cleaner Production*, 126, pp. 667–676.
Sari, A. and Tuzen, M. (**2014**) 'Cd(II) adsorption from aqueous solution by raw and modified kaolinite', *Applied Clay Science*. Elsevier B.V., 88–89, pp. 63–72.
Sasaki, T., Iizuka, A., Watanabe, M., Hongo, T. and Yamasaki, A. (**2014**) 'Preparation and performance of arsenate (V) adsorbents derived from concrete wastes', *Waste Management*, 34(10), pp. 1829–1835.
Schoonheydt, R. A. (**2014**) 'Functional hybrid clay mineral films', *Applied Clay Science*. Elsevier B.V., 96, pp. 9–21.
Shaban, M., Abukhadra, M. R., Khan, A. A. P. and Jibali, B. M. (**2018**) 'Removal of Congo red, methylene blue and Cr(VI) ions from water using natural serpentine', *Journal of the Taiwan Institute of Chemical Engineers*. Elsevier B.V., 82, pp. 102–116.
Shaban, M., Sayed, M. I., Shahien, M. G., Abukhadra, M. R. and Ahmed, Z. M. **(2018**) 'Adsorption behavior of inorganic- and organic-modified kaolinite for Congo red dye from water, kinetic modeling, and equilibrium studies', *Journal of Sol-Gel Science and Technology*. Springer US. doi: 10.1007/s10971-018-4719-6.
Środoń, J. (**2013**) 'Identification and Quantitative Analysis of Clay Minerals', in *Developments in Clay Science*, pp. 25–49.
Struijk, M., Rocha, F. and Detellier, C. (**2017**) 'Novel thio-kaolinite nanohybrid materials and their application as heavy metal adsorbents in wastewater', *Applied Clay Science*. Elsevier, 150(September), pp. 192–201.
Sun, D., Zhang, X., Wu, Y. and Liu, T. (**2013**) 'Kinetic mechanism of competitive adsorption of disperse dye and anionic dye on fly ash', *International Journal of Environmental Science and Technology*, 10(4), pp. 799–808.
Sun, K., Shi, Y., Chen, H., Wang, X. and Li, Z. (**2017**) 'Extending surfactant-modified 2:1 clay minerals for the uptake and removal of diclofenac from water', *Journal of Hazardous Materials*. Elsevier B.V., 323, pp. 567–574.
Sutar, H., Mishra, S. C., Sahoo, S. K., Prasad, A. and Maharana, H. S. (**2014**) 'Progress of Red Mud Utilization : An Overview', *American Chemical Science*

Journal, 4(3), pp. 255–279.
Taamneh, Y. and Sharadqah, S. (**2017**) 'The removal of heavy metals from aqueous solution using natural Jordanian zeolite', *Applied Water Science*. Springer Berlin Heidelberg, 7(4), pp. 2021–2028.
Tan, K. L. and Hameed, B. H. (**2017**) 'Insight into the adsorption kinetics models for the removal of contaminants from aqueous solutions', *Journal of the Taiwan Institute of Chemical Engineers*. Elsevier B.V., 74, pp. 25–48.
Te, B., Wichitsathian, B. and Yossapol, C. (**2015**) 'Modification of Natural Common Clays as Low Cost Adsorbents for Arsenate Adsorption', *International Journal of Environmental Science and Development*, 6(11), pp. 799–804.
Thinakaran, N., Panneerselvam, P., Baskaralingam, P., Elango, D. and Sivanesan, S. (**2008**) 'Equilibrium and kinetic studies on the removal of Acid Red 114 from aqueous solutions using activated carbons prepared from seed shells', *Journal of Hazardous Materials*, 158(1), pp. 142–150.
Thommes, M., Kaneko, K., Neimark, A. V., Olivier, J. P., Rodriguez-Reinoso, F., Rouquerol, J. and Sing, K. S. W. (**2015**) 'Physisorption of gases, with special reference to the evaluation of surface area and pore size distribution (IUPAC Technical Report)', *Pure and Applied Chemistry*, 87(9–10), pp. 1051–1069.
Thue, P. S., Sophia, A. C., Lima, E. C., Wamba, A. G. N., Alencar, W. S. De, Glaydson, S., Rodembusch, F. S. and Dias, S. L. P. (**2018**) 'Synthesis and characterization of a novel organic-inorganic hybrid clay adsorbent for the removal of acid red 1 and acid green 25 from aqueous solutions', *Journal of Cleaner Production*. Elsevier Ltd, 171, pp. 30–44.
Tireli, A. A., Guimarães, I. do R., Terra, J. C. de S., da Silva, R. R. and Guerreiro, M. C. (**2014**) 'Fenton-like processes and adsorption using iron oxide-pillared clay with magnetic properties for organic compound mitigation', *Environmental Science and Pollution Research*, 22, pp. 870–881.
Toczyłowska-Mamińska, R. (**2017**) 'Limits and perspectives of pulp and paper industry wastewater treatment – A review', *Renewable and Sustainable Energy Reviews*, 78(November 2016), pp. 764–772.
Toor, M. and Jin, B. (**2012**) 'Adsorption characteristics, isotherm, kinetics, and diffusion of modified natural bentonite for removing diazo dye', *Chemical Engineering Journal*, 187(Supplement C), pp. 79–88.
Tran, H. N., You, S. J. and Chao, H. P. (**2016**) 'Thermodynamic parameters of cadmium adsorption onto orange peel calculated from various methods: A comparison study', *Journal of Environmental Chemical Engineering*. Elsevier B.V., 4(3), pp. 2671–2682.
Tran, H. N., You, S. J., Hosseini-Bandegharaei, A. and Chao, H. P. (**2017**) 'Mistakes and inconsistencies regarding adsorption of contaminants from aqueous solutions: A critical review', *Water Research*. Elsevier Ltd, pp. 88–116.
Tran, V. S., Ngo, H. H., Guo, W., Zhang, J., Liang, S., Ton-That, C. and Zhang, X. (**2015**) 'Typical low cost biosorbents for adsorptive removal of specific organic pollutants from water', *Bioresource Technology*. Elsevier Ltd, 182, pp. 353–363.
Tripathi, A. and Rawat Ranjan, M. (**2015**) 'Heavy Metal Removal from Wastewater Using Low Cost Adsorbents', *Journal of Bioremediation & Biodegradation*, 06(06). doi: 10.4172/2155-6199.1000315.

Tu, Y.-J., You, C.-F., Chang, C.-K., Wang, S.-L. and Chan, T.-S. (**2013**) 'Adsorption behavior of As(III) onto a copper ferrite generated from printed circuit board industry', *Chemical Engineering Journal*, 225, pp. 433–439.
Turk Sekulić, M., Pap, S., Stojanović, Z., Bošković, N., Radonić, J. and Šolević Knudsen, T. (**2018**) 'Efficient removal of priority, hazardous priority and emerging pollutants with Prunus armeniaca functionalized biochar from aqueous wastes: Experimental optimization and modeling', *Science of the Total Environment*, 613–614, pp. 736–750.
Tyagi, S., Rawtani, D., Khatri, N. and Tharmavaram, M. (**2018**) 'Strategies for Nitrate removal from aqueous environment using Nanotechnology: A Review', *Journal of Water Process Engineering*. Elsevier, 21, pp. 84–95.
Uddin, M. K. (**2017**) 'A review on the adsorption of heavy metals by clay minerals, with special focus on the past decade', *Chemical Engineering Journal*. Elsevier B.V., 308, pp. 438–462.
Unuabonah, E. I., Adebowale, K. O., Olu-Owolabi, B. I., Yang, L. Z. and Kong, L. X. (**2008**) 'Adsorption of Pb (II) and Cd (II) from aqueous solutions onto sodium tetraborate-modified Kaolinite clay: Equilibrium and thermodynamic studies', *Hydrometallurgy*, 93(1–2), pp. 1–9.
Vasconcelos, P. N. M., Lima, W. S., Silva, M. L. P., Brito, A. L. F., Laborde, H. M. and Rodrigues, M. G. F. (**2013**) 'Adsorption of Zinc from Aqueous Solutions Using Modified Brazilian Gray Clay', *American Journal of Analytical Chemistry*, 4(September), pp. 510–519.
Vicente, M. A., Gil, A. and Bergaya, F. (**2013**) 'Pillared Clays and Clay Minerals', *Developments in Clay Science*, 5, pp. 523–557.
Vimonses, V., Jin, B. and Chow, C. W. K. (**2010**) 'Insight into removal kinetic and mechanisms of anionic dye by calcined clay materials and lime', *Journal of Hazardous Materials*. Elsevier B.V., 177(1–3), pp. 420–427.
Vimonses, V., Lei, S., Jin, B., Chow, C. W. K. and Saint, C. (**2009**) 'Adsorption of congo red by three Australian kaolins', *Applied Clay Science*. Elsevier B.V., 43(3–4), pp. 465–472.
Vimonses, V., Lei, S., Jin, B., Chow, C. W. K. and Saint, C. (**2009**) 'Kinetic study and equilibrium isotherm analysis of Congo Red adsorption by clay materials', *Chemical Engineering Journal*, 148(2–3), pp. 354–364.
Wan Ngah, W. S., Teong, L. C. and Hanafiah, M. A. K. M. (**2011**) 'Adsorption of dyes and heavy metal ions by chitosan composites: A review', *Carbohydrate Polymers*. Elsevier Ltd., pp. 1446–1456.
Wang, J., Li, Y., Huang, J., Yan, T. and Sun, T. (**2016**) 'Growing water scarcity, food security and government responses in China', *Global Food Security*. Elsevier B.V., 14(August 2016), pp. 9–17.
Wang, L. and Wang, A. (**2008**) 'Adsorption properties of Congo Red from aqueous solution onto surfactant-modified montmorillonite', *Journal of Hazardous Materials*, 160, pp. 173–180.
Wang, Y., Wang, W. and Wang, A. (**2013**) 'Efficient adsorption of methylene blue on an alginate-based nanocomposite hydrogel enhanced by organo-illite/smectite clay', *Chemical Engineering Journal*. Elsevier B.V., 228, pp. 132–139.
Weir, A. H., Ormerod, E. C. and El Mansey, I. M. I. (**1975**) 'Clay mineralogy of

sediments of the western Nile Delta', *Clay Minerals*, 10(5), pp. 369–386.
Xia, C., Jing, Y., Jia, Y., Yue, D., Ma, J. and Yin, X. (2011) 'Adsorption properties of congo red from aqueous solution on modified hectorite: Kinetic and thermodynamic studies', *Desalination*. Elsevier B.V., 265(1–3), pp. 81–87.
Xu, M. and McKay, G. (**2017**) 'Removal of Heavy Metals, Lead, Cadmium, and Zinc, Using Adsorption Processes by Cost-Effective Adsorbents', in Bonilla-Petriciolet, A., Mendoza-Castillo, D. I., and Reynel-Ávila, H. E. (eds) *Adsorption Processes for Water Treatment and Purification*. Cham: Springer International Publishing, pp. 109–138.
Xu, Y., Liang, X., Xu, Y., Qin, X., Huang, Q., Wang, L. and Sun, Y. (**2017**) 'Remediation of Heavy Metal-Polluted Agricultural Soils Using Clay Minerals: A Review', *Pedosphere*, 27(2), pp. 193–204.
Yadav, D., Kapur, M., Kumar, P. and Mondal, M. K. (**2015**) 'Adsorptive removal of phosphate from aqueous solution using rice husk and fruit juice residue', *Process Safety and Environmental Protection*, 94(Suppl. C), pp. 402–409.
Yadava, K. P., Tyagi, B. S. and Singh, V. N. (**1988**) 'Removal of arsenic(III) from aqueous solution by china clay', *Environmental Technology Letters*. Taylor & Francis, 9(11), pp. 1233–1244.
Yagub, M. T., Sen, T. K., Afroze, S. and Ang, H. M. (**2014**) 'Dye and its removal from aqueous solution by adsorption: A review', *Advances in Colloid and Interface Science*. Elsevier B.V., pp. 172–184.
Yang, S., Gao, M., Luo, Z. and Yang, Q. (**2015**) 'The characterization of organo-montmorillonite modified with a novel aromatic-containing gemini surfactant and its comparative adsorption for 2-naphthol and phenol', *Chemical Engineering Journal*. Elsevier B.V., 268, pp. 125–134.
Yang, S., Wu, Y., Aierken, A., Zhang, M., Fang, P., Fan, Y. and Ming, Z. (**2016**) 'Mono/competitive adsorption of Arsenic(III) and Nickel(II) using modified green tea waste', *Journal of the Taiwan Institute of Chemical Engineers*. Elsevier Ltd., 60, pp. 213–221.
Youssef AM, A. M. and Al-Awadhi MM (**2013**) 'Adsorption of Acid Dyes onto Bentonite and Surfactant-modified Bentonite', *Journal of Analytical & Bioanalytical Techniques*, 04(04). doi: 10.4172/2155-9872.1000174.
Yu, J. xia, Xiong, W. li, Zhu, J., Chen, J. dong and Chi, R. an (**2017**) 'Removal of Congo red from aqueous solution by adsorption onto different amine compounds modified sugarcane bagasse', *Clean Technologies and Environmental Policy*. Springer Berlin Heidelberg, 19(2), pp. 517–525.
Yu, X., Wei, C., Ke, L., Hu, Y., Xie, X. and Wu, H. (**2010**) 'Development of organovermiculite-based adsorbent for removing anionic dye from aqueous solution', *Journal of Hazardous Materials*. Netherlands, 180(1–3), pp. 499–507.
Yu, Y. W., Zhao, H. T. and Vance, G. F. (**2001**) 'Removal of Arsenite from Aqueous Solutions by Anionic Clays', *Environmental Technology*. Taylor & Francis, 22(12), pp. 1447–1457.
Zaini, M. A. A., Zakaria, M., Mohd.-Setapar, S. H. and Che-Yunus, M. A. (**2013**) 'Sludge-adsorbents from palm oil mill effluent for methylene blue removal', *Journal of Environmental Chemical Engineering*, 1(4), pp. 1091–1098.
Zare, H., Heydarzade, H., Rahimnejad, M., Tardast, A., Seyfi, M. and

Peyghambarzadeh, S. M. (**2015**) 'Dried activated sludge as an appropriate biosorbent for removal of copper (II) ions', *Arabian Journal of Chemistry*. King Saud University, 8(6), pp. 858–864.
Zehhaf, A., Benyoucef, A., Quijada, C., Taleb, S. and Morallón, E. (**2013**) 'Algerian natural montmorillonites for arsenic(III) removal in aqueous solution', *International Journal of Environmental Science and Technology*, 12(2), pp. 595–602.
Zenasni, M. A., Meroufel, B., Merlin, A. and George, B. (**2014**) 'Adsorption of Congo Red from Aqueous Solution Using CTAB-Kaolin from Bechar Algeria', *Journal of Surface Engineered Materials and Advanced Technology*, 04(06), pp. 332–341.
Zhang, L., Zhang, B., Wu, T., Sun, D. and Li, Y. (**2015**) 'Adsorption behavior and mechanism of chlorophenols onto organoclays in aqueous solution', *Colloids and Surfaces A: Physicochemical and Engineering Aspects*. Elsevier B.V., 484(August), pp. 118–129.
Zhang, R., Zhang, J., Zhang, X., Dou, C. and Han, R. (**2014**) 'Adsorption of Congo red from aqueous solutions using cationic surfactant modified wheat straw in batch mode: Kinetic and equilibrium study', *Journal of the Taiwan Institute of Chemical Engineers*, 45(5), pp. 2578–2583.
Zhang, Z., Moghaddam, L., O'Hara, I. M. and Doherty, W. O. S. (**2011**) 'Congo Red adsorption by ball-milled sugarcane bagasse', *Chemical Engineering Journal*, 178(Supplement C), pp. 122–128.
Zhao, K., Guo, H. and Zhou, X. (**2014**) 'Adsorption and heterogeneous oxidation of arsenite on modified granular natural siderite: Characterization and behaviors', *Applied Geochemistry*. Elsevier Ltd, 48, pp. 184–192.
Zhou, C. H. and Keeling, J. (**2013**) 'Fundamental and applied research on clay minerals: From climate and environment to nanotechnology', *Applied Clay Science*. Elsevier B.V., 74, pp. 3–9.
Zhou, X. and Zhou, X. (**2014**) 'the Unit Problem in the Thermodynamic Calculation of Adsorption Using the Langmuir Equation', *Chemical Engineering Communications*, 201(11), pp. 1459–1467.
Zhu, L., Wang, L. and Xu, Y. (**2017**) 'Chitosan and surfactant co-modified montmorillonite: A multifunctional adsorbent for contaminant removal', *Applied Clay Science*, 146(May), pp. 35–42.
Zou, J., Dai, Y., Wang, X., Ren, Z., Tian, C., Pan, K., Li, S., Abuobeidah, M. and Fu, H. (**2013**) 'Structure and adsorption properties of sewage sludge-derived carbon with removal of inorganic impurities and high porosity.', *Bioresource technology*. England, 142, pp. 209–217.
Zou, W. H., Zhao, L. and Zhu, L. (**2012**) 'Efficient uranium(VI) biosorption on grapefruit peel: kinetic study and thermodynamic parameters', *Journal of Radioanalytical and Nuclear Chemistry*, 292(3), pp. 1303–1315.

Appendixes

Energy dispersive X ray images for the samples

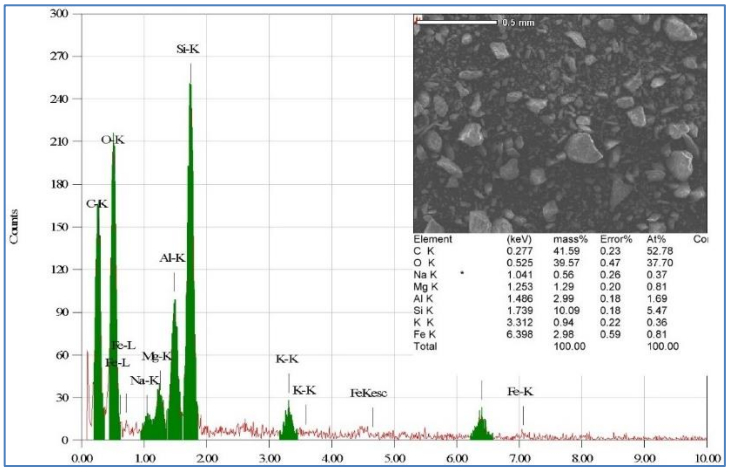

EDX image for Na-MO sample

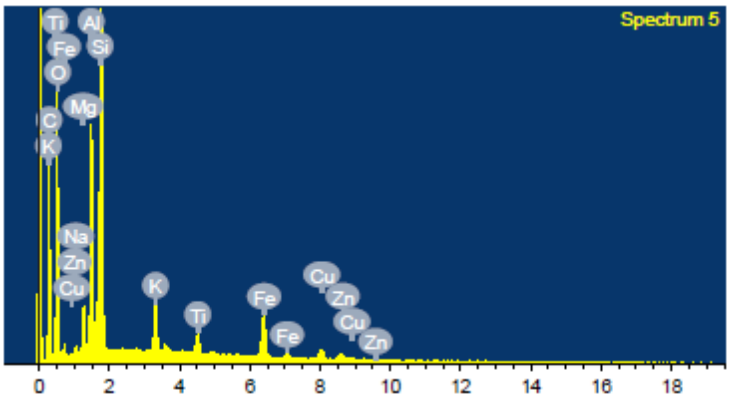

EDX image for Surf-MO sample

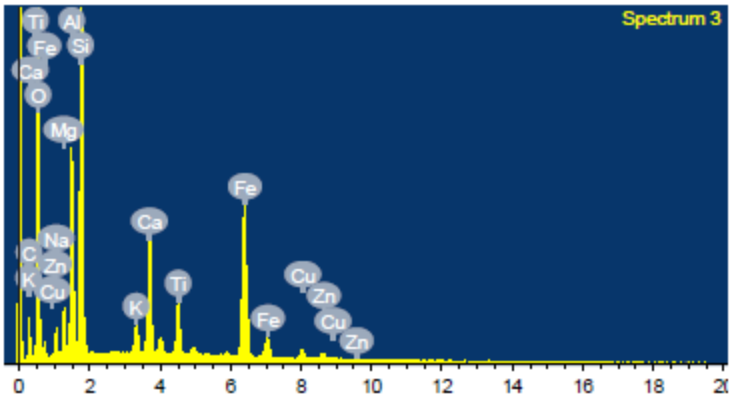

EDX image for Na-NI sample

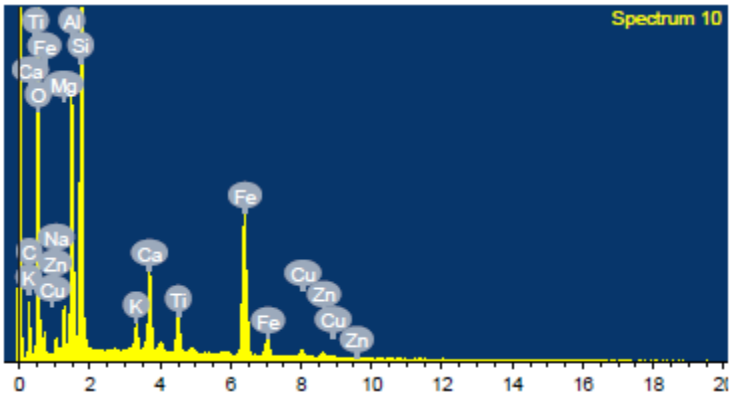

EDX image for Surf-NI sample

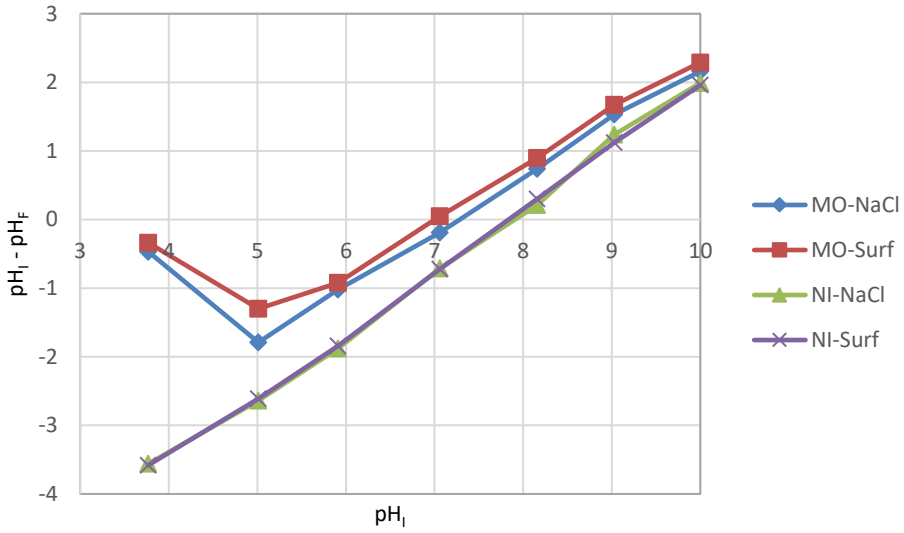

Calibration curves for CV, MB, CR and phenol (PH)

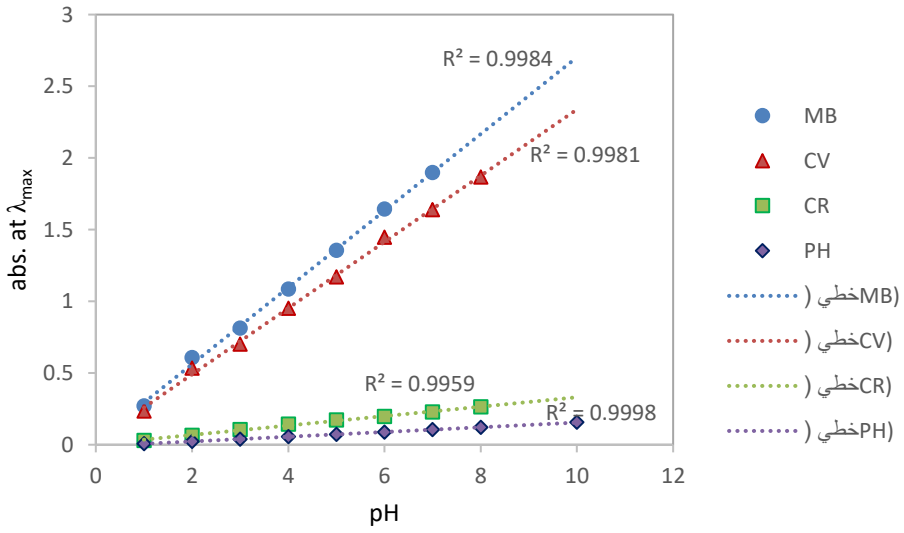

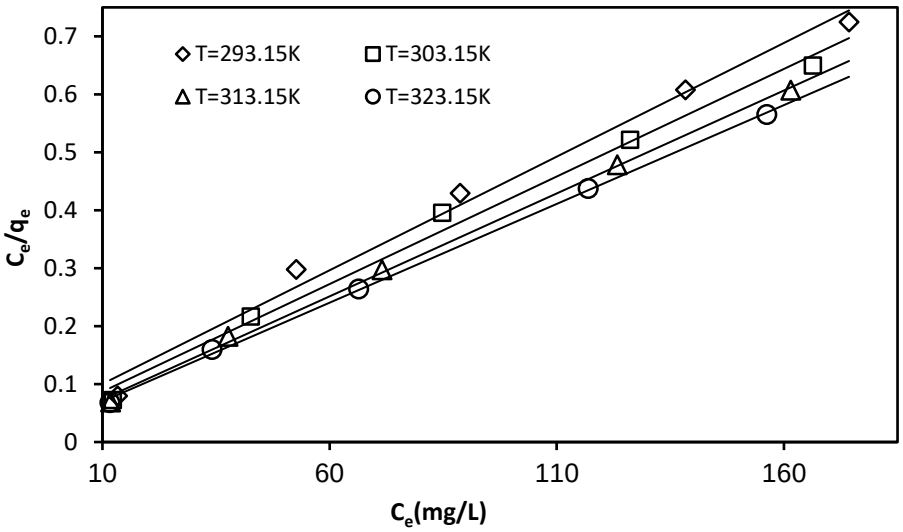

Langmuir plot for the adsorption of CV onto Na-MO

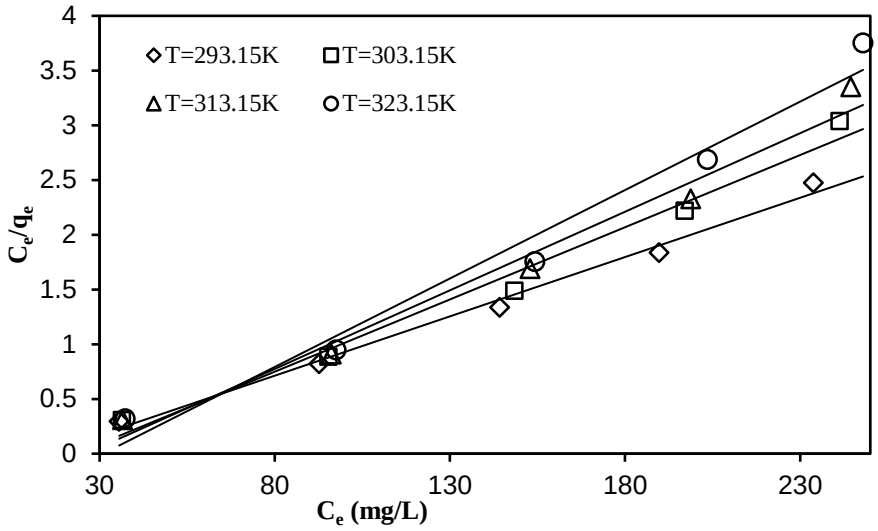

Langmuir plot for the adsorption of MB onto Na-MO

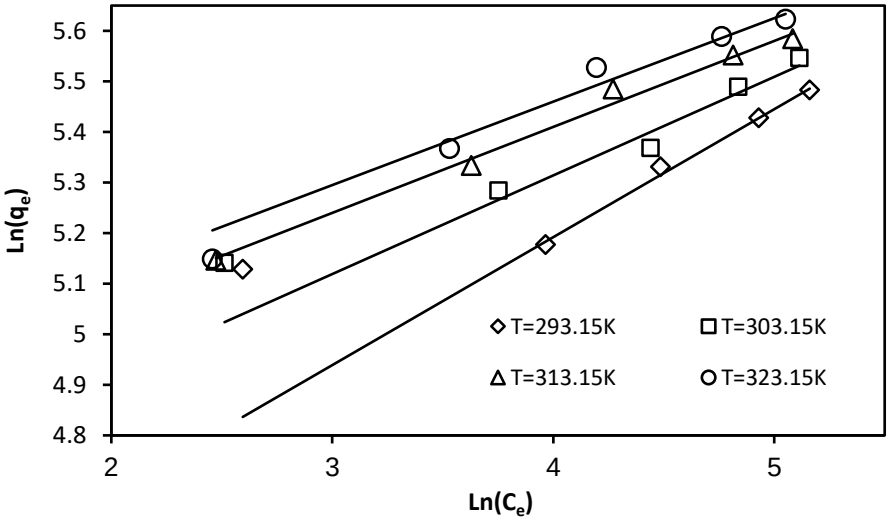

Freundlich plots for the adsorption of CV onto Na-MO

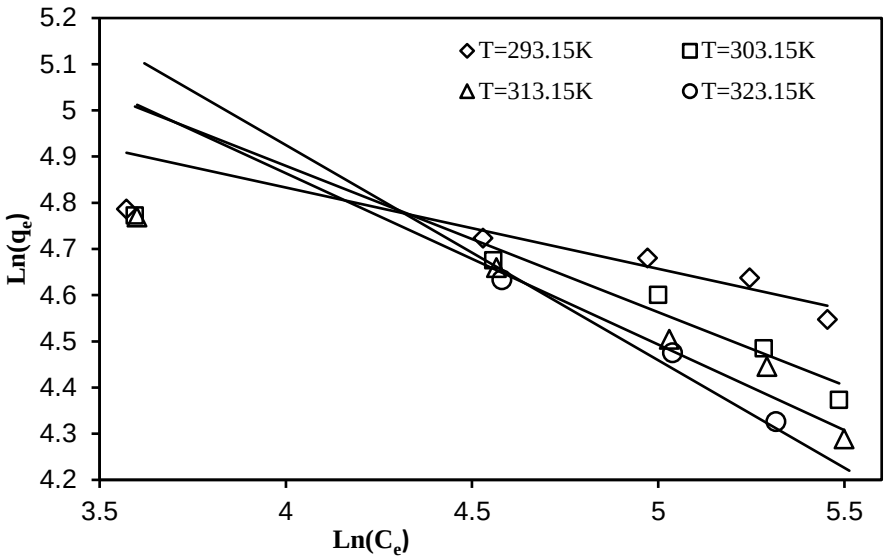

Freundlich plots for the adsorption of MB onto Na-MO

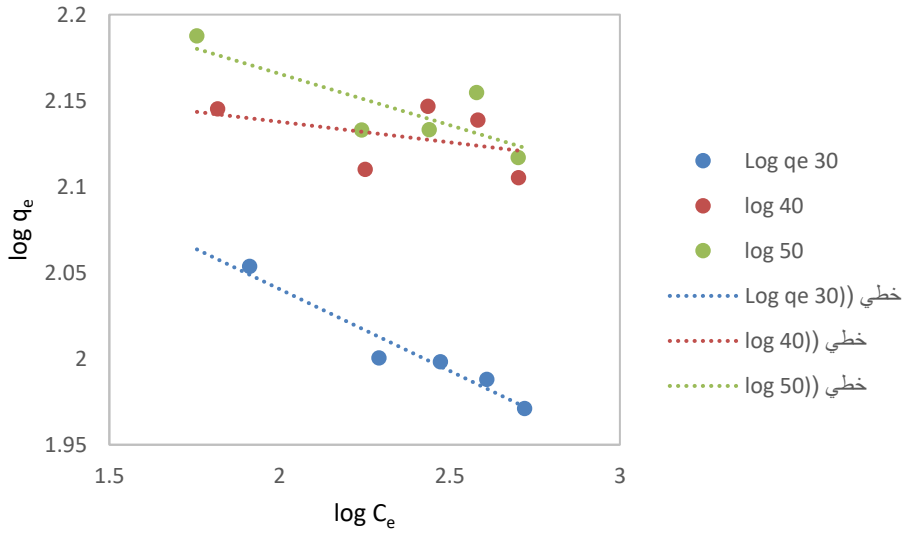

Freundlich plots for the adsorption of CR onto Surf-NI

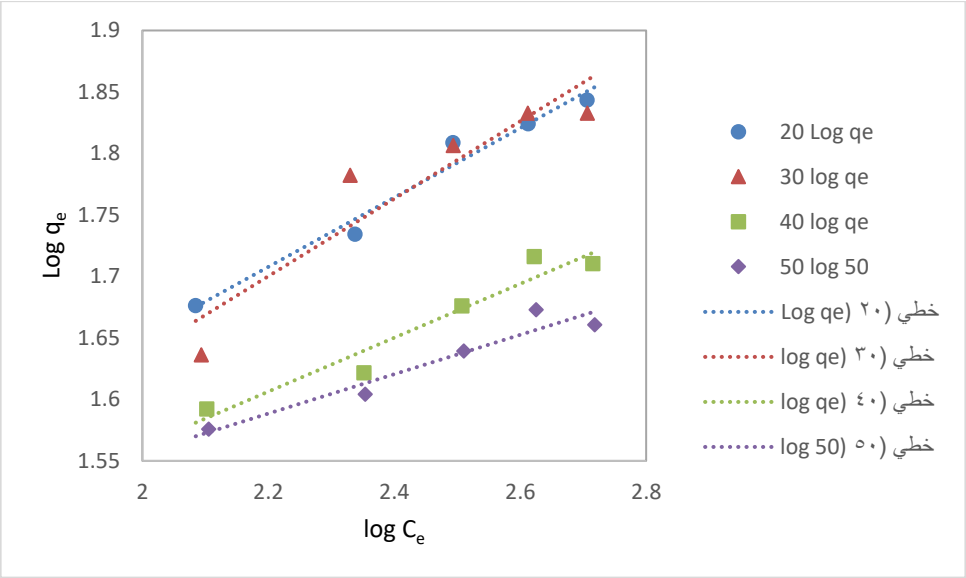

Freundlich plots for the adsorption of CR onto Surf-MO

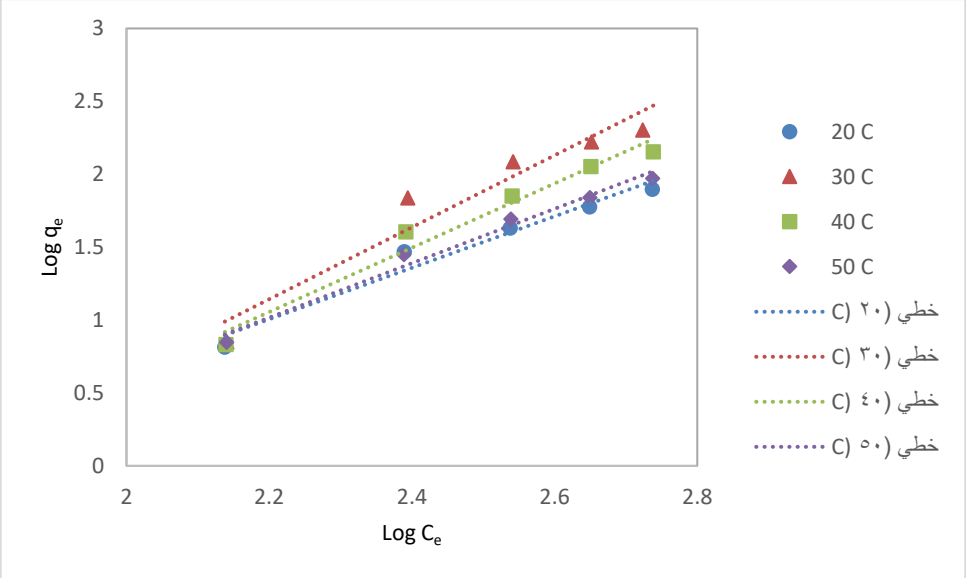

Freundlich plots for the adsorption of CR onto Na-MO

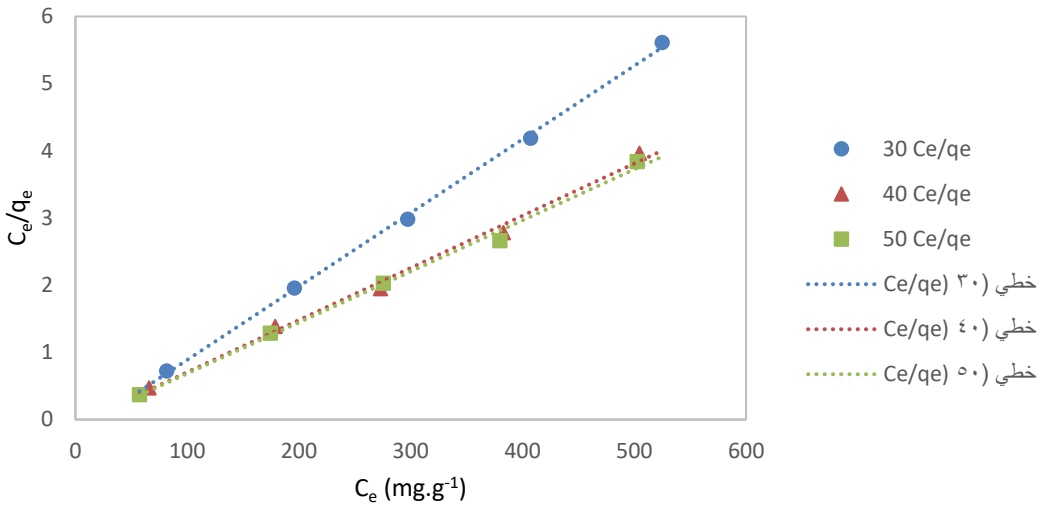

Langmuir plots for the adsorption of CR onto Surf-NI

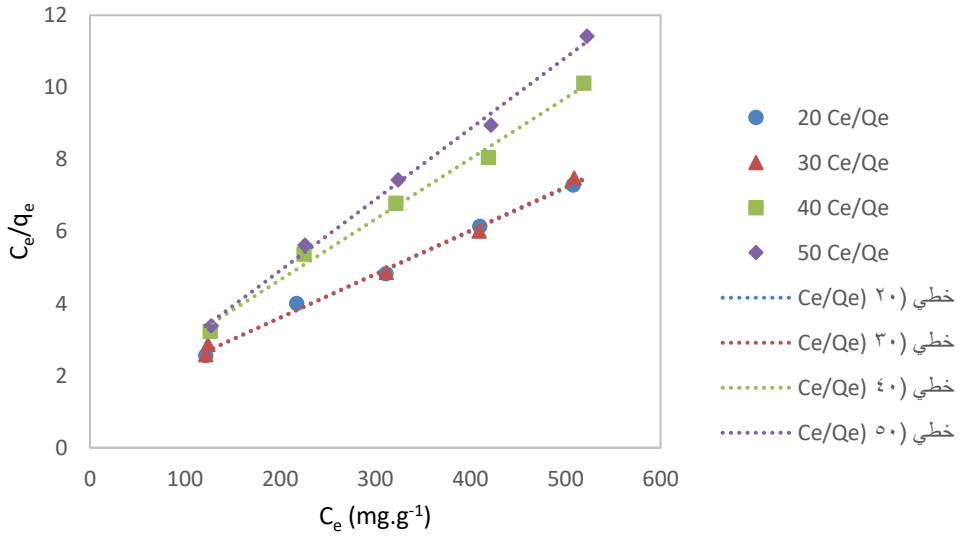

Langmuir plots for the adsorption of CR onto Surf-MO

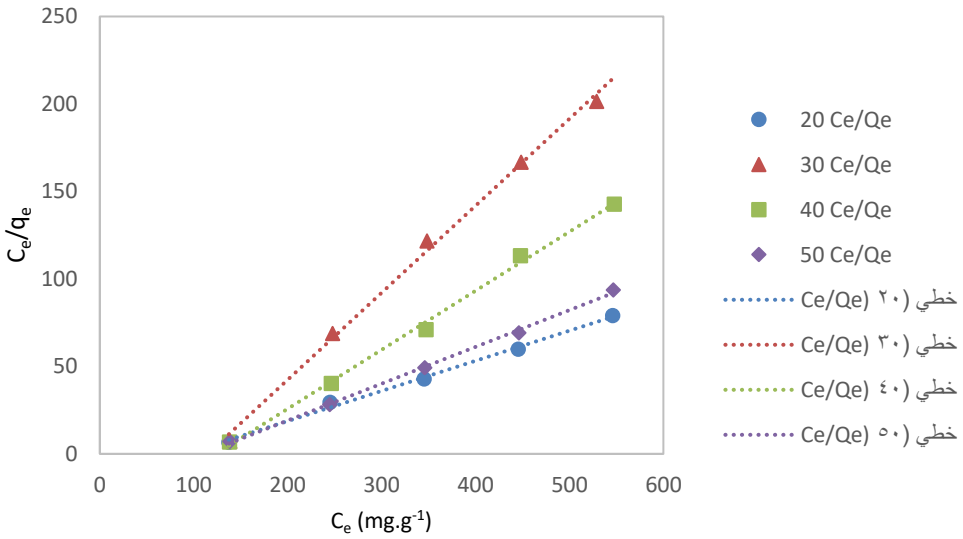

Langmuir plots for the adsorption of CR onto Na-MO